STUDY OF MAGNETIC AND OPTICAL BEHAVIOURS OF SOME RARE-EARTH COMPLEXES

THESIS SUBMITTED FOR THE DEGREE OF
DOCTOR OF PHILOSOPHY (SCIENCE)
OF THE
UNIVERSITY OF NORTH BENGAL

By
ASOKE NATH
DEPARTMENT OF MAGNETISM
INDIAN ASSOCIATION FOR THE CULTIVATION OF SCIENCE
CALCUTTA - 700 032
AUGUST, 1983

ST - VERP

STOCK TAKING - 2011

DEDICATED TO THE MEMORY

OF MY MOTHER

ACKNOWLEDGEMENT

The investigations presented in this thesis have been carried out under the direct and active guidance of Dr. U.S.Ghosh, Reader in Physics, Magnetism Department, Indian Association for the Cultivation of Science, Jadavpur, Calcutta 700032, India . I express my sincerest gratitude to him for giving me an opportunity to work with him and his keen interest, invaluable suggestions, constant help and encouragement throughout the progress of the work. Frequent discussions with him about the work presented here as well as about other related topics have helped me in better understanding of the subject and in broadening my scientific outlook.

I am indebted to Professor M.Chowdhury, Head of the Department of Physical Chemistry, Indian Association for the Cultivation of Science, for kindly extending his ideas to me and constant encouragement during the course of my work and finally collaborating with me for a part of this work.

I feel indebted to Dr. (Mrs.) C.Basu, Mr. Prabir K. Chatterjee for their valuable suggestions and constant assistance during the progress of the work.

I wish to thank Mr. Tapan Kumar Moulik for his careful typing of the manuscript and all others, those who helped me during the preparation of the thesis.

I am indebted to my father and grateful to my wife for their keen interest in my research work. Their understanding and patience have helped me to face the stress and strain which I had to undergo during the course of my work.

Lastly, I am thankful to the authorities of the Indian Association for the Cultivation of Science for providing me the necessary facilities for my work and for the award of research fellowship.

Calcutta
August/1983

(ASOKE NATH)

LIST OF PUBLICATIONS

1 Configuration mixing and crystal field splitting of Fe^{2+} and Cu^{2+} ions,
A. Nath, C. Basu and U. S. Ghosh,
Indian J. Phys. 55A, 277 (1981).

2 Ligand field theory of the magnetic behaviours of neodymium ethyl sulphate nonahydrate,
A. Nath and U. S. Ghosh,
Phys. Stat. Sol. (b) 112, 187 (1982).

3 Interpretation of the optical, magnetic and thermal behaviours of thulium ethyl sulphate,
A. Nath, Indian J. Phys. (in press).

4 Interpretation of the optical and magnetic behaviours of $Pr_2Mg_3(NO_3)_{12}\cdot 24H_2O$,
A. Nath, J. Phys. Soc. Japan (in press).

5 Absorption and circular dichroism spectra of $K_3Pr_2(NO_3)_9$ single crystal,
P. K. Chatterjee, A. Nath, A. C. Sen and M. Chowdhury,
J. Chem. Soc. Farad. Tr. II. (in press).

SYNOPSIS

The present thesis is devoted to the theoretical studies on magnetic, thermal, e.p.r and optical absorption results of some rare-earth complexes. Attempts have also been made here to present a model calculation on the optical activity of a rare-earth double nitrate crystal. The thesis consists of four chapters and we give below a brief description of the contents of the different chapters.

Chapter I opens with a general introduction of the crystal field (CF) and its modifications to what is called ligand field theory followed by a qualitative discussion on the effect of configuration interaction (C.I.) in the rare-earth group. This chapter also discusses the origin of paramagnetic behaviours of rare-earth complexes. The phenomenon of optical activity of some types of rare-earth complexes is also discussed at the end of this chapter.

Chapter II discusses the mathematical preliminaries specifically necessary for our work in the subsequent chapters. In order to make the thesis self sufficient we have started with a discussion of the Hamiltonian of an ion embedded within a crystal lattice. Then we have mentioned the different coupling schemes that are used generally in the calculation of atomic energy levels. The scheme of perturbation calculation

depending on the relative magnitudes of the various interactions present in the case of rare-earth complexes as well as the forms of the crystal field under various symmetries of the ion are also discussed systematically. The tensor operator technique has been discussed fully along with the concept of coefficient of fractional parentage (c.f.p). The tensor operator technique in the calculation of CF problems in the case of rare-earth ions has also been discussed. The method of calculation of magnetic susceptibility, g-value of a paramagnetic ion has been indicated. The introduction of the covalency reduction factor of the orbital angular momentum operator has also been discussed. The concept of charge and polarizability contribution to the CF parameter and the method of calculation of electric-dipole transition moment from both static and dynamic contribution have been dealt with in this chapter. The method of calculation of the magnetic dipole transition moment for $f \rightarrow f$ transition is also discussed. Finally, we give in this chapter the theoretical method of calculation of the rotational strength of an optically active RE ion.

The chapter III describes a consistent interpretation of the principal magnetic susceptibilities, g-values, optical absorption spectra and the magnetic heat capacity (where available) for various rare-earth ions namely Nd^{3+}, Pr^{3+}, Tm^{3+} in ethyl sulphate lattice and Pr^{3+} in double nitrate

lattice with the aid of a unified theory that simultaneously explains the results of all the different types of experiments mentioned above. Each system was treated rigorously with due consideration of intermediate coupling (IC) scheme and different J-mixing under the crystal field. The effect of C.I. in the CF level pattern were also taken into account in the case of praseodymium ethyl sulphate where the inclusion of this effect is found to be indispensable. A rigorous treatment gives a very reliable information regarding the crystal field (CF) parameters, interelectronic repulsion parameters (ES) and the spin-orbit (SO) coupling coefficient of the rare-earth ion. Investigation by direct diagonalisation of the complete energy matrix (consisting of SO, ES and CF interactions in general) is presented in case of Pr^{3+} and Tm^{3+} ion. It gives the full J-mixing. The theoretical interpretation on the optical, magnetic and e.p.r behaviours (and also specific heat behaviour where available) has been done for the concentrated crystal of Pr^{3+}, Nd^{3+} and Tm^{3+} ions in ethyl sulphate lattice and the Pr^{3+}-ion in double nitrate lattice. Systematic analysis for each sample is given separately in the different sections under this chapter. The results show that in the case of Nd^{3+} in ethyl sulphate we have an excellent agreement between the theory and experiment when a small covalency reduction is introduced in the orbital angular momentum during the calculation of magnetic susceptibility and the g-values.

The results obtained for Pr^{3+}, Tm^{3+} show that the theory simultaneously describes both the aspects of magnetic and optical behaviours within certain limitations. Further scope for future refinement of the theory has been mentioned. Moreover, the need of more experimental work with the presently available refined techniques has been pointed out.

The chapter IV describes a model calculation on the optical activity of anhydrous $K_3Pr_2(NO_3)_9$ single crystal. A brief account of the experimental details of both optical absorption and circular dichroism spectra has been described. The rotational strength was theoretically obtained by evaluating the imaginary part of the product of electric dipole transition moment and the magnetic dipole transition moment and then it was checked with the experimental value for both magnitude and relative sign for different transitions obtained. The calculation of electric dipole transition moment uses the odd order harmonics of the crystal field and the odd order harmonics were calculated with the point charge model including polarizability contribution. The CF energy level calculations were done first by the parameters obtained from point charge model and polarizability contribution and then the values of even order CF parameters thus obtained were adjusted to give the best fit to the experimental CF levels and also the rotational strengths. The contributions of both the electric

and magnetic dipole transition moments were calculated after due consideration of the J-mixing in the CF states. It is to be noted that for electric dipole transition moment both the static and dynamic contribution were taken into consideration. We also have mentioned the few discrepancies that arise in this model calculation.

The investigations presented in the chapters III and IV contain the original work of the candidate, most of which have been published in different journals (see the list of publications). No part of this thesis has been submitted for any degree elsewhere.

CONTENTS

CHAPTER IV : INTERPRETATION OF THE ABSORPTION AND CIRCULAR DICHROISM SPECTRA OF THE OPTICALLY ACTIVE $K_3Pr_2(NO_3)_9$ SINGLE CRYSTAL

CHAPTER I

GENERAL INTRODUCTION

I. GENERAL INTRODUCTION

The crystalline electric field theory formulated by J.H. Van Vleck[1] was established on a firm basis fairly long ago. This could explain in general, the paramagnetic behaviours of crystalline solids containing ions of the iron and transition group elements. Subsequently the crystalline electric field theory was developed to throw light on the electronic energy level pattern of iron and transition metal ions embedded in crystals and to explain the electronic spectrum of the ions. It is well known that the unpaired electrons in the incomplete inner shells of these groups of elements are responsible for the paramagnetism of their compounds. In the rare-earth compounds some of the 4f electrons of the rare-earth atom are often left out unpaired and would result in paramagnetism of the complexes and reflected finally in the crystals constituted by them in the solid state. We shall be mainly interested in the present thesis with the salts of rare-earth complexes.

The rare-earth or 'lanthanide' series forms a distinctive group whose chemical properties are remarkably similar. The valency is usually 3 . The interesting feature of the lanthanide group is the partial filling of the inner 4f shell inside a completely filled outer 5s and 5p shell. The closed shells of the electrons form the xenon core i.e. $1s^2 2s^2 2p^6 3s^2 3p^6 3d^{10}$

$4s^2 4p^6 4d^{10} 5s^2 5p^6$, which is the spectroscopic state of La^{3+} and Ce^{4+}. One more interesting point regarding lanthanides is that most compounds exhibit sharp lines in their optical spectra, particularly at low temperatures. These give us a detailed information for both ground and excited states.

Van Vleck[1] discussed in detail the paramagnetic behaviour of an assembly of non-interacting or free atoms each possessing identical or nonidentical quanta of magnetic moments associated with its resultant orbital and spin angular momenta arising due to statistical mixture of its electronic configuration in thermal equilibrium. The expressions for paramagnetic susceptibility under the three possible conditions, the multiplet intervals larger than, smaller than and comparable to kT, the average thermal energy deciding the distribution of population among the various quantum states of the system, have been derived by Van Vleck[1]. He showed that the paramagnetic susceptibility of such a system of free atoms can be described, in general, by a simple Curie-law, except when the multiplet intervals are comparable to kT, in which case the resultant atomic magnetic moment is itself a function of absolute temperature. When a paramagnetic ion goes to form a complex molecule, obviously some of the freedom of the unpaired electrons in the ion is destroyed. Whatever, if any are left free will be able to constitute the paramagnetism of the molecule in the free state, which can be estimated on the basis of the electronic configuration of the

molecule. This will be further modified when the ions or their complexes go into the solid crystalline state in two ways (1) by further association between complexes tending to pair off residual electronic moments, (2) by causing the ions or complexes to take up crystalline anisotropic orientations and thus only the average moments of complexes are found to be along the crystalline directions and as a result the molecular anisotropies are reflected in crystalline anisotropies.

From the early measurements of the susceptibility of the lanthanides at the room temperature it was found that in most of the cases it was generally rather close to that expected from an assembly of free ions and Curie's law was fairly obeyed and the spectral lines found in the rare-earth salts are very sharp. These phenomena can be explained by the fact that 4f electrons are shielded by 5s and 5p subshell from the valence fields of the co-ordinating atoms called ligands. The spin-orbit interaction in case of rare-earth complexes is very high and so L and S are not the good quantum numbers in case of rare-earth complexes but J remains a good quantum number. Now the strong electric fields from ligands and exchange fields from close neighbouring ions are still often effective enough to cause the J-degeneracy to be removed sufficiently. Van Vleck[1] established a number of essential features regarding the behaviours of paramagnetic salts from the quantum mechanical

description. He took into account the correct description of the symmetry properties of the crystal field and also the group theoretical approach given by Bethe[2] . The complete description of the pattern of the eigenstates generated by splitting the ground manifold of the free ion in presence of the ligand atoms depends upon the strength of binding as well as the symmetry of the cluster of ligand atoms. This theory of Bethe[2] and Van Vleck[1] is called the 'crystalline field theory', the ligands are assumed to produce static electric field.

Elliott and Stevens[3] tried to explain the magnetic susceptibilities and the e.p.r g-values of rare-earth ethyl sulphates with the help of the crystalline field theory. The optical spectra of the rare-earth complexes was explained with the help of crystal field theory by a number of workers[4-38] . The same type of calculations was done by Judd[39] also. Their aim was to examine the consistency of the crystalline field theory in explaining mostly the spectral and e.p.r behaviours of rare-earth complexes. It is now well established that elementary crystal field theory though need some modifications, is still fruitful to a first approximation for the interpretation of the optical and magnetic behaviours of rare-earth substances. In the crystal field theory the covalent metal-ligand interaction is ignored. In the rare-earth complexes, though this interaction is small due to shielding effect, sometimes it is

necessary to take into account the metal-ligand covalency effect to interpret the optical and magnetic results. So one has to incorporate the molecular orbital formalism due to Mulliken[40] in the frame of the crystal field theory. This inclusion of the M.O. method in the crystal field theory resulted in the development of what is known as ligand field theory[41-47] . The full M.O. calculation of rare-earth complexes is extremely complicated. However, in most of the cases ligand field theory which incorporates in it the essential features of M.O. theory by introducing the covalency reduction of some parameters directly or indirectly, is enough for explaining the optical e.p.r and magnetic susceptibility results.

Most of the crystal field calculations of rare-earth complexes are done within the same configuration. The calculations were confined within the ground configuration and thus the mixing of the excited configuration with the ground configuration i.e. the configuration interaction is ignored. The diagonalisation of the combined electrostatic and spin-orbit interaction matrices (for free rare-earth atoms) for a particular configuration yields energy levels which disagree with the experimental value substantially very frequently. This mismatch is due to neglect of configuration interaction. Configuration interaction plays a very important and frequently unrecognized role in the electronic properties of rare-earths, which sometimes, has a profound effect on their hyperfine

structure, spectral intensities and their behaviour in crystal fields. The configuration interaction in free rare-earth atom may be divided into two classes :

(1) strong configuration interactions where the perturbing configurations are energetically close to the perturbed configuration and there is appreciable coupling of the configurations by way of the Coulomb field,

(2) weak configuration interactions where the perturbing configurations are well separated from perturbed configuration and the coupling of the configurations in the Coulomb field is weak.

Where the configuration interaction is strong it becomes necessary to diagonalise energy matrices which include all the electrostatic interactions within and between the configurations. The eigenvectors resulting from the diagonalisation then allow us to express the states in terms of linear combinations of the states of the connected configurations. The effect of configuration interaction can be accomodated by introducing effective operators that act only within the configuration under study. The additional parameters that enter in the lowest order of perturbation theory are associated with two body operators (α, β, γ are the three related parameters) introduced by Rajnak and Wybourne[49] or with three electron operators (T^1, T^2, T^3, T^4, T^5, T^6) introduced by Judd[50] . Another contribution of the configuration interaction in the free

atom coming from spin-spin and spin-other-orbit which is called by Judd et al.[51] as 'Intra-atomic magnetic interactions for f electrons' (the related parameters are M^0, M^2, M^4, M^6 and P^0, P^2, P^4, P^6). To improve the free ion calculation of the rare-earth crystals this C.I. part should be taken into consideration. Recently Carnall et al[11] did this type of calculation for the rare-earth complexes to improve the theoretical crystal field levels and hence to have a good fit with the experimental levels. In the case of rare-earth ion embedded in a crystal lattice, the configuration interaction is brought about in the second order by both the crystal field interaction and inter-electronic repulsion. The odd harmonics of the crystal field interaction are known to have a profound effect on the intensity of transition between crystal field levels.[52-53]

The theoretical approach for interpreting the spectral, magnetic, e.p.r and specific heat consists in finding a unique set of relevant parameters which enter into the theory and consistent with the results of all the aforesaid experiments. These parameters in the case of rare-earth complexes are the Slater-Condon parameters[54] for the electrostatic part (F_2, F_4, F_6), spin-orbit (SO) coupling constant (ζ) and crystal field (CF) parameters and sometimes some additional parameters such as two and three body parameters, intra-atomic magnetic interaction

parameters mentioned earlier and covalency reduction factors[55] for the orbital angular momentum may be necessary. It may be noted that covalency affects almost all the parameters. However, in a theory where the parameters are deduced from experiments by adjusting them to give a good fit between the theory and experiment, the covalency effect on the parameters is automatically included in them.

The information obtained from optical spectra, electron paramagnetic resonance, magnetic specific heat of the rare-earth ions in crystalline solid can be supplemented with magnetic susceptibility and anisotropy results. When the results of the optical spectra are not available in detail, it is difficult to get a unique set of parameters from the optical experiments alone. Even when the fine structure details are available, the validity of the parameters deduced from such optical experiments can only be confirmed if they are consistent with other experimental results. So by studying the susceptibility, anisotropy and $g_{\perp}$ values we have an opportunity to check the validity of the crystal field parameters suggested by optical data.

Optical activity[56-61] is the ability to rotate the plane of polarization of circularly polarized light. An optically active medium may owe its rotatory power to one or both of two causes: molecular dissymmetry and macroscopic anisotropy, the latter of these two may be due to the spatial arrangement of molecules (e.g.

crystal lattice) or to the presence of fields (e.g. the Faraday effect).

The circular dichroism (CD) is the differential absorption of left circularly polarized light and right circularly polarized light. After eventual transmission from the system the incident circularly polarized light gets elliptically polarized due to the differential absorption. Circular dichroism (CD) and optical activity are like twins with their origins in the dyssmetric environment, the former being related to the difference in imaginary parts of the refractive indices of right and left circularly polarized light and the latter to the real parts. An important application of CD measurements lies in the identification of magnetic dipole transitions, since the magnitude of these effects depends on the product of electric dipole transition moment and the magnetic dipole transition moment. It has been found that the weak f→f transition (oscillator strength $f \leqslant 10^{-6}$) has some magnetic dipole character and in some special cases, magnetic dipole transitions have actually been detected.[62-64]

We have chosen trivalent RE compound ($K_3Pr_2(NO_3)_9$) for our optical activity calculation. The $f^N \rightarrow f^N$ transitions in trivalent RE complexes are frequently forced electric dipole allowed[65-66], sometimes magnetic dipole allowed.[62-63] We discuss a model calculation regarding the electric dipole moment and the magnetic dipole moment of the aforesaid compound. Rotational

strength[67] is then calculated by considering the imaginary contributions of their product. Static and dynamic contribution to the electric dipole moment were calculated after Richardson and Faulkner[68] . The contribution of the magnetic dipole moment for term to term was calculated after Sen and Chowdhury.[69] The rotational strength can also be obtained from experiment.[70] The relative changes in sign of the rotational strengths of CF transitions were compared with the experimental CD spectrum.

CHAPTER II

MATHEMATICAL PRELIMINARIES

II.1. INTERACTIONS PRESENT IN A PARAMAGNETIC ION EMBEDDED IN A CRYSTAL

When a paramagnetic ion is embedded in a magnetically dilute crystal the Hamiltonian in presence of an externally applied magnetic field can be written as

$$H = H_F + H_{SO} + H_C + H_{\mathcal{H}} \qquad \text{(II.1.1)}$$

where, H_F = nonrelativistic Hamiltonian for a free ion excluding magnetic interactions of electron orbits and spins.

H_{SO} = spin-orbit interaction energy,

H_C = crystal field interaction,

$H_{\mathcal{H}}$ = interaction energy due to the application of the external magnetic field $\mathcal{H}$. The spin-spin interaction, the exchange interaction of electrons, nuclear interaction and other possible interactions are usually small and have been neglected in our calculation. The non relativistic free atom Hamiltonian H_F is

$$H_F = \sum_i \left(T_i - \frac{Ze^2}{r_i}\right) + \sum_{i<j} \frac{e^2}{r_{ij}} \qquad \text{(II.1.2)}$$

where T_i = K.E. of the i-th electron and $\frac{-Ze^2}{r_i}$ = P.E. of the i-th electron in the attractive coulomb field of the nucleus. $\frac{e^2}{r_{ij}}$ = electron electron repulsion term. If we neglect the inter-electronic repulsion term then the method of separation

of variables can be applicable and the Schrödinger equation corresponding to (II.1.2) can be solved. But this term is too large to be dropped and treated later by perturbation theory. So the general procedure for solving the eigenvalue problem of H_F is then to use the central field approximation. This means actually that it is fairly good approximation first to replace H_F by a central field Hamiltonian H_o which takes into account of the fact that each electron moves independently of the others in an effective central potential V(r) representing the combined effects of the attraction by the nuclear charge and a suitably averaged repulsion by the other electrons. Now we define $(H_F - H_o)$ as the residual interaction H_r , which is treated as the perturbation potential. Thus we can write

$$H_F - H_o = H_r \qquad \text{(II.1.3)}$$

where H_o = central field Hamiltonian and is given by

$$H_o = \sum_i \left[T_i + V_{eff}(r_i) \right] \qquad \text{(II.1.4)}$$

$V_{eff}(r_i)$ = P.E. energy of the i-th electron in the effective central field. The residual interaction H_r is given by[71]

$$\begin{aligned} H_r &= H_F - H_o \\ &= \sum_i \left(- V_{eff}(r_i) - \frac{Ze^2}{r_i} \right) + \sum_{i<j} \frac{e^2}{r_{ij}} \end{aligned} \qquad \text{(II.1.5)}$$

H_r thus consists of one and two electron terms represented by

$$H_r^{ii} = \sum_i \left(- V_{eff}(r_i) - \frac{Ze^2}{r_i} \right) \qquad \text{(II.1.6)}$$

and

$$H_r^{ij} = \sum_{i<j} \frac{e^2}{r_{ij}} \qquad \text{(II.1.7)}$$

Now when one is interested entirely within the structure of a single configuration, the one electron term H_r^{ii} may be omitted in H_r since its effect is simply to shift a configuration as a whole. So we drop this term as calculations involving different electronic configurations will not be dealt with in the present thesis.

Thus we can write finally the total effective Hamiltonian (II.1.1) of a paramagnetic ion embedded in a crystalline lattice in presence of external field $\mathcal{H}$ using the central field approximation for free ion as follows :

$$H = H_o + H_r^{ij} + H_C + H_{SO} + H_{\mathcal{H}} \qquad \text{(II.1.8)}$$

The eigen value problem of the total Hamiltonian H given in (II.1.8) is tackled by treating H_o as the unperturbed Hamiltonian and $(H-H_o)$ as the perturbation Hamiltonian. Further the perturbation $(H-H_o)$ consists of a number of parts in order of decreasing strength, and the perturbation problem is tackled by applying these parts in stages in order of decreasing strength on the low lying states resulting from the previous perturbation part. The calculation of the matrix elements of the perturbation Hamiltonian is facilitated by defining a complete set of basis states in some well defined coupling schemes which are discussed in the next section.

II.2. COUPLING SCHEME

We consider the following three coupling schemes that are used in the theory of atomic spectra

(a) L-S coupling scheme

The free atom Hamiltonian H_F , L^2, S^2, L_z , S_z are mutually commuting dynamical variables where L and S are the resultants of individual electronic orbital angular momenta, ℓ's and spin angular momenta, s's respectively. That means H_F , L^2, S^2, L_z and S_z have simultaneous eigenstates and L, S, M_L , M_S are good quantum numbers or in other words L^2, S^2, L_z and S_z are constants of motion. From the same argument we can have simultaneous eigen states of H_F , L^2, S^2, J^2 and J_z where J, the total angular momentum, is the resultant of L and S and also L^2, S^2, J^2 and J_z are constants of motion. We can then classify the energy eigen states of the atom by the eigen value of the constants of motion i.e., by specifying the definite values of L, S, M_L , M_S or L, S, J, M_J . This description of the atom is valid only when H_{SO} is neglected in the free atom since otherwise L^2 or S^2 will not commute with the Hamiltonian. So in case of lighter atoms for which atomic number is small and H_{SO} is weak it is a good approximation to take H_{SO} as a small perturbation on the states represented by $|SLM_SM_L\rangle$ or $|SLJM_J\rangle$ in the basis of which L^2 and S^2 are diagonal. Any set

of states in which L^2 and S^2 are diagonal is referred to as Russel-Saunder's coupling scheme.

(b) jj coupling scheme

For heavy atoms (large atomic number), H_{SO} can no longer be treated as a perturbation on L-S coupling states $|SLM_SM_L\rangle$ or $|SLJM_J\rangle$ but must be taken into account at the very begining in the original single particle orbitals from which the resultant atomic states are built. This actually means that electronic wave functions are no longer simultaneous eigen-states of n, ℓ, m_s, m_ℓ but the simultaneous eigen states of n, ℓ, j, m where j is the total angular momentum (resultant of ℓ and s) of a single electron. The individual electronic j's then combine to produce the total J and its component M_J of the atom as constants of motion. The scheme characterised by the set of quantum numbers n, ℓ, j for each electron and JM_J for the whole atom is known as the jj coupling scheme. In this scheme H_{SO} is diagonal and coulomb repulsion term is then taken as perturbation.

(c) Intermediate coupling scheme

When the coulomb repulsion and the spin-orbit interaction terms are comparable, neither L-S nor j-j coupling gives a good approximation, since the Hamiltonian of a free atom (which

includes H_{SO}) is not diagonal in either case. In this case we have to diagonalize the Hamiltonian matrix which includes both coulomb repulsion and SO interaction exactly and its diagonalization gives a representation in which both H_r^{ij} and H_{SO} are diagonal. This is known as the intermediate coupling. The wave function in this scheme is a linear combination of states represented by $|SLJM_J\rangle$.

II.3. SCHEMES OF PERTURBATION CALCULATION DEPENDING ON THE MAGNITUDE OF CRYSTAL FIELD RELATIVE TO OTHER INTERACTIONS

The coupling scheme indicates the basis states necessary for starting perturbation calculation. The coupling schemes already stated are for the case of a free atom. The above description has to be modified in the case of paramagnetic ion occupying a site in the crystalline lattice i.e. if H_c is included in the perturbation $(H-H_o)$, the different parts of which are applied in stages as mentioned earlier. So we have to know how H_c compares in order of magnitude with the other perturbing quantities of equation (II.1.8) particularly H_{SO} and H_r^{ij} part of H_r . We shall confine our discussion to the rare-earth groups only with which the present thesis is concerned.

Now in case of rare-earth complexes, $H_r^{ij} \approx H_{SO} \gg H_c$. Evidently the intermediate coupling scheme described earlier

in the case of free atom is the most suitable one in this case and it is the most realistic approach for the perturbation procedure in rare-earth complexes. H_c is to be applied then on the Intermediate coupling states.

II.4. TENSOR OPERATORS AND THEIR USES IN THE PRESENT THESIS

For the calculation of the matrix elements of H_r , H_{SO} , H_c (H_c = crystal field interaction) etc between the atomic states we can expand the atomic states in terms of antisymmetrized product of one electron wave functions following the method of Slater[72] and the matrix elements of the operators are then evaluated in the manner as described by Slater[72] and Condon and Shortley[54] . But this method, though in principle applicable to most of the cases, is very cumbersome and extremely tedious in complex configurations. An alternative and much simpler but most powerful and elegant method known as tensor operator method has been developed in conjunction with group theory and concept of fractional parentage by Racah[73] and Wigner[74] .

II.4(a). DEFINITION OF A TENSOR OPERATOR

An irreducible tensor operator of rank k is defined by Racah[75] as an operator $T^{(k)}$ whose $(2k+1)$ components satisfy

the same commutation rule with respect to the total angular momentum J as the spherical harmonic operators Y_k^q i.e.

$$\left[(J_x \pm iJ_y),\ T_q^{(k)}\right] = \left[(k \mp q)(k \pm q + 1)\right]^{1/2} T_{q\pm1}^{(k)} \qquad \text{(II.4.1)}$$

$$\left[J_z\ ,\ T_q^{(k)}\right] = q\, T_q^{(k)} \qquad \text{(II.4.2)}$$

Evidently, the spherical harmonics are themselves tensor operators. One can easily show from the above definition that suitable linear combinations of the components of the orbital angular momentum or the spin or the cartesian (x,y,z) operator are the components of tensor operators with $k = 1$. The tensor operator form of x,y,z may also be easily obtained by expressing them in terms of the components of the first order spherical harmonics.[76]

II.5. COEFFICIENT OF FRACTIONAL PARENTAGE

Calculation with the help of Racah formalism needs frequent use of the concept of fractional parentage. The idea is as follows :

Any state $\Psi(\ell^n \alpha S L M_S M_L)$ of the configuration ℓ^n may be expanded in terms of the products of states $\Psi(\ell^{n-1} \alpha_1 S_1 L_1 M_S M_L)$ of the first (n-1) electrons with those of the n-th electron having the same ℓ value as follows :

$$\Psi(\ell^n \alpha S L M_S M_L) = \sum_{\alpha_1 S_1 L_1} \left\langle \ell^{n-1}(\alpha_1 S_1 L_1)\ell;\ SL \right\} \ell^n \alpha S L \rangle \sum_{M_{S_1} M_{L_1} m_s m_\ell} \langle S_1\ \tfrac{1}{2}\ S M_S |$$

$$S_1\ \tfrac{1}{2}\ M_{S_1} m_s \rangle \langle L_1 \ell L M_L | L_1 \ell M_{L_1} m_\ell \rangle \Psi(\ell^{n-1}(\alpha_1 S_1 L_1 M_{S_1} M_{L_1})) \Phi(\ell, m_\ell, m_s) \tag{II.5.1}$$

where $\Phi(\ell, m_\ell, m_s)$ represents the state of the n-th electron having quantum numbers ℓ , m_ℓ , m_s . The first summation extends over all the terms $\Psi(\ell^{n-1}(\alpha_1 S_1 L_1))$ of the complete set for the ℓ^{n-1} configuration and the second sum merely performs the vector coupling of the total S and L values. In other words the state $\Psi(\ell^n \alpha S L)$ representing a term of the ℓ^n configuration may be written as the following linear combination

$$\Psi(\ell^n \alpha S L) = \sum_{\alpha_1 S_1 L_1} \Psi(\ell^{n-1}(\alpha_1 S_1 L_1)\ell; SL) \left\langle \ell^{n-1}(\alpha_1 S_1 L_1)\ell; SL \right\} \ell^n \alpha S L \rangle \tag{II.5.2}$$

The term $\alpha_1 S_1 L_1$ of the ℓ^{n-1} configuration is known as the parent of the term $\alpha S L$ of the ℓ^n configuration and the co-efficient $\left\langle \ell^{n-1}(\alpha_1 S_1 L_1)\ell; SL \right\} \ell^n \alpha S L \rangle$ commonly abbreviated as $\langle \bar{\Psi} | \} \Psi \rangle$ is known as the coefficient of fractional parentage (c.f.p.) . The c.f.p. describes how the resultant state Ψ is built up from its possible parents $\bar{\Psi}$ when another electron with the same ℓ quantum number is added to the parent and can be looked upon as defining the state. They are chosen to yield the properly antisymmetrized eigenfunctions of the ℓ^n configuration and are zero for all the forbidden states of the configuration.

Due to the equivalence of the electrons the matrix element of the sum of a single particle operator $F = \sum_i f_i$ between two states of the configuration ℓ^n is n times the corresponding matrix element for f_i where f_i is a single particle operator for the i-th particle, that is

$$\langle \ell^n \alpha S L | F | \ell^n \alpha' S' L' \rangle = n \langle \ell^n \alpha S L | f_i | \ell^n \alpha' S' L' \rangle \qquad \text{(II.5.3)}$$

Making use of (II.5.2) we get

$$\langle \ell^n \alpha S L \, M_S M_L | F | \ell^n \alpha' S' L' M_S' M_L' \rangle = n \sum_{\alpha_1 S_1 L_1} \langle \ell^n \alpha S L \{ | \ell^{n-1} (\alpha_1 S_1 L_1) \ell \, S L \rangle$$

$$\langle S_1 L_1 \ell_n S L \, M_S M_L | f_i | S_1 L_1 \ell_n S' L' M_S' M_L' \rangle \langle \ell^{n-1} (\alpha_1 S_1 L_1) \ell S' L' | \} \ell^n \alpha' S' L' \rangle \qquad \text{(II.5.4)}$$

The matrix element of f_i can be evaluated by expressing f_i in terms of the appropriate tensor operator and then using the tensor operator technique. The problem then reduces to finding the coefficients $\langle \ell^n \alpha S L \{ | \ell^{n-1} (\alpha_1 S_1 L_1) \ell S L \rangle$ and $\langle \ell^{n-1} (\alpha_1 S_1 L_1) \ell S' L' | \} \ell^n \alpha' S' L' \rangle$. We shall assume that the phases of the states of the configurations ℓ^n, ℓ^{n-1} and ℓ have been chosen to ensure that the coefficients are real, hence

$$\langle \ell^n \alpha S L \{ | \ell^{n-1} (\alpha_1 S_1 L_1) \ell S L \rangle = \langle \ell^{n-1} (\alpha_1 S_1 L_1) \ell S L | \} \ell^n \alpha S L \rangle \qquad \text{(II.5.5)}$$

For matrix element of a single-particle operator F between two states of different configurations we can write following Racah[73]

$$\langle \ell^n \alpha S L \, M_S M_L | F | \ell^{n-1} (\alpha_1 S_1 L_1) \ell' S' L' M_S' M_L' \rangle$$

$$= n^{1/2} \langle \ell^n \alpha S L \{ | \ell^{n-1} (\alpha_1 S_1 L_1) \ell S L \rangle \langle S_1 L_1 \ell_n S L \, M_S M_L | f_n | S_1 L_1 \ell_n' S' L' M_S' M_L' \rangle \qquad \text{(II.5.6)}$$

The coefficients of fractional parentages for d^n and f^n configurations have been tabulated in a convenient form by Nielson and Koster[77] . These tables are available for configurations upto half-filled shell. For configurationsmore than the half-filled shell, the c.f.p may be easily calculated from the recursion formula given by Racah[73]

$$\left\langle \ell^{4\ell+1-n}(\alpha' S' L')\ell SL \right\} \ell^{4\ell+2-n}\alpha S L\rangle$$

$$= (-1)^{S+S'+L+L'-\ell-\frac{1}{2}} \left[\frac{(n+1)(2S'+1)(2L'+1)}{(4\ell+2-n)(2S+1)(2L+1)}\right]^{1/2}$$

$$\left\langle \ell^n(\alpha SL)\, \ell\, S' L' \right\} \ell^{n+1}\alpha' S' L'\rangle \qquad \text{(II.5.7)}$$

II.6. REPRESENTATION OF A WAVE FUNCTION BY RACAH'S CONVENTION IN THE CASE OF f^n CONFIGURATION

In the particular case of the f shell, Racah[78] introduced two groups providing two sets of quantum numbers W and U. The first is a set of three integral numbers $W = (w_1 w_2 w_3)$ with $w_1 \geqslant w_2 \geqslant w_3 \geqslant 0$ and all $w \leqslant 2$, while the second is a set of two integral numbers $U \equiv (u_1 u_2)$. With a few exceptions these labels distinguish all states of the f shell and using the symbol α to separate these exceptions, the wave functions are denoted by

$$\Psi(f^n \alpha\ W\ U\ S\ L\ M_S M_L) \ . \qquad \text{(II.6.1)}$$

The states of any rare-earth ion having a configuration represe-

ted in general by $^4f^n$ are listed by Nielson and Koster[77] using this representation. In earlier work Racah used a 'seniority number' v, which is essentially equivalent to W, to label the states. The corresponding notation alternative to (II.6.1) is

$$\Psi(f^n \alpha\ U\ v\ SL\ M_S M_L) \quad . \qquad \text{(II.6.2)}$$

II.7. ELECTROSTATIC ENERGY FOR f^n CONFIGURATION

By expanding the electrostatic interaction between electrons in Legendre polynomials of the cosine of the angle between them, the electrostatic energy $\mathcal{E}$ may be written as a linear combination of Slater radial integrals[54], F_K

$$\mathcal{E} = \sum_{k=0}^{2l} f^k F_k \ , \quad k \text{ is even} \qquad \text{(II.7.1)}$$

For the two electron configuration the coefficients f^k are simply angular integrals over spherical harmonics. Using the calculated c.f.p. together with equation (1) of Racah[78] to derive the coefficients of the F_k in the configuration ℓ^n from those in the configuration ℓ^{n-1}, we may build up a chain process from the known ℓ^2 coefficients; but in the f shell such a process is tedious.

To simplify the calculation, Racah observed that, in the two-electron problem, the coefficient f^k is essentially the expectation value of the scalar product operator $(y_k(1).y_k(2))$ of two spherical harmonics. Although this operator is a scalar

with respect to rotations in three dimensions it is neither scalar nor has simple properties with respect to the more general groups of transformations used to classify the wave functions. However, by taking certain linear combinations of these operators one may construct new operators which have simple transformation properties under the groups employed. The energy becomes

$$\mathcal{E} = \sum_{k=0} e_k E^k , \qquad \text{(II.7.2)}$$

where the e_k are the expectation values of the new operators and the E^k's are linear combinations of the F_k's.

In the f shell we have

$$\begin{aligned} E^0 &= F_0 - 10F_2 - 33F_4 - 286F_6 , \\ E^1 &= \tfrac{1}{9}(70F_2 + 231F_4 + 2002F_6), \\ E^2 &= \tfrac{1}{9}(F_2 - 3F_4 + 7F_6) \\ E^3 &= \tfrac{1}{3}(5F_2 + 6F_4 - 91F_6) \end{aligned} \qquad \text{(II.7.3)}$$

For configuration f^n Racah[78] has shown that both e_o and e_1 are diagonal in the UvSL scheme with values,

$$\begin{aligned} e_o &= \tfrac{1}{2} n(n-1) , \\ e_1 &= \tfrac{9}{2}(n-v) + \tfrac{1}{4} v(v+2) - S(S+1) \end{aligned} \qquad \text{(II.7.4)}$$

The remaining co-efficients are more difficult to derive and necessitate the use of the c.f.p. discussed in II.5 . Using these, Racah has prepared subsidiary tables from which the

values of e_2 and e_3 may be derived in any configuration f^n. One can calculate the electrostatic part of any f^n system by using the above mentioned procedure. However, Nielson and Koster[77] gave extensive tables where they gave the electrostatic part of any of f^n system in terms of E^0, E^1, E^2, E^3 and we have used this table in dealing with the problems discussed in the present thesis.

II.8. MATRIX ELEMENTS OF THE SPIN-ORBIT INTERACTION

Using the tensor operator methods of Racah[75] together with the fractional parentage coefficients, the matrix element of the spin-orbit operator $\zeta\sum_i (\underset{\sim}{s}_i \cdot \underset{\sim}{\ell}_i)$ between two general states Ψ_{JM}, Ψ'_{JM} of the configuration ℓ^n is given by

$$(\Psi_{JM}|\zeta\sum_i (\underset{\sim}{s}_i \cdot \underset{\sim}{\ell}_i)|\Psi'_{JM}) = -n\,\zeta\{3\ell(\ell+1)(2\ell+1)(2L+1)(2L'+1)(2S+1)(2S'+1)/2\}^{1/2} (-1)^{J+L+S'+1} \begin{Bmatrix} J & L & S \\ 1 & S' & L' \end{Bmatrix}$$
$$\sum_{\bar{\Psi}} \langle \Psi \{| \bar{\Psi}\rangle \langle \Psi' \{| \bar{\Psi}\rangle (-1)^{S+\bar{S}+L+\bar{L}+\ell+\frac{1}{2}} \begin{Bmatrix} \bar{S} & S & \frac{1}{2} \\ 1 & \frac{1}{2} & S' \end{Bmatrix} \begin{Bmatrix} \bar{L} & L & \ell \\ 1 & \ell & L' \end{Bmatrix} \qquad \text{(II.8.1)}$$

where $\langle \Psi \{| \bar{\Psi}\rangle$ stands for the coefficient of fractional parentage. The SO matrix element in terms of ζ has been calculated by several workers. Spedding[79] calculated the SO matrix elements for f^2 system and Judd and Loudon[80] calculated the matrix elements for f^3 system. Later Nielson and Koster[77] has given

the values of the matrix elements of SO interaction in a tabular form for all f^n systems.

II.9. THE CRYSTAL FIELD

Assuming that the crystal field potential V satisfies Laplace's equation over the space not occupied by charges, it can be expanded as a sum of spherical harmonics as follows :

$$V(r,\Theta,\Phi) = \sum_{k=0}^{\infty} \sum_{q=-k}^{k} a_{kq}\, r^k\, Y_k^q(\Theta,\Phi) \qquad \text{(II.9.1)}$$

with the sign convention $(Y_k^q)^* = (-1)^q Y_k^{-q}$. It is to be noted that V is real which imposes the condition $a_{kq} = (-1)^q a_{k-q}^*$. The quantities a_{kq}'s are known as crystal field coefficients.

The number of terms in the potential expression may be considerably limited following the three rules.

i) If there is a centre of inversion there will be no harmonics of odd k in the potential expression.

ii) Odd harmonics may also be omitted for non-centro-symmetric ion site provided we confine ourselves within a given configuration. To show this we consider the state of an ion written in terms of product of one-electron wave functions $\Phi_i(n^a \ell^a m_\ell^a m_s^a)$ (i refers to the i-th electron). The matrix element of crystal field interaction between two such states reduces to sum of one electron integrals $\int \Phi_i^*(n\ell m_\ell^a m_s^a)\, V \Phi_i(n\ell m_\ell^b m_s^b)\, d\tau$.

The parity of two Φ functions are the same for a given configuration. When V is odd the integral becomes an odd function and therefore the integral vanishes. However, such odd order potentials may admix different configurations and will have to be considered in the case of configuration mixing.

iii) For the integral $\int \Phi_i^*(n\ell m_\ell^a m_s^a) V \Phi_i(n\ell m_\ell^b m_s^b) d\tau$ to be non-vanishing it has to fulfil the triangular condition (the triangle formed by the values representing order of the three spherical harmonics i.e. ℓ for both wave functions and k for the potential) which gives $k \leqslant 2\ell$. Hence, all terms in (II.9.1) having $k > 2\ell$ may be omitted.

It may be shown that when we confine ourselves to a single configuration ℓ^n the matrix element of the k-th harmonics of the crystal field interaction between two states of the ion contains the reduced matrix element $\langle \ell \| C^{(k)} \| \ell \rangle$ as a factor where $C^{(k)}$ is an irreducible tensor operator corresponding to the k-th harmonic of the potential. The reduced matrix element is non-vanishing only when,

(a) $\ell+k+\ell$ is even i.e. k is even.

(b) ℓ, k, ℓ satisfies the triangular condition i.e. $k \leqslant 2\ell$.

The above two rules thus immediately follow .

Again the number of terms will also be reduced by the symmetry of the surroundings of the ion and that the terms occurring depend very much on the co-ordinate axes chosen and are in their simplest form when the axes coincide with the

symmetry axes of the point group. The present thesis deals with 4f electrons of rare-earth group so we shall retain the terms upto k = 6 .

If we take a common example, the D_{3h} symmetry, which means there is a threefold axis, a twofold axis perpendicular to it, and a reflection plane perpendicular to the threefold axis which makes a_{66} real (a crystal symmetry that is found approximately in the RE ethyl sulphates), the development can be written

$$V_{D_{3h}} = a_{20}r^2Y_2^o + a_{40}r^4Y_4^o + a_{60}r^6Y_6^o + a_{66}r^6(Y_6^6 + Y_6^{-6}) \quad \text{(II.9.2)}$$

where for convenience the summation over i, the number of 4f electrons has been dropped out.

This can be again rewritten as,

$$V_{D_{3h}} = a_{20}U_o^{(2)} + a_{40}U_o^{(4)} + a_{60}U_o^{(6)} + a_{66}(U_6^{(6)} + U_{-6}^{(6)}) \quad \text{(II.9.3)}$$

where $U_q^{(k)} = r^kY_k^q$, which is called as the tensor operator of rank k and having q-th component. The quantities a_{kq}'s are called the crystal field coefficients. The crystal field interaction of an ion having n electrons in the unfilled shell is

$$H_c = -\sum |e| V \quad \text{(II.9.4)}$$

$$= -\sum_{k,q} |e| a_{kq}r^kY_k^q = -\sum_{k,q} |e| a_{kq}U_q^{(k)} \quad \text{(II.9.5)}$$

where the summation in (II.9.4) and first summation in (II.9.5) extend over all the n electrons. The quantities $-|e| a_{kq}\langle r^k\rangle_{n\ell}$

which occur in crystal field calculations are known as crystal field parameters where $_{n\ell}\langle r^k\rangle_{n\ell}$ is the radial integral given by $_{n\ell}\langle r^k\rangle_{n\ell} = \int \Psi^*_{n\ell}\Psi_{n\ell} r^k r^2 dr$ and $\Psi_{n\ell}$ is the radial part of the wave function of the electron corresponding to the $n\ell$ subshell.

II.10. MATRIX ELEMENTS OF CRYSTAL FIELD INTERACTION IN THE CASE OF RARE-EARTH IONS

The fundamental problem is to calculate the matrix elements of the form

$$(f^n \alpha U v S L J M_J | U^{(k)}_q | f^n \alpha' U' v' S' L' J' M'_J)$$

Since $U^{(k)}_q$ does not contain any spin variables so we have $S = S'$. By applying Wigner Eckart[81,82] theorem we have

$$(f^n \alpha U v S L J M_J | U^{(k)}_q | f^n \alpha' U' v' S L' J' M'_J)$$

$$= (-1)^{J-M_J} \begin{pmatrix} J & k & J' \\ -M_J & q & M'_J \end{pmatrix} (f^n \alpha U v S L J | U^{(k)} | f^n \alpha' U' v' S L' J') \quad \text{(II.10.1)}$$

Again

$$(f^n \alpha U v S L J | U^{(k)} | f^n \alpha' U' v' S L' J')$$

$$= (-1)^{S+k+J+L'} \begin{Bmatrix} J & J' & S \\ L & L' & k \end{Bmatrix} \left[(2J+1)(2J'+1)\right]^{1/2}$$

$$(f^n \alpha U v S L \,||U^{(k)}|| f^n \alpha' U' v' S L') \quad \text{(II.10.2)}$$

Therefore (II.10.1) becomes

$$(-1)^{2J+S+k+L'-M_J} \left[(2J+1)(2J'+1)\right]^{1/2} \begin{pmatrix} J & k & J' \\ -M_J & q & M'_J \end{pmatrix} \begin{Bmatrix} J & J' & S \\ L & L' & k \end{Bmatrix}$$

$$(f^n \alpha U v S L \,||U^{(k)}|| f^n \alpha' U' v' S L') \quad \text{(II.10.3)}$$

where,

$$(f^n \alpha U v S L \,||U^{(k)}|| \, f^n \alpha' U' v' S L')$$

is called the reduced matrix element which is tabulated by Nielson and Koster[77] . The same thing can be further reduced by using the fractional parentage as follows :

$$(f^n \alpha U v S L \,||U^{(k)}|| \, f^n \alpha' U' v' S L')$$

$$= n \sum_{\bar{\Psi}} (\Psi \{| \bar{\Psi}) (\Psi' \{| \bar{\Psi}) (-1)^{L+k+3-L'+L+L'+3+3}$$

$$\begin{Bmatrix} L & L & \bar{L} \\ 3 & 3 & k \end{Bmatrix} \left[(2L+1)(2L'+1)\right]^{1/2} (f \,||U^{(k)}|| \, f)$$

$$= n \sum_{\bar{\Psi}} (\Psi \{| \bar{\Psi}) (\Psi' \{| \bar{\Psi}) (-1)^{\bar{L}+k+3+L} \begin{Bmatrix} L & L' & \bar{L} \\ 3 & 3 & k \end{Bmatrix} \left[(2L+1)(2L'+1)\right]^{1/2}$$

$$(f \,||U^{(k)}|| \, f) \qquad \text{(II.10.4)}$$

Therefore

$$(f^n \alpha U v S L J M_J \,|U_q^{(k)}\,| f^n \alpha' U' v' S L' J' M_J')$$

$$= n \sum_{\bar{\Psi}} (-1)^{2J+S+2k+L'-M_J+\bar{L}+3+L} (\Psi \{| \bar{\Psi}) (\Psi' \{| \bar{\Psi}) \begin{pmatrix} J & k & J' \\ -M_J & q & M_J' \end{pmatrix}$$

$$\begin{Bmatrix} L & L' & \bar{L} \\ 3 & 3 & k \end{Bmatrix} \begin{Bmatrix} J & J' & S \\ L & L' & k \end{Bmatrix} \left[(2J+1)(2J'+1)(2L+1)(2L'+1)\right]^{1/2} (f \,||U^{(k)}|| \, f)$$

(II.10.5)

$$= n \sum_{\bar{\Psi}} (-1)^{2J+S+L'+L-M_J+3+\bar{L}} (\Psi \{| \bar{\Psi}) (\Psi' \{| \bar{\Psi}) \begin{pmatrix} J & k & J' \\ -M_J & q & M_J' \end{pmatrix}$$

$$\begin{Bmatrix} L & L' & \bar{L} \\ 3 & 3 & k \end{Bmatrix} \begin{Bmatrix} J & J' & S \\ L & L' & k \end{Bmatrix} \left[(2J+1)(2J'+1)(2L+1)(2L'+1)\right]^{1/2} (f \,||U^{(k)}|| \, f)$$

(II.10.6)

where $(\Psi \{| \bar{\Psi})$ are the coefficient of fractional parentages (c. f. p)

and

$$(f \| U^{(k)} \| f) = \left[\frac{2k+1}{4\pi}\right]^{1/2} {}_{4f}\langle r^k \rangle_{4f} \; (f \| C^k \| f)$$

$$= \left[\frac{2k+1}{4\pi}\right]^{1/2} {}_{4f}\langle r^k \rangle_{4f} \; (-1)^3 \left[(2\cdot 3+1)(2\cdot 3+1)\right]^{1/2} \begin{pmatrix} 3 & k & 3 \\ 0 & 0 & 0 \end{pmatrix}$$

$$= -7 \left[\frac{2k+1}{4\pi}\right]^{1/2} \begin{pmatrix} 3 & k & 3 \\ 0 & 0 & 0 \end{pmatrix} {}_{4f}\langle r^k \rangle_{4f} \qquad \text{(II.10.7)}$$

The quantities like $-|e| a_{kq} {}_{4f}\langle r^k \rangle_{4f}$ have been treated as crystal field parameters and a simple symbol A_{kq} has been used for $-|e| a_{kq} {}_{4f}\langle r^k \rangle_{4f}$.

The similar type of calculation can be done by using operator equivalent method which has been discussed by Stevens[83]. When Steven's operator equivalent method is used the CF potential is expressed in cartesian form and the CF parameters are obtained in Steven's form and they are denoted by B_k^q's instead of A_{kq}'s. In our subsequent calculation we shall use A_{kq}'s which are the CF parameters in tensor operator form. B_k^q's are related with A_{kq}'s by simple constant factors given below

$$A_{20} = 4\sqrt{\frac{\pi}{5}}\, B_2^0 \; ; \qquad A_{40} = \frac{16}{3}\sqrt{\pi}\, B_4^0 \; ; \qquad A_{60} = 32\sqrt{\frac{\pi}{13}}\, B_6^0$$

$$A_{66} = 32\sqrt{\frac{\pi}{3003}}\, B_6^6 \; ; \quad A_{63} = 16\sqrt{\frac{\pi}{1365}}\, B_6^3 \; ; \quad A_{43} = \frac{4}{3}\sqrt{\frac{\pi}{35}}\, B_4^3$$

Since the operator equivalent technique was not used in the subsequent CF calculation, so the details of that is not discussed here.

II.11. CALCULATION OF MAGNETIC SUSCEPTIBILITY

A free paramagnetic ion in the absence of an external magnetic field, will in general have a number of degenerate and non-degenerate states. These states are classified according to their energy values into different groups labelled by the index m ; degenerate states having the same energy form a group, each non-degenerate state is a group by itself. Suppose a correct zeroth order state $\Psi_{m\ell,i}$ assumes an energy $W_{m\ell,i}$ in the magnetic field $\mathcal{H}$ which is applied in the direction i ($i \equiv x, y, z$). The additional suffix ℓ is used to specify a particular component state when it belongs to a degenerate group i.e. $\Psi_{m\ell,i}$ is the correct zeroth order ℓ-th state belonging to the m-th group, the correct zeroth order states of a degenerate group being decided by the fact that the Zeeman perturbation $\beta\mathcal{H}(L_i+2S_i)$ is diagonal in a basis of these states. The general expression for the ionic paramagnetic susceptibility of a system of free ions[1] is given by

$$K_i = \lim_{\mathcal{H}\to 0} -\frac{N}{\mathcal{H}} \frac{\sum_{m\ell} \frac{\partial W_{m\ell,i}}{\partial \mathcal{H}} \exp\left(-\frac{W_{m\ell,i}}{kT}\right)}{\sum_{m\ell} \exp\left(-\frac{W_{m\ell,i}}{kT}\right)} \qquad \text{(II.11.1)}$$

$$= \lim_{\mathcal{H}\to 0} \frac{NkT}{\mathcal{H}} \frac{\partial}{\partial \mathcal{H}} \ln Z_i \qquad \text{(II.11.2)}$$

where

$$Z_i = \sum \exp\left(-\frac{W_{m\ell,i}}{kT}\right) \qquad \text{(II.11.3)}$$

where the summation extends over all indices m, ℓ corresponding to all states.

Van Vleck has also given a more convenient expression e.g.

$$K_i = \frac{\sum_m \left[\frac{\left(W^{(1)}_{m\ell,i}\right)^2}{kT} - 2W^{(2)}_{m\ell,i} \right] \exp\left(-\frac{W^{(0)}_m}{kT}\right)}{\sum_{m\ell} \exp\left(-\frac{W^{(0)}_m}{kT}\right)} \qquad \text{(II.11.4)}$$

where $W^{(0)}_m$, $W^{(1)}_{m\ell,i}$ and $W^{(2)}_{m\ell,i}$ are defined by the expansion of energy $W_{m\ell,i}$ in a power series in the applied field $\mathcal{H}$ as follows :

$$W_{m\ell,i} = W^{(0)}_m + W^{(1)}_{m\ell,i}\mathcal{H} + W^{(2)}_{m\ell,i}\mathcal{H}^2 + \cdots \qquad \text{(II.11.5)}$$

Thus $W^{(0)}_m$ is the unperturbed energy in the zero magnetic field (the indices ℓ and i are superfluous in the zeroth order energy and hence are omitted in $W^{(0)}_m$). $W^{(1)}_{m\ell,i}\mathcal{H}$ and $W^{(2)}_{m\ell,i}\mathcal{H}^2$ are the first and second order Zeeman perturbation when a magnetic field $\mathcal{H}$ is applied along the direction i . The quantities $W^{(1)}_{m\ell,i}$ and $W^{(2)}_{m\ell,i}$ are explicitly given as follows.

$$W^{(1)}_{m\ell,i} = \langle \Psi_{m\ell,i} | \beta(L_i + 2S_i) | \Psi_{m\ell,i} \rangle \qquad \text{(II.11.6)}$$

$$W^{(2)}_{m\ell,i} = -\sum_{np} \frac{\left| \langle \Psi_{m\ell,i} | \beta(L_i + 2S_i) | \Psi_{np,i} \rangle \right|^2}{W^{(0)}_n - W^{(0)}_m} \qquad \text{(II.11.7)}$$

The expression (II.11.4) can be obtained from (II.11.1) using the expansion (II.11.5) and assuming that (i) the Zeeman terms are very much smaller than kT so that exponentials when expanded can be approximated by neglecting higher terms in their

expansion and (ii) there is no permanent polarization in zero magnetic field i.e.

$$\sum_{m\ell} W^{(1)}_{m\ell,i} \exp\left(-\frac{W^{(0)}_{m\ell}}{kT}\right) = 0$$

The above derivation of susceptibility is quite general and holds good so far as any magnetic degeneracy is left over even in the process of molecules or solid state formations.

II.12. CALCULATION OF g-VALUES

Electron paramagnetic resonance spectrum corresponds to transition between the two components into which the lowest doublet (Φ_1 , Φ_1') splits when an external magnetic field is applied. We shall assume uniaxial symmetry of the ion so that e.p.r spectrum for the two cases, magnetic field parallel and perpendicular to the symmetry axis will be considered. Diagonalisation of the Zeeman perturbation $\beta\mathcal{H}(L_z + 2S_z)$ constructed in a basis of two component states Φ_1 and Φ_1' of the lowest doublet gives the energies of the two components into which the doublet (Φ_1 , Φ_1') splits when $\mathcal{H} \| Z$ and the energy separation ΔW^Z between the two components when $\mathcal{H} \| Z$ is given by

$$\Delta W^Z = \beta\mathcal{H} \left| \langle \Phi_1 | L_z + 2S_z | \Phi_1 \rangle - \langle \Phi_1' | L_z + 2S_z | \Phi_1' \rangle \right|$$

Thus

$$g_{\|} = g_z = \frac{\Delta W^Z}{\beta\mathcal{H}} \left| \langle \Phi_1 | L_z + 2S_z | \Phi_1 \rangle - \langle \Phi_1' | L_z + 2S_z | \Phi_1' \rangle \right| \qquad \text{(II.12.1)}$$

Similarly diagonalisation of the matrix of Zeeman perturbation $\beta\mathcal{H}(L_\alpha + 2S_\alpha)$ constructed in a basis of the states Φ_1 and $\Phi_{1'}$ when $\mathcal{H} \| \alpha$ (α = x or y) gives the value of the splitting as

$$\Delta W^\alpha = 2\beta\mathcal{H}\left|\left\langle \Phi_1 \left| L_\alpha + 2S_\alpha \right| \Phi_{1'} \right\rangle\right|$$

where α = x or y and

$$g_\perp = g_x = g_y = \frac{\Delta W^\alpha}{\beta\mathcal{H}}$$

$$= 2\left|\left\langle \Phi_1 \left| L_x + 2S_x \right| \Phi_{1'} \right\rangle\right| = 2\left|\left\langle \Phi_1 \left| L_y + 2S_y \right| \Phi_{1'} \right\rangle\right| \qquad \text{(II.12.2)}$$

II.13. CALCULATION OF THE MATRIX ELEMENT OF THE TYPE $\left\langle SLJM \left| (L_i + 2S_i) \right| SL'JM' \right\rangle$

To calculate the matrix element of $\left\langle SLJM \left| (L_i + 2S_i) \right| SL'J'M' \right\rangle$ we have to express L_i and S_i in tensor operator form as follows:

For i = Z

L_Z and S_Z can be treated as $T_o^{(1)}$ tensor operator. For i = x, L_x or S_x can be written as,

$$\sqrt{\frac{1}{2}}(T_{-1}^{(1)} - T_1^{(1)})$$

And for i = y, L_y or S_y can be written as,

$$i\sqrt{\frac{1}{2}}\,(T_1^{(1)} + T_{-1}^{(1)})$$

And if the tensor operator form be applied here we shall obtain the following results :

$$\left\langle SLJM_J \left| L_Z \right| SLJM_J \right\rangle = M_J \frac{L(L+1)+J(J+1)-S(S+1)}{2J(J+1)}$$

$$\langle SLJM_J | S_Z | SLJM_J \rangle = M_J \frac{S(S+1)+J(J+1)-L(L+1)}{2J(J+1)}$$

$$\langle SLJM_J | L_Z | SLJ+1M_J \rangle = -\langle SLJM_J | S_Z | SLJ+1M_J \rangle$$

$$= -\left[\frac{(J+M_J+1)(J-M_J+1)(S+L+J+2)(S+L-J)(S-L+J+1)(-S+L+J+1)}{(2J+3)(2J+2)^2(2J+1)}\right]^{1/2}$$

$$\langle SLJM_J | L_x | SLJM_J+1 \rangle = \frac{\left[(J-M_J)(J+M_J+1)\right]^{1/2}}{4J(J+1)} \left[J(J+1)-S(S+1)+L(L+1)\right]$$

$$\langle SLJM_J | S_x | SLJM_J+1 \rangle = \frac{\left[(J-M_J)(J+M_J+1)\right]^{1/2}}{4J(J+1)} \left[J(J+1)+S(S+1)-L(L+1)\right]$$

$$\langle SLJM_J | L_x | SLJM_J-1 \rangle = \frac{\left[(J+M_J)(J-M_J+1)\right]^{1/2}}{4J(J+1)} \left[J(J+1)+L(L+1)-S(S+1)\right]$$

$$\langle SLJM_J | S_x | SLJM_J-1 \rangle = \frac{\left[(J+M_J)(J-M_J+1)\right]^{1/2}}{4J(J+1)} \left[J(J+1)+S(S+1)-L(L+1)\right]$$

$$\langle SLJM_J | L_x | SLJ+1M_J+1 \rangle = -\langle SLJM_J | S_x | SLJ+1M_J+1 \rangle$$

$$= \frac{1}{4(J+1)}\left[\frac{(J+M_J+1)(J+M_J+2)(J+L+S+2)(-J+L+S)(J-L+S+1)(J+L-S+1)}{(2J+1)(2J+3)}\right]^{1/2}$$

$$\langle SLJM_J | L_x | SLJ+1M_J-1 \rangle = -\langle SLJM_J | S_x | SLJ+1M_J-1 \rangle$$

$$= -\frac{1}{4(J+1)}\left[\frac{(J-M_J+1)(J-M_J+2)(J+L+S+2)(-J+L+S)(J-L+S+1)(J+L-S+1)}{(2J+1)(2J+3)}\right]^{1/2}$$

II.14. COVALENCY REDUCTION OF ORBITAL ANGULAR MOMENTUM

Since the magnetic properties and optical absorption are connected with the orbitals of the unfilled shell of the central metal atoms, such aspects of them as are determined by the behaviour of electrons close to the nucleus of the central

metal ion will be reduced if the orbitals overspill on the ligands. Particularly the orbital angular momentum and the spin-orbit coupling co-efficient will be effectively reduced by such covalency effect from their respective free ion values. Now the covalency effect in the case of rare-earth ion, although small has been felt necessary for the past few years. We also find during our calculations that unless a reduction of the orbital moment matrices presumably due to the covalency effect is assumed, it becomes impossible to achieve a good fit to the g-values and magnetic susceptibilities in some of the rare-earth complexes. The covalency effect implies that the electrons in the unfilled shell of the rare-earth ion do not move in pure f-orbitals, they move in modified orbitals, the so called molecular orbitals, in which the f-orbitals of the metal atom are admixed slightly with the orbitals of the ligand electrons as required by the symmetry of the complex. Denoting the molecular orbital corresponding to a pure f-orbital by f^{mol} we define the covalency reduction factor for the orbital angular momentum operator by the ratios:

$$\frac{\langle f_a^{mol} | \ell_i | f_b^{mol} \rangle}{\langle f_a | \ell_i | f_b \rangle} = k_i^{ab} \quad (i \equiv x, y, z) \qquad (II.14.1)$$

For rare-earth ions k_i^{ab} will be very near to but slightly less than unity. The matrix elements of L_i $(i \equiv x, y, z)$ that occur in the calculation of g-values and magnetic susceptibilities

are of the type

$$\langle SLJM|L_i|S'L'J'M'\rangle \qquad \text{(II.14.2)}$$

In (II.14.2) the states between which the matrix element of the resultant orbital angular momentum L_i is considered refer to the whole atom built up from the individual electron states. Now if the electrons are of pure f-type, the matrix element in (II.14.2) will be denoted by Q_i . If they are not of pure f-type its value will be modified from the value that one would obtain when the resultant atomic states are built up from pure f-electrons and will be denoted by Q_i^m . This modified value Q_i^m has to be used in place of Q_i . To find the relation between Q_i and Q_i^m one should express the states $|SLJM\rangle$ and $|S'L'J'M'\rangle$ in terms of determinantal product states and then replace the individual pure f-states of electrons by their corresponding molecular orbital states f^{mol} . We now make a simplifying approximation that k_i^{ab} is the same for all pairs of orbitals and further consider that the reduction factor partakes of the symmetry of the complex. In the case of uniaxial symmetry of the complex (e.g. D_{3h}) we will have only two covalency reduction factors $k_{\parallel}$ ($=k_z$) and $k_{\perp}$ ($=k_x$ or k_y). In the case of rare-earth ions these reduction factors are all very near to unity and the above approximation may be considered as quite reasonable. With the above approximation we shall have $Q_i^m = k_i Q_i$ ($i \equiv x, y, z$). In the case of uniaxial

symmetry when i refers to the z direction we shall denote k_i by $k_{||}$ and when i = x or y , k_i will be denoted by $k_{\perp}$. This means that in order to take the effect of covalency into account we have to replace the operator L_i by the effective operator $k_i L_i$ in the matrix element between two resultant atomic states. In the present thesis $k_{||}$ and $k_{\perp}$ will be treated as two additional parameters to be evaluated from experiment.

II.15. ELECTRIC DIPOLE TRANSITION MOMENTS

The crystal field of Ln^{3+} ion in either a crystalline or molecular environment, is pictured as arising from the electrostatic potential due to the net charges of the surrounding ligands[84] . This electrostatic potential then acts to split the Ln^{3+} free ion electronic energy levels in the familiar weak field approximation. But this idea is not general while calculating the crystal field splittings from parameters based solely on the net charges and spatial distribution of the ligands because the predicted splittings are often much smaller in magnitude than the observed level spacings.

We take a lanthanide ion surrounded by N ligands. We also consider that the ligands are non-interacting and partition the total system into two. The Ln^{3+} ion subsystem is designated by A and the ligand subsystem by B and an individual ligand will be denoted by L .

So the complete hamiltonian of our system can be written as follows :

$$H = H_A^o + H_B^o + H_{AB} \qquad \text{(II.15.1)}$$

where

$H_A^o = L_n^{3+}$ free ion hamiltonian .

$H_B^o = \sum_L h_L$

h_L = hamiltonian for the L-th ligand.

H_{AB} = A-B interaction hamiltonian.

The interaction hamiltonian may be expanded in metal ion-ligand pairwise potentials :

$$H_{AB} = \sum_L \sum_{\ell_A} \sum_{\ell_L} V_L(\ell_A \, , \, \ell_L) \qquad \text{(II.15.2)}$$

where $V_L(\ell_A, \ell_L)$ = electrostatic potential between the ℓ_A-th multipole of the lanthanide ion charge distribution and ℓ_L-th multipole of the charge distribution of the L-th ligand.

$V_L(\ell_A \, , \, \ell_L)$ may again be partitioned as follows :

$$H_{AB} = \sum_L \sum_{\ell_A} V_L(\ell_A, 0) + \sum_L \sum_{\ell_A} \sum_{\ell_L \geq 1} V_L(\ell_A, \ell_L) \qquad \text{(II.15.3)}$$

$$= \mathcal{V} + \mathcal{U} \qquad \text{(II.15.4)}$$

The operator $\mathcal{V}$ represents the electrostatic interactions between the metal ion multipoles and the ligand monopoles (net charges) and as such represents the standard point charge

crystal field. $\mathcal{U}$ is the interaction between the metal ion multipoles and the higher ($\ell_L \geqslant 1$) multipoles of the ligands. In the present thesis we take $\ell_L = 1$.

$$\mathcal{U} = \sum_L \sum_{\ell_A} V_L(\ell_A , 1)$$

Richardson termed $\mathcal{V}$ as the 'static-coupling' operator and $\mathcal{U}$ as the 'dynamic coupling operator' .

II.15(a). POINT CHARGE PART

Now let us try to find out the expression for the crystal field parameter for static coupling operator (which is actually called the point charge part). In absence of any external radiation the central metal ion and the ligand charges may be treated as point charges. i.e. the charge distribution of the central metal ion and the ligands are assumed to be centred to two points. This is the basic consideration of the point charge model. The theory disregards the metal-ligand electron exchange. In case of point charge model it is generally considered that a particular charge distribution of the ligands taken to be that of the ground state, perturbs all the electronic states of the metal-ion. On expansion of the potential provided by the point charges around the central metal ion we have the form of the potential as

$$\mathcal{V} = \sum_{\ell} \sum_{\ell_A} V_L(\ell_A , 0)$$

by expanding the CF potential the following form of the CF parameters will come as

$$A_{kq}(chg) = (-1)^q \, 7e \begin{pmatrix} 3 & k & 3 \\ 0 & 0 & 0 \end{pmatrix} \sum_L q_L \; R_L^{-(k+1)}$$

$$\left[\frac{4\pi}{2k+1}\right]^{1/2} Y_{\ell}^{-m}(\Theta_L \, , \, \Phi_L) \; {}_{4f}\langle r^k \rangle_{4f} \qquad \text{(II.15(a).1)}$$

where

$(R_L \, , \; \Theta_L \, , \, \Phi_L)$ = spherical polar co-ordinates of the ligand group L .

II.15(b). POLARIZABILITY CONTRIBUTION

From the dynamic contribution on the crystal field potential we have the crystal field parameters due to the polarizability contribution. An approximation to the CF potential is afforded by a multipole expansion of each of the charge distributions of metal ion and the ligand, centred upon their respective co-ordinate origins, and the truncation of each series is done after the leading term. The term retained for the ligand group charge distributions is up to the electric dipole. The allowed electric charge distributions of an $\ell \rightarrow \ell$ metal ion transition are the even multipole moments, 2^n-poles, with $n = 2, 4, \ldots 2\ell$, each having $(2n+1)$ components. In the ligand polarization model the electron exchange between the

ligands and the metal ions is also neglected as in the case of point charge model.

The polarizability contribution thus comes from the interaction of the dipole moment of the ligand with the quadrupole, hexadecapole etc. moment of the central metal ion. And this comes out as second order effect and should be included in the crystal field parameter. This contribution in the crystal field was extensively used by Mason[85] . Later Richardson and Faulkner[68] introduced this polarizability contribution in the CF level calculations.

The polarizability contribution to the crystal field parameter is given by[68]

$$A_{kq}(pol) = 14e(k+1)(-1)^q \begin{pmatrix} 3 & k & 3 \\ 0 & 0 & 0 \end{pmatrix} q_A \sum_L \bar{\alpha}_L R_L^{-(k+4)} \left[\frac{4\pi}{2k+1}\right]^{1/2} Y_\ell^{-m}(\Theta_L, \Phi_L) \langle r^k \rangle_{4f} \qquad \text{(II.15(b).1)}$$

where

q_A = net charge on Ln^{3+} = 3,

$\bar{\alpha}_L$ = 'mean' isotropic polarizability of ligand L .

This is a constant for a particular ligand group. Saxe et al.[86] gave the values of $\bar{\alpha}_L$ in a tabular form for different ligand groups.

So the resultant crystal field parameter is obtained from both the charge and the polarizability contribution :

$$A_{kq} = A_{kq}(chg) + A_{kq}(pol)$$

II.15(c). STATIC-COUPLING MECHANISM IN THE ELECTRIC DIPOLE TRANSITION MOMENT

The static-coupling contribution to the electric dipole transition moment is defined as that arising from $\mathcal{V}$ part of H_{AB}. This operator operates only on metal ion (A) wave functions and it connects metal ion states of opposite parity. That means the matrix element (or the electric dipole moment) of this operator only exists between one state in $4f^n$ configuration and the other in $4f^{n-1}n''d$ or $4f^{n-1}n''g$. Following Judd-Ofelt[52-53] mechanism Richardson and Faulkner[68] obtained the static contribution to the electric dipole transition moment from a state $|A_o\rangle$ to an excited state $|A_a\rangle$ as follows :

$P_{oa}^{(S)}$ = Static contribution of the electric dipole moment.

$$= e^2 \sum_q \sum_{\ell_A(odd)} \sum_{m_A} \sum_L q_L \frac{(-1)^{\ell_A+m_A}}{R_L^{\ell_A+m_A}} \sum_\lambda (-1)^{m_A+q+J-M_J}$$

$$(2\lambda+1) \begin{pmatrix} 1 & \lambda & \ell_A \\ q & -m_A-q & m_A \end{pmatrix} \begin{pmatrix} J & \lambda & J' \\ -M_J & m_A+q & M_J' \end{pmatrix} (-1)^{S+L'+J+\lambda}$$

$$\left[(2J+1)(2J'+1)\right]^{1/2} \begin{Bmatrix} L & \lambda & L' \\ J' & S & J \end{Bmatrix} (SL \| U^{(\lambda)} \| SL') \; H(\ell_A, \lambda) \qquad \text{(II.15(c).1)}$$

where

$$\boxplus(\ell_A,\lambda) = 2\sum_{n''\ell''}(2\ell+1)(2\ell''+1)(-1)^{\ell+\ell''}\begin{pmatrix}1 & \lambda & \ell_A\\ \ell & \ell'' & \ell\end{pmatrix}$$

$$\begin{pmatrix}\ell & 1 & \ell''\\ 0 & 0 & 0\end{pmatrix}\begin{pmatrix}\ell'' & \ell_A & \ell\\ 0 & 0 & 0\end{pmatrix}(4f\|r\|n''\ell'')(n''\ell''\|r^{\ell_A}\|4f)/\Delta(n''\ell'')$$

The summation $\sum_{n''\ell''}$ is taken over n''d and n''g and for f system $\ell = 3$. The calculation of $\boxplus(\ell_A, \lambda)$ has been discussed by Krupke[87] . $\Delta(n''\ell'')$ is defined as an 'average energy' parameter. $(SL\|U^{(\lambda)}\|SL')$ is called the reduced matrix element which can be obtained from, Nielson and Koster's table.

II.15(d). DYNAMIC COUPLING MECHANISM IN THE ELECTRIC DIPOLE TRANSITION MOMENT

In the Judd-Ofelt[52,53] theory the ligands surrounding the lanthanide ion are considered only in as much as their ground state field produces the perturbation required to mix excited configuration into the 4f configurations. But the ligand wave functions are also perturbed by the metal ion. Now we try to explain what is meant by Dynamic Coupling mechanism. Let us call the metal ground and excited functions as $|M_o\rangle$ and $|M_a\rangle$ and those of the ligand as $|L_o\rangle$ and $|L_b\rangle$. The combined wave function of the total system will be simply the product functions i.e. $|M_oL_o\rangle$.

The first order perturbed ground and excited states $|A\rangle$ and $|B\rangle$ as

$$|A\rangle = |M_o L_o\rangle - \sum_b \frac{\langle M_a L_b | \underset{\sim}{V} | M_o L_o \rangle}{E_a + E_b} |M_a L_b\rangle$$

$$|B\rangle = |M_a L_o\rangle - \sum_b \frac{\langle M_a L_b | \underset{\sim}{V} | M_a L_o \rangle}{E_a - E_b} |M_o L_b\rangle$$

where

$E_a = |M_a\rangle \leftarrow |M_o\rangle$ transitional energy.

$E_b = |L_b\rangle \leftarrow |L_o\rangle$ transitional energy.

The summation on the right hand side of $|A\rangle$ and $|B\rangle$ runs over all transitions of the ligand which are electric dipole allowed.

$\underset{\sim}{V}$ represents the coulombic interaction of the charge distributions on metal and ligand.

The $f \leftrightarrow f$ transition thus acquires a first order electric dipole transition moment which is given by :

$$e\langle A | D_q^{(1)} | B\rangle = e \sum_b 2E_b (E_b^2 - E_a^2)^{-1} \langle M_o M_a | \underset{\sim}{V} | L_o L_b \rangle \langle L_o | D_q^{(1)} | L_b \rangle$$

$D_q^{(1)}$ = induced dipole operator. The electric dipole moments $\langle L_o | D_q^{(1)} | L_b \rangle$ located on the ligand are correlated coulombically with the charge distribution at the lanthanide ion caused by the $f \leftrightarrow f$ transition. The correlation is given by the matrix element $\langle M_o M_a | \underset{\sim}{V} | L_o L_b \rangle$.

Now applying the Judd-Ofelt mechanism and by expressing the wave function in $|4f^{\alpha}[SL]\, JM\rangle$ form we ultimately have the contribution of the electric dipole moment due to dynamic coupling as[68]

$P_{oa}^{(d)}$ = Dynamic contribution of the electric dipole moment from a state $|A_o\rangle$ to an excited state $|A_a\rangle$

$$= e\langle A_o | D_q^{(1)} | A_a \rangle$$

$$= \sum_q \sum_{\ell_A} \sum_{m_A} \sum_L (-1)^q \bar{\alpha}_L(qq) T^{(\ell_A,1)}_{m_A-q}(L) Z^{(d)}_{oa}(\ell_A, m_A) \qquad \text{(II.15(d).1)}$$

where

$$T^{(\ell_A,1)}_{m_A,-q}(L) = \frac{(-1)^{1+m_A+q}}{R_L^{\ell_A+2}} \left[\frac{(\ell_A+1+m_A-q)!(\ell_A+1-m_A+q)!}{(\ell_A+m_A)!(\ell_A-m_A)!(1-q)!(1+q)!}\right]^{1/2}$$

$$C^{\ell_A+1}_{-m_A+q}(\Theta_L, \Phi_L)$$

$$Z^{(d)}_{oa}(\ell_A, m_A) = (A_o | D^{\ell_A}_{m_A} | A_a) = -e \sum_\alpha r_\alpha^{\ell_A} \langle A_o | C^{\ell_A}_{m_A}(\Theta_\alpha, \Phi_\alpha) | A_a \rangle$$

$\bar{\alpha}_L(qq)$ = q-th diagonal component of the polarizability tensor for the L-th ligand group.

$$= \sum_b \frac{2E_b e^2 \langle L_o | D_q^{(1)} | L_b \rangle^2}{E_b^2 - E_a^2}$$

and

$$C^{\ell_A}_{m_A}(\Theta_\alpha, \Phi_\alpha) = \left[\frac{4\pi}{2\ell_A+1}\right]^{1/2} Y^{m_A}_{\ell_A}(\Theta_\alpha, \Phi_\alpha)$$

since the transition charge distribution, arises entirely from within the $4f^n$ configuration of the metal ion, the only values of ℓ_A leading to nonvanishing values of $Z^{(d)}_{oa}$ are ℓ_A = 2, 4 and 6 . Other terms are already explained before. The computational model is followed from the procedures of Mason, Peacock and Stewart[88], Richardson and Faulkner[68] .

II.16. MAGNETIC DIPOLE TRANSITION MOMENT

The theory of magnetic dipole transitions is well known[53], and therefore we are interested only in the application to the crystal field problem. Generally the magnetic dipole transitions are 10^{-6} times less intense than the electric dipole transition. But in cases of parity-forbidden (i.e. $g \rightarrow g$, $u \rightarrow u$) transitions in complexes, having inversion symmetry, the electric dipole moment will vanish owing to symmetry reasons but magnetic dipole moment may play a significant role in making the purely electronic O-O band allowable.

The magnetic dipole moment operator is given by

$$M = -\frac{e}{2mc} \sum_i (\underset{\sim}{L}_i + 2\underset{\sim}{S}_i) \qquad \text{(II.16.1)}$$

Expressing $\underset{\sim}{L}_i$ and $\underset{\sim}{S}_i$ in tensor operator and utilizing the intermediate coupling notation for the metal ion ($f \rightarrow f$) states, the magnetic dipole transition moment for the transition

$$|\Psi\,[SL]\,JM\rangle \rightarrow |\Psi'\,[S'L']\,J'M'\rangle$$

is given by

$$M_{\Psi\Psi'} = \langle \Psi\,[SL]\,JM | \underset{\sim}{m}_q | \Psi'\,[S'L']\,J'M' \rangle$$

$$= \delta(\Psi,\Psi')\,\delta(S,S')\,\delta(L,L')\,(-1)^{J-M} \begin{pmatrix} J & 1 & J' \\ -M & q & M' \end{pmatrix}$$

$$\langle [SL]\,J \,\|\underset{\sim}{m}\|\, [SL]\,J' \rangle \qquad \text{(II.16.2)}$$

where $\underset{\sim}{m}_q$ is the q-th (spherical) component of the magnetic dipole moment operator. The reduced matrix elements of $\underset{\sim}{m}$ are given by

$$\left\langle [SL]J \,\|\underset{\sim}{m}\|\, [SL]J \right\rangle = \frac{1}{2}\,\mu_\beta \left[\frac{(2J+1)}{J(J+1)}\right]^{1/2}$$

$$\left\{(g_s-1)\left[S(S+1)-L(L+1)\right]+(g_s+1)J(J+1)\right\} \qquad \text{(II.16.3)}$$

$$\left\langle [SL]J \,\|\underset{\sim}{m}\|\, [SL]J+1 \right\rangle = \frac{1}{2}\,\mu_\beta(g_s-1)\left\{\left[(S+L+1)^2-(J+1)^2\right]\right.$$

$$\left.\left[(J+1)^2-(L-S)^2\right](J+1)^{-1}\right\}^{1/2} \qquad \text{(II.16.4)}$$

and

$$\left\langle [SL]J \,\|\underset{\sim}{m}\|\, [SL]J-1 \right\rangle = \frac{1}{2}\,\mu_\beta(g_s-1)\left\{\left[(S+L+1)^2-J^2\right]\right.$$

$$\left.\left[J^2-(L-S)^2\right](J)^{-1}\right\}^{1/2} \qquad \text{(II.16.5)}$$

In equations (II.16.3) - (II.16.5)

$$\mu_B = -\frac{e\hbar}{2mc}$$

g_s = gyromagnetic ratio of the electron.

To compute the magnetic dipole transition moment for a transition between crystal field levels, the spherical basis results of equation (II.16.2) can be converted into the crystal field basis using appropriate crystal field wave functions. It is important to emphasize, however, that a simple symmetry transformation of the spherical into the crystal field basis is inadequate in this case. In particular for $J \rightarrow J\pm 2$ transitions it is the inter-term crystal field mixings that

contributes to the magnetic dipole intensity. It is essential then, that crystal field induced J-mixing be included in the magnetic-dipole moment calculations.

II.17. CALCULATION OF ROTATIONAL STRENGTH

The electric and magnetic field vector of a right/left circularly polarised light wave along the +Z direction is given by

$$E_x \cos\omega t \mp E_y \sin\omega t = \frac{1}{2}(E_x + iE_y)e^{-i\omega t} + \frac{1}{2}(E_x - iE_y)e^{i\omega t}$$

$$H_x \sin\omega t \mp H_y \cos\omega t = \frac{1}{2}(H_y + iH_x)e^{-i\omega t} + \frac{1}{2}(H_y - iH_x)e^{i\omega t}$$

When we are considering the case of an absorption, the term containing $e^{-i\omega t}$ will only be important for bringing about transition (Rotating wave approximation). For circularly polarized light $E_x = E_y = E$ (say) and $H_x = H_y = \mathcal{H}$ (say).
So we can write

$$E(\cos\omega t \pm \sin\omega t) \longrightarrow \frac{1}{2} E(1 \pm i)e^{-i\omega t} \qquad \text{(II.17.1)}$$

$$\mathcal{H}(\sin\omega t \pm \cos\omega t) \longrightarrow \frac{1}{2} \mathcal{H}(1 \pm i)e^{-i\omega t} \qquad \text{(II.17.2)}$$

neglecting the term containing $e^{i\omega t}$ for the problem under discussion. The time average of (II.17.1) and (II.17.2) gives $E/2$ and $\mathcal{H}/2$. Now the Hamiltonian of interaction between the light wave and molecule is given by

$$\underset{\sim}{E}\cdot e\underset{\sim}{r} \mp \underset{\sim}{H}\cdot\underset{\sim}{\mu}$$

$$= e\frac{E}{2}(\underset{\sim}{x} \pm i\underset{\sim}{y}) + \frac{e}{2mc}\frac{\hbar}{2}(\underset{\sim}{L}_y \pm i\underset{\sim}{L}_x)$$

$$= (e\frac{E}{2}\underset{\sim}{x} + \frac{e}{2mc}\frac{\hbar}{2}\underset{\sim}{L}_y) \pm i(e\frac{E}{2}\underset{\sim}{y} + \frac{e}{2mc}\frac{\hbar}{2}\underset{\sim}{L}_x)$$

Let

$$\hat{\alpha} = eE\underset{\sim}{x} + \frac{e}{2mc}\hbar\,\underset{\sim}{L}_y$$

$$\hat{\beta} = eE\,\underset{\sim}{y} + \frac{e}{2mc}\hbar\,\underset{\sim}{L}_x$$

$\therefore$ H_{int} = interaction hamiltonian $= \frac{1}{2}\hat{\alpha} \pm \frac{1}{2}i\hat{\beta} = \hat{\alpha}' \pm i\hat{\beta}'$.

The probability of absorption of right and left circularly polarised light corresponding to transition between non-degenerate level $a \rightarrow b$ is given by the well-known expression

$$P_R = \frac{2\pi}{\hbar}\langle a|\hat{\alpha}' + i\hat{\beta}'|b\rangle\langle a|\hat{\alpha}' + i\hat{\beta}'|b\rangle^* \delta_{a,b+\omega}$$

$$P_L = \frac{2\pi}{\hbar}\langle a|\hat{\alpha}' - i\hat{\beta}'|b\rangle\langle a|\hat{\alpha}' - i\hat{\beta}'|b\rangle^* \delta_{a,b+\omega}$$

The circular dichroism is the difference of absorption of right and left circularly polarised light. Therefore the difference in absorption

$$P_R - P_L = \frac{2\pi}{\hbar}\Big[\langle a|\hat{\alpha}' + i\hat{\beta}'|b\rangle\langle a|\hat{\alpha}' + i\hat{\beta}'|b\rangle^* - \langle a|\hat{\alpha}' - i\hat{\beta}'|b\rangle\langle a|\hat{\alpha}' - i\hat{\beta}'|b\rangle^*\Big]\delta_{a,b+\omega}$$

where

$$\langle a|\hat{\alpha}' + i\hat{\beta}'|b\rangle\langle a|\hat{\alpha}' + i\hat{\beta}'|b\rangle^* - \langle a|\hat{\alpha}' - i\hat{\beta}'|b\rangle\langle a|\hat{\alpha}' - i\hat{\beta}'|b\rangle^*$$

$$= 2\Big[-i\langle a|\hat{\alpha}'|b\rangle\langle a|\hat{\beta}'|b\rangle^* + i\langle a|\hat{\beta}'|b\rangle\langle a|\hat{\alpha}'|b\rangle^*\Big]$$

$$= -2i\langle a|\hat{\alpha}'|b\rangle\langle a|\hat{\beta}'|b\rangle^{*} + 2i\langle a|\hat{\beta}'|b\rangle\langle a|\hat{\alpha}'|b\rangle^{*}$$

$$= -2i\left[\langle a|\hat{\alpha}'|b\rangle\langle a|\hat{\beta}'|b\rangle^{*} - \left\{\langle a|\hat{\alpha}'|b\rangle\langle a|\hat{\beta}'|b\rangle^{*}\right\}^{*}\right]$$

$$= -2 \times 2 \times i \times i \times \text{Imaginary part of } \langle a|\hat{\alpha}'|b\rangle\langle a|\hat{\beta}'|b\rangle^{*}$$

$$= 4 \times \text{Imaginary part of } \left[\langle a|\hat{\alpha}'|b\rangle\langle a|\hat{\beta}'|b\rangle^{*}\right]$$

$$= 4\times\tfrac{1}{2}\times\tfrac{1}{2}\times \text{Imaginary part of}\left[\langle a|\hat{\alpha}|b\rangle\langle a|\beta|b\rangle^{*}\right]$$

$$= \text{Im}\,\langle a|\hat{\alpha}|b\rangle\langle b|\hat{\beta}|a\rangle$$

$$= \text{Im}\,\langle a|eE\,\underset{\sim}{x} + \frac{e}{2mc}\mathcal{H}\,\underset{\sim}{L}_y|b\rangle\langle b|e\,E\,\underset{\sim}{y} + \frac{e}{2mc}\mathcal{H}\,\underset{\sim}{L}_x|a\rangle$$

$$= \text{Im}\left[\left\{eE\langle a|\underset{\sim}{x}|b\rangle + \frac{e\mathcal{H}}{2mc}\langle a|\underset{\sim}{L}_y|b\rangle\right\}\left\{eE\langle b|\underset{\sim}{y}|a\rangle + \frac{e\mathcal{H}}{2mc}\langle b|\underset{\sim}{L}_x|a\rangle\right\}\right]$$

$$= \text{Im}\Big[e^2E^2\langle a|\underset{\sim}{x}|b\rangle\langle b|\underset{\sim}{y}|a\rangle + \frac{e^2E\mathcal{H}}{2mc}\langle a|\underset{\sim}{x}|b\rangle\langle b|\underset{\sim}{L}_x|a\rangle$$

$$+ \frac{e^2\mathcal{H}E}{2mc}\langle a|\underset{\sim}{L}_y|b\rangle\langle b|\underset{\sim}{y}|a\rangle + \frac{e^2\mathcal{H}^2}{4m^2c^2}\langle a|\underset{\sim}{L}_y|b\rangle\langle b|\underset{\sim}{L}_x|a\rangle$$

In the above expression $e^2E^2\langle a|\underset{\sim}{x}|b\rangle\langle b|\underset{\sim}{y}|a\rangle$ and $\frac{e^2\mathcal{H}^2}{4m^2c^2}\langle a|\underset{\sim}{L}_y|b\rangle\langle b|\underset{\sim}{L}_y|a\rangle$ are real so we can omit these. So the above expression becomes

$$= \text{Im}\,\frac{e^2E\mathcal{H}}{2mc}\left[\langle a|\underset{\sim}{x}|b\rangle\langle b|\underset{\sim}{L}_x|a\rangle + \langle a|\underset{\sim}{L}_y|b\rangle\langle b|\underset{\sim}{y}|a\rangle\right]$$

$$= \text{Im}\left[\langle a|eE\underset{\sim}{x}|b\rangle\langle b|\frac{e\mathcal{H}}{2mc}\underset{\sim}{L}_x|a\rangle + \langle a|\frac{e\mathcal{H}}{2mc}\underset{\sim}{L}_y|b\rangle\langle b|eE\underset{\sim}{y}|a\rangle\right]$$

$$= \text{Im}\left[\langle a|eE\,(\underset{\sim}{x}+i\underset{\sim}{y})|b\rangle\langle b|\frac{e\mathcal{H}}{2mc}\,(\underset{\sim}{L}_y + i\underset{\sim}{L}_x)|a\rangle\right]$$

This expression is for oriented set of molecules with light propagating along Z direction. For randomly oriented molecules, we have to take the average over all possible orientations and then the above expression turns to Imaginary part

of $\langle a|\underset{\sim}{r}|b\rangle\langle b|\underset{\sim}{M}|a\rangle$. Hence the Rotational strength in proper unit is given by

$$R_K = \text{Im}\,\langle a|\underset{\sim}{r}|b\rangle \cdot \langle b|\underset{\sim}{M}|a\rangle \cdot$$

The above derivation seems to be the most straight forward and simplest way of deriving an expression for CD[70] .

CHAPTER III

THEORETICAL INVESTIGATIONS ON THE OPTICAL ABSORPTION, MAGNETIC SUSCEPTIBILITY, g-VALUES AND MAGNETIC HEAT CAPACITY OF SOME RARE-EARTH COMPLEXES

This chapter deals with the interpretation of the optical, thermal and magnetic behaviours of some rare-earth complexes. A number of theoretical calculations on optical absorption[89] and e.p.r[90,91] spectra of various rare-earth complexes have been done earlier. Theoretical works on the susceptibility of some RE complexes have also been done earlier[92-95]. Special mention may be made to the RE chlorides and ethyl sulphates which have been studied extensively and parameters giving a good fit to the optical results have been already evaluated. Some workers[3,92-95] also tried to fit the magnetic data. But still we find that there is no unified approach to explain the magnetic susceptibilities, g-values and the CF levels of RE crystals with a single set of parameters. Sometimes, this may be due to insufficient data. But in many cases we find that no rigorous approach to interpret simultaneously the e.p.r, the magnetic susceptibility and the optical absorption data of RE complexes have been taken recourse to. While rigorous approach by using intermediate coupling and J-mixing is found in the case of interpreting many optical results, the theoretical interpretation of magnetic susceptibility and e.p.r results of same RE ions considered only the lowest Russel-Saunders term. We have chosen the $4f^2$, $4f^3$ and $4f^{12}$ electronic configurations for our theoretical study on the optical absorption, the magnetic

susceptibility results, the g-values and in one case the magnetic heat capacity of a specific complex. In the present chapter we confine our attention mainly to some RE ethyl sulphates and double nitrates of the above mentioned system such as (i) Nd^{3+} ethyl sulphate, (ii) Tm^{3+} ethyl sulphate, (iii) Pr^{3+} ethyl sulphate, (iv) Pr^{3+} double nitrate. These complexes received attention fairly long ago, but a unified theory to interpret consistently and simultaneously all the different experimental results is still lacking. We enumerate the reasons for the choice of these complexes :

(i) The magnetic susceptibility and anisotropy data are available in full details but the correct interpretation was not found.

(2) Due to the simple electronic configuration it is easy to diagonalise the hamiltonian giving rigorous solution of the eigenvalue problem. The intermediate coupling and different J-mixing under the crystal field are then automatically taken into account in the rigorous solution.

(3) The interpretation of the optical data of RE ethyl sulphates or double nitrates has been reliably done earlier. But in most cases the attempts were not done to test whether the interpretation of the optical result is also consistent with the magnetic susceptibility results and the g-values. i.e., whether the parameters which reproduce the CF levels faithfully can also successfully explain the magnetic susceptibilities and the g-values or not .

(4) Some of the early CF calculations regarding the RE ethyl sulphates or double nitrates are in R.S. coupling scheme which are totally inadequate to explain the other experimental data like magnetic susceptibility and the g-values.

So this invokes us to take up these problems. Our aim is to see how CF theory can successfully explain the optical absorption spectra and then to see whether the same theory can reproduce the magnetic and e.p.r data faithfully. During calculation we have considered not only the intermediate coupling scheme but also the J-mixing and in case of $4f^2$ and $4f^{12}$ a rigorous approach which considers diagonalisation of the complete energy matrix has been adopted. The results were then used to calculate the susceptibility and the g-values (for $4f^{12}$ system magnetic heat capacity is also calculated). In all cases we made an attempt to explain the optical absorption results, the susceptibility and g-values simultaneously from a single set of parameters.

III.1. INTERPRETATION OF THE MAGNETIC BEHAVIOURS OF NEODYMIUM ETHYL SULPHATE

III.1.1. INTRODUCTION

In this section we shall make an attempt to give a theoretical interpretation of the magnetic susceptibility

values at different temperature, g values and also the optical spectra of Neodymium ethyl sulphate and we shall show that all these experimental results can be successfully explained by using a unique set of theoretical parameters, which will be evaluated from the experimental results themselves. Elliott and Stevens[3] were the first to give a theoretical interpretation of the e.p.r results of rare-earth ethylsulphates in terms of the crystal field theory. They considered a crystal field of D_{3h} symmetry of the rare-earth ions in the ethyl sulphate lattice and in the case of NES (neodymium ethylsulphate) they achieved some success in interpreting the e.p.r and magnetic susceptibility data with the following set of crystal field parameters: $B_2^o = -15\ cm^{-1}$, $B_4^o = -35\ cm^{-1}$, $B_6^o = -60\ cm^{-1}$ and $B_6^6 = 640\ cm^{-1}$. The theory used the Russel Saunder's (R.S.) coupling scheme and mixing of only $^4I_{11/2}$ with the free-ion ground level $^4I_{9/2}$. The predicted crystal field energy levels were found later to deviate considerably from the observed optical data of Gruber and Satten[96] for the concentrated crystals of NES not only in magnitude but also in the order of some of the levels. It now appears that Elliott and Stevens[3] tried to fit the e.p.r results of diluted crystal on the one hand and magnetic data of concentrated crystal on the other with the same set of parameters. The calculated g-values (i.e. $g_{\parallel} = 3.56$, $g_{\perp} = 2.12$), are not in good agreement with the latest experimental result

$g_{\parallel} = 3.594$ and $g_{\perp} = 2.039$ of Fisher et al[97] for the concentrated crystals of NES and the fitting of magnetic data is also not very satisfactory.

Gruber and Satten[96], in their theory, took intermediate coupling (IC) scheme into account although in an indirect way and used the mixing of the J-levels $^4I_{11/2}$, $^4I_{13/2}$ and $^4I_{15/2}$ with $^4I_{9/2}$. With the set of parameters $B_2^o = 58.4\ cm^{-1}$, $B_4^o = -68.2\ cm^{-1}$, $B_6^o = -42.7\ cm^{-1}$ and $B_6^6 = 595\ cm^{-1}$, a set quite different from that of Elliott and Stevens[3], they were able to fit the observed crystal field levels in their optical absorption experiment on concentrated crystals of NES within a mean deviation of only $4\ cm^{-1}$. However, they did not test whether the parameters quoted by them could faithfully reproduce the observed g-values and magnetic susceptibilities. Moreover, they did not actually carry out the IC calculation for NES, instead they used the IC wave functions of Neodymium chloride given by Wybourne[98] to calculate the crystal field levels of NES. In fact, with the crystal field parameters given by Gruber and Satten and the correct IC wave functions of NES obtained from direct IC calculation we found that the predicted crystal field levels deviate from the values calculated by Gruber and Satten and also from the experimental values (see table III.1.5), the calculated g-values ($g_{\parallel} = 3.559$, $g_{\perp} = 2.15$) do not agree well with the observed values for the concentrated crystal and the calculated magnetic

susceptibilities at different temperatures also deviate significantly from the experimental values.

In the back-drop of discrepancies mentioned above we have reinvestigated the problem rigorously by carrying out the actual IC calculation and using different J-mixing of $^4I_{11/2}$, $^4I_{13/2}$ and $^4I_{15/2}$ with $^4I_{9/2}$. Attempts are then made to evaluate a unique set of parameters that will make the theory consistent with the e.p.r, optical absorption and magnetic susceptibility experiments simultaneously. A consistent interpretation of observed g-values, optical and magnetic susceptibility results in terms of a unique set of parameters has been possible only after we introduce a very small covalency reduction of the orbital angular momentum which effectively lowers the g-values and susceptibilities without altering the crystal field levels in the frame work of our theory. Indeed, a very good fit of all the above-mentioned experimental data has been achieved with a single set of parameters by introducing covalency reduction factors for the orbital moment very slightly less than unity into the present theory.

III.1.2. CRYSTALLOGRAPHIC BACKGROUND OF RARE-EARTH ETHYL SULPHATES

Lanthanide ethyl sulphates, $Ln(C_2H_5SO_4)_3.9H_2O$, whose X-ray crystallography was investigated by Ketelaar[99] (see Fig. III.1.1) and more

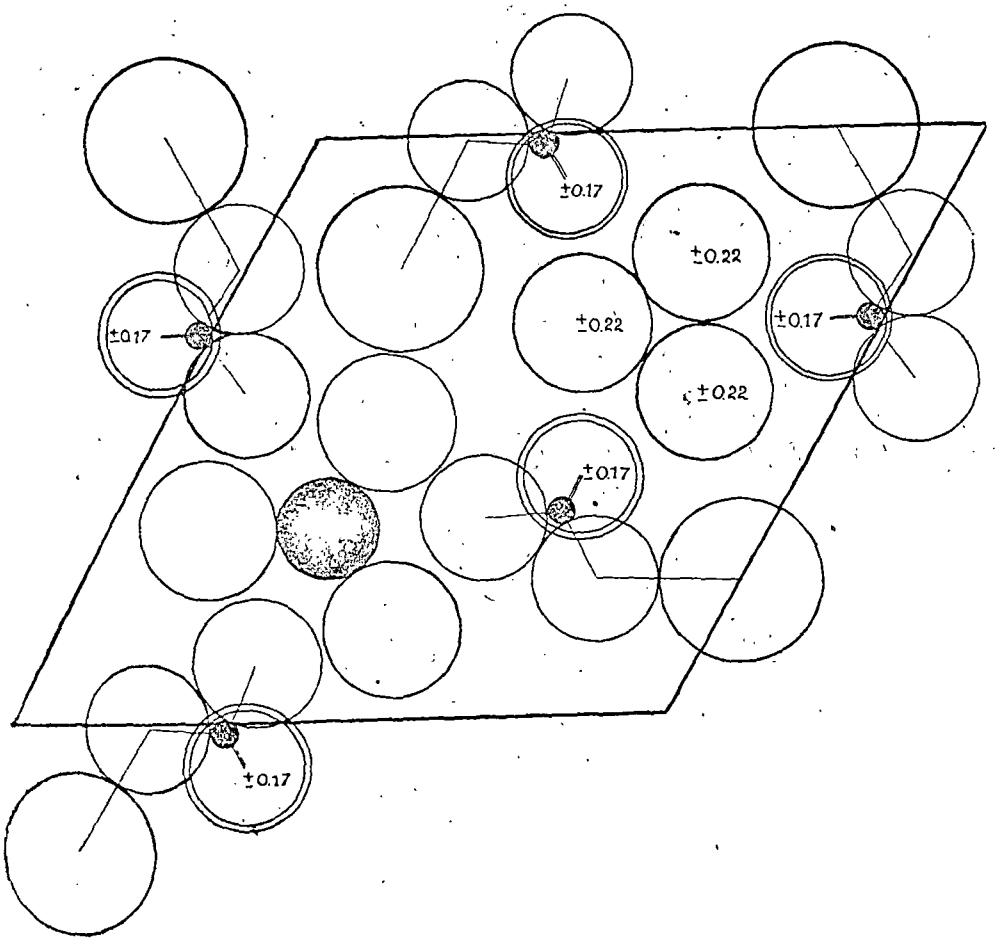

Fig. III.1.1. Projection of the lower half of the elementary cell on a plane at right angles with the c-axis on 1/4 of its height. The numbers indicate the distance to the plane of projection in fractions of the elementary period.
S = ● , Ce = ◉, O = O, H_2O = O, C_2H_5 = O . (The diameter of the various circles represents on scale the size of the atoms).

recently by Fitzwater and Rundle[100] . They studied the crystallographic structure of Pr, Er and Y . The latter workers showedthat all heavy atoms are found in the space group $P^6 3/m$ and that probably the hydrogen positions also conform to this space group. The point symmetry at the lanthanide ion is C_{3h} . This ion has nine water molecules as nearest neighbours; six form a triangular prism with three above and three below the mirror plane containing the other three water oxygens and the lanthanide ion (Fig. III.1.2) . In Erbium compound the Er-O distances to the prism are 0.237 nm, and the remaining three distances are 0.252 nm . If all but the nearest oxygen positions are neglected, the symmetry about the lanthanide ion is almost D_{3h} . This structure has a vertical threefold axis of symmetry; if the structure were exactly D_{3h} there would also be both a vertical and horizontal plane of reflection symmetry. The compounds are isomorphous throughout the group from La^{3+} to Lu^{3+} and also Y^{3+} .

III.1.3. METHOD OF CALCULATION

The Nd^{3+}-ion in the ethyl sulphate lattice is under a crystal field of hexagonal symmetry. Using thecentral field approximation the effective Hamiltonian of Nd^{3+}-ion in the crystal is given by

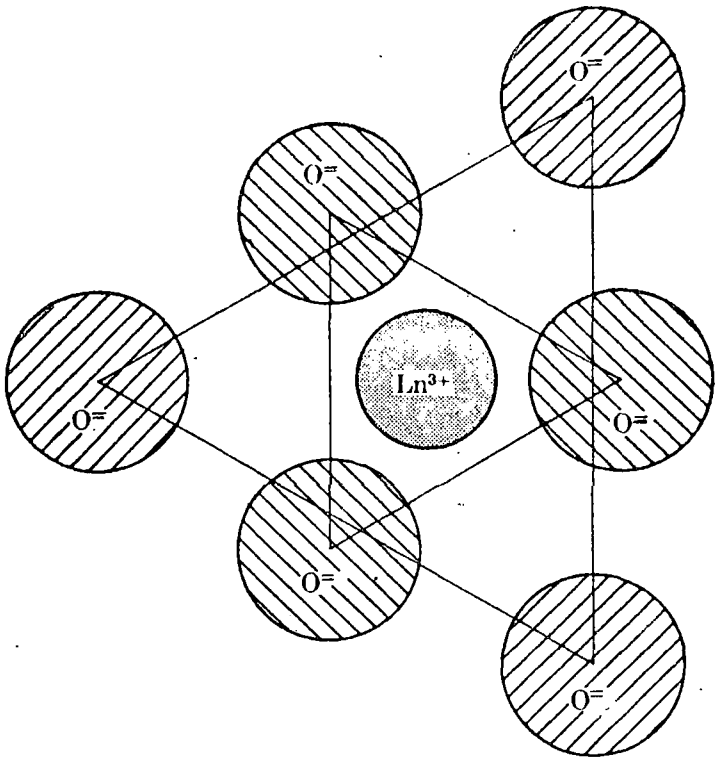

Fig. III.1.2. Arrangement of the double triangular prism of water oxygen ions in the lanthanide ethylsulphates, in a plan view as seen along the crystallographic c-axis. In (R, Θ, Φ) coordinates, the Ln^{3+} ion is at the origin; there are three $O^{=}$ ions in the same plane at $(0.252\ nm, \pi/2, \Phi = (2n+1)\pi/3)$, and six $O^{=}$ ions (above and below) at $(0.237\ nm, \Theta, \Phi = 2n\pi/3)$ and $(0.237\ nm, \pi-\Theta, \Phi = 2n\pi/3)$ with Θ approximately 40°. The values of R, Θ vary slightly with the lanthanide ion; the values of R given are for Er^{3+}. The radii of the circles denoting ions are drawn on about half scale relative to the inter-ionic distances.

$$\mathcal{H}_{eff} = H_r^{ij} + H_{SO} + H_C = \sum_{i<j} \frac{e^2}{r_{ij}} + \zeta \sum_i \underset{\sim}{l}_i \cdot \underset{\sim}{s}_i + H_C$$

Using the intermediate coupling scheme we first diagonalise the matrix of $H_r^{ij} + H_{SO}$ constructed in a basis of states represented by $|U\vartheta SLJM\rangle$, where the symbol ϑ within the ket notation has been discussed in chapter II. The crystal field interaction, H_C is then treated as a perturbation over the resulting states which are actually the intermediate coupling wave functions.

Finally we apply Zeeman perturbation caused by an external magnetic field $\mathcal{H}$ along and perpendicular to the symmetry axis of the ion in the form $\beta\mathcal{H}(k_{\parallel} L_Z + 2S_Z)$ and $\beta\mathcal{H}(k_{\perp} L_X + 2S_X)$ respectively where the covalency effect on the orbital angular momentum is introduced by associating the reduction factors $k_{\parallel}$ and $k_{\perp}$ with L_Z and L_X respectively. This way of introducing covalency reduction of orbital moment into the theory has been discussed earlier (chapter II). We ultimately obtain the principal g-values ($g_{\parallel}$ and $g_{\perp}$) and principal magnetic susceptibilities ($K_{\parallel}$ and $K_{\perp}$) of Nd^{3+}-ion .

III.1.4. INTERMEDIATE COUPLING WAVE FUNCTIONS

The diagonalisation of the matrix of $H_r^{ij} + H_{SO}$ yields what are known as intermediate coupling wave-functions and their eigenvalues. For this we need the matrix elements of

H_r^{ij} and H_{SO} both. The spin-orbit matrix element for $4f^3$ configuration has been calculated by Judd and Loudon[80]. This can also be calculated by the general formula (II.8.1) given in chapter II along with the use of the tables of c.f.p. given by Nielson and Koster. The method of calculation of the matrix elements of electrostatic interaction H_r^{ij} has been described in chapter II. Gruber and Satten, in order to fit the 'free-ion' spectrum, deduced the values of the electrostatic parameters $F_2 = 331.33\ cm^{-1}$, $F_4 = 47.956\ cm^{-1}$, $F_6 = 5.313\ cm^{-1}$ and SO coupling parameter $\zeta = 880.11\ cm^{-1}$ for NES from those of $NdCl_3$ following a procedure developed by Wong[101] without carrying out the IC calculation. We have used the same values for the parameters to calculate the numerical values of the IC matrix elements. The matrix of $H_r^{ij} + H_{SO}$ constructed thus in a basis of states $|U\nu SLJM\rangle$ reduces to block form and each block corresponds to a particular value of J.

However, we need to consider only the four block matrices corresponding to J = 9/2, 11/2, 13/2 and 15/2 in our calculation and the results for other values of J are not needed since the energy levels corresponding to other values of J are too high (more than $10,000\ cm^{-1}$) to be included in the calculation of different J-mixing under the crystal field and of magnetic susceptibilities. It is to be noted that we need only the following four lowest wave functions and their corresponding energies in our subsequent calculation :

$$\Psi_1 = 0.0031\left|{}^4F_{9/2}\right\rangle - 0.0170\left|{}^2G_{9/2}(20)\right\rangle + 0.0151\left|{}^2G_{9/2}(21)\right\rangle$$
$$+ 0.0076\left|{}^4G_{9/2}\right\rangle + 0.0577\left|{}^2H_{9/2}(11)\right\rangle - 0.1636\left|{}^2H_{9/2}(21)\right\rangle$$
$$+ 0.9845\left|{}^4I_{9/2}\right\rangle$$

with energy $E_{\Psi_1}^{(0)} = 0$ (zero of the energy scale is taken at $E_{\Psi_1}^{(0)}$),

$$\Psi_2 = 0.0071\left|{}^4G_{11/2}\right\rangle + 0.0367\left|{}^2H_{11/2}(11)\right\rangle - 0.0945\left|{}^2H_{11/2}(21)\right\rangle$$
$$- 0.0151\left|{}^2I_{11/2}\right\rangle + 0.9947\left|{}^4I_{11/2}\right\rangle$$

with energy $E_{\Psi_2}^{(0)} = 1867.66\ cm^{-1}$,

$$\Psi_3 = -0.0231\left|{}^2I_{13/2}\right\rangle + 0.0644\left|{}^2K_{13/2}\right\rangle + 0.9977\left|{}^4I_{13/2}\right\rangle$$

with energy $E_{\Psi_3}^{(0)} = 3856.16\ cm^{-1}$,

$$\Psi_4 = 0.9930\left|{}^4I_{15/2}\right\rangle + 0.1174\left|{}^2K_{15/2}\right\rangle - 0.0090\left|{}^4I_{15/2}\right\rangle$$

with energy $E_{\Psi_4}^{(0)} = 5921.36\ cm^{-1}$.

III.1.5. CRYSTAL FIELD ENERGY LEVELS

For our purpose we actually need to calculate the crystal field effect only on the lowest intermediate coupling wave function Ψ_1. The effect of the crystal field is obtained by first diagonalising the matrix of H_c constructed in a basis of 10 states represented by $\left|\Psi_1 J_Z\right\rangle$ where $J_Z = \pm 9/2, \pm 7/2, \pm 5/2, \pm 3/2$ and $\pm 1/2$. This will give the first order correc-

tion to the energy of Ψ_1 yielding a splitting of Ψ_1 into five doublets and the correct zeroth order states for each component of the five doublets. The first order correction of the state is obtained by using the perturbation formula which involves the mixing of each of the aforesaid correct zeroth order state having J = 9/2 with the states belonging to Ψ_2 , Ψ_3 and Ψ_4 having J-values equal to 11/2, 13/2 and 15/2 respectively. Thus the different J-mixing under the crystal field is obtained from the first order correction to the states.

The Nd^{3+} ion in ethyl sulphate lattice is under a crystal field of C_{3h} symmetry. However, as pointed out by Wybourne[102] and Abragam and Bleaney[103] we can also safely replace C_{3h} symmetry by a D_{3h} symmetry for the sake of calculation and indeed this has been the usual practice in treating the rare-earth ethyl sulphate ions. The CF interaction H_c assuming D_{3h} symmetry is given by

$$H_c = A_{20}U_o^{(2)} + A_{40}U_o^{(4)} + A_{60}U_o^{(6)} + A_{66}(U_6^{(6)} + U_{-6}^{(6)})$$

The CF parameters A_{kq}'s are not the same as B_k^q's which are obtained when Stevens operator equivalent method is used and they are related as shown in chapter II.

By extensive trial method we have obtained the following set of parameters :

$A_{20} = 180\ cm^{-1}$, $A_{40} = -645\ cm^{-1}$, $A_{60} = -730\ cm^{-1}$, $A_{66} = 624\ cm^{-1}$,

and the corresponding B_k^q values are $B_2^o = 56.8\ cm^{-1}$, $B_4^o = -68.2\ cm^{-1}$, $B_6^o = -46.4\ cm^{-1}$, $B_6^6 = 602.8\ cm^{-1}$. Using these values of the parameters the diagonalisation of the matrix of H_c constructed in a basis of the ten states $|\Psi_1 J_Z\rangle$ where $J_Z = \pm 9/2, \pm 7/2, \pm 5/2, \pm 3/2, \pm 1/2$ yields the following zeroth order CF states comprising five doublets and the first-order energy correction

$$\left.\begin{aligned}\Phi_1^{(o)} &= 0.9105|\Psi_1\ 7/2\rangle + 0.4136|\Psi_1 -5/2\rangle \\ \Phi_{1'}^{(o)} &= 0.9105|\Psi_1 -7/2\rangle + 0.4136|\Psi_1\ 5/2\rangle\end{aligned}\right\} \quad \varepsilon_1^{(1)} = -183.19\ cm^{-1},$$

$$\left.\begin{aligned}\Phi_2^{(o)} &= 0.7552|\Psi_1\ 9/2\rangle + 0.6555|\Psi_1 -3/2\rangle \\ \Phi_{2'}^{(o)} &= 0.7552|\Psi_1 -9/2\rangle + 0.6555|\Psi_1\ 3/2\rangle\end{aligned}\right\} \quad \varepsilon_2^{(1)} = -21.46\ cm^{-1},$$

$$\left.\begin{aligned}\Phi_3^{(o)} &= |\Psi_1\ \tfrac{1}{2}\rangle \\ \Phi_{3'}^{(o)} &= |\Psi_1 -\tfrac{1}{2}\rangle\end{aligned}\right\} \quad \varepsilon_3^{(1)} = -30.96\ cm^{-1},$$

$$\left.\begin{aligned}\Phi_4^{(o)} &= -0.6555|\Psi_1\ 9/2\rangle + 0.7552|\Psi_1 -3/2\rangle \\ \Phi_{4'}^{(o)} &= -0.6555|\Psi_1 -9/2\rangle + 0.7552|\Psi_1\ 3/2\rangle\end{aligned}\right\} \quad \varepsilon_4^{(1)} = 125.18\ cm^{-1},$$

$$\left.\begin{aligned}\Phi_5^{(o)} &= -0.4136|\Psi_1\ 7/2\rangle + 0.9105|\Psi_1 -5/2\rangle \\ \Phi_{5'}^{(o)} &= -0.4136|\Psi_1 -7/2\rangle + 0.9105|\Psi_1\ 5/2\rangle\end{aligned}\right\} \quad \varepsilon_5^{(1)} = 110.44\ cm^{-1}$$

Next, we take the effect of J-mixing. Remembering that $E_{\Psi_1}^{(o)}$ is the zero of the energy scale, the state correct to first order due to J-mixing is given by

$$\Phi_i = N\left[\Phi_i^{(o)} - \sum_{\Psi_t} \frac{\langle\Psi_t|H_c|\Phi_i^{(o)}\rangle}{E_{\Psi_t}^{(o)}}|\Psi_t\rangle\right] \qquad \text{(III.1.1)}$$

where t = 2, 3, 4 and N is the normalization factor so that $\langle \Phi_i | \Phi_i \rangle = 1$ and the CF energy correct to second order is

$$\varepsilon_i = \varepsilon_i^{(1)} - \sum_t \left| \langle \Psi_t | H_c | \Phi_i^{(0)} \rangle \right|^2 / E_{\Psi_t}^{(0)} \qquad \text{(III.1.2)}$$

there exist selection rules for M_J (the crystal quantum number is conserved) which strongly reduce the number of matrix elements to be considered in sum in (III.1.1) and (III.1.2).

The above crystal field states forming five doublets and originating from the lowest intermediate coupling wave function Ψ_1 comprise the lowest group of levels originating from Ψ_2.

III.1.6. COVALENCY REDUCTION OF ANGULAR MOMENTUM

We find that unless a reduction of the orbital momentum matrices is assumed presumably due to the covalency effect implying motion of the magnetic electrons in molecular orbitals, it becomes impossible to achieve a good fit to the g-values and magnetic susceptibilities. It has been discussed in chapter II that the matrix elements of L that occur in the calculation of g-values and magnetic susceptibilities are of the type

$$\langle SLJM | L_\alpha | S' L' J' M' \rangle \qquad \text{(III.1.3)}$$

where

$$\alpha \equiv x,\ y,\ z$$

in which the states refer to the whole atom built up from the individual electron state which are not pure f states but slightly modified due to covalency effect. It has also been discussed in chapter II that the effect of covalency on such matrix element will be to reduce the operator L_α to $k_\alpha L_\alpha$ and then calculate the matrix element of $k_\alpha L_\alpha$ between the atomic states built up from pure f electronic states. The k_α is the orbital reduction factor. Further it was shown in chapter II that in case of uniaxial symmetry we will have only two covalency reduction factors $k_{\parallel}$ ($= k_z$) and $k_{\perp}$ ($= k_x$ or k_y). In the present theory the orbital reduction factors $k_{\parallel}$ and $k_{\perp}$ will be treated as two additional parameters to be evaluated from experiment.

III.1.7. CALCULATION OF g-VALUES

For the calculation of the principal g-values one is interested only in the lowest doublet (Φ_1 , $\Phi_{1'}$) in the CF level pattern. With the introduction of covalency reduction factors for the orbital momentum the expressions for the g-values are

$$g_{\parallel} = g_z = \left|\langle\Phi_1|k_{\parallel}L_z + 2S_z|\Phi_1\rangle - \langle\Phi_{1'}|k_{\parallel}L_z + 2S_z|\Phi_{1'}\rangle\right| ,$$

$$g_{\perp} = g_x = g_y = 2\left|\langle\Phi_1|k_{\perp}L_x + 2S_x|\Phi_{1'}\rangle\right| = 2\left|\langle\Phi_1|k_{\perp}L_y + 2S_y|\Phi_{1'}\rangle\right|$$

III.1.8. CALCULATION OF SUSCEPTIBILITY

A significant contribution to the magnetic susceptibility comes from only the lowest group of ten CF states Φ_i forming five doublets. The general expression for the ionic paramagnetic susceptibility is obtained by the same way as described in chapter II.

III.1.9. RESULTS AND DISCUSSION

The values of the parameters used in the theory are : $F_2 = 331.33\ cm^{-1}$, $F_4 = 47.956\ cm^{-1}$, $F_6 = 5.313\ cm^{-1}$, $\zeta = 880.11\ cm^{-1}$, $B_2^o = 56.8\ cm^{-1}$, $B_4^o = -68.2\ cm^{-1}$, $B_6^o = -46.4\ cm^{-1}$, $B_6^6 = 602.8\ cm^{-1}$, $k_{||} = 0.987$, $k_{\perp} = 0.997$. The values of the crystal field energy levels, g-values ($g_{||}$ and $g_{\perp}$) and magnetic susceptibility values $K_{||}$ and $K_{\perp}$ at different temperatures of Nd^{3+} ion in NES calculated with the parameters mentioned above are shown in the tables III.1.5 - III.1.7 . The symbols || and $\perp$ are used as suffix to indicate the quantities along the parallel and perpendicular to the symmetry axis of the ion. These tables also show the experimental values to facilitate comparison of the theory with the experiment.

Before we start interpreting the experimental results with the theory presented here we make a brief survey of the experimental results which are of interest to us. The principal

magnetic susceptibilities $K_{\parallel}$ and $K_{\perp}$ of Nd^{3+}-ion in the undiluted NES are available at different temperatures ranging from 14K to 291K from the works of Van den Handel and Hupse[104] (see table III.1.7). From the optical absorption experiment at 77K on undiluted NES Gruber and Satten gave the details of the crystal field energy levels into which the ground $^4I_{9/2}$ level of the free ion splits (see table III.1.5). However, the resonance g-values that are available in the literature for the undiluted NES appear to be a little confusing. A magnetic resonance value $g_{\parallel} = 3.61$ and $g_{\perp} = 2.05$ for undiluted NES were quoted by Elliott and Stevens[3], although the source was not mentioned. For NES which was diluted 200:1 with La-ethyl sulphate Bleaney et al[91] gave the following g-values for their e.p.r experiment at 20K : $g_{\parallel} = 3.53$, $g_{\perp} = 2.08$. They further reported that for concentrated NES similar values were obtained, of course with a less degree of accuracy. It is not clear whether these 'similar' values which refer to the concentrated crystal were identical with those for the diluted crystal. On the other hand, very recently Fisher et al.[97] from magneto-thermodynamic studies at extremely low temperature (about 4K) found the accurate g-values of the concentrated crystals to be $g_{\parallel} = 3.594$ and $g_{\perp} = 2.039$ which is very close to the values quoted by Elliott and Stevens[3] .

Without actually carrying out the diagonalisation of IC matrices of NES, Gruber and Satten evaluated the electrostatic parameters F_2 , F_4 , F_6 and SO parameter ζ in the new system of NES from those of $NdCl_3$ following a method developed by Wong[105] in which a Taylor series expansion of the energy values was used. Wong also indicated that Taylor series expansion method can also be applied to find the wave function in the new system. Gruber and Satten did not make any attempt to find the wave function of NES from those of $NdCl_3$ and instead he used those of $NdCl_3$ for further calculation of crystal field splitting. We have used the values of the above parameters to calculate the IC wave functions by diagonalisation of IC matrices and the corresponding energy values calculated with these values of F_2 , F_4 , F_6 and ζ are presented in tables III.1.1 - III.1.4 . As expected, the 'free-ion' levels of NES that are obtained thus from actual diagonalisation of IC matrices are in exact agreement with those obtained by Gruber and Satten using Wong's procedure. However, the IC wave functions for NES obtained from diagonalisation of the IC matrices are slightly different from those of $NdCl_3$ since the parameters in the two systems are slightly different.

The crystal field parameters A_{20} , A_{40} , A_{60} and A_{66} are then chosen by an exhaustive trial method and so as to

fit the theory with the observed crystal field spectra as close as possible. The parameters giving the best fit are shown in table III.1.5, the predicted and observed crystal field levels agree almost exactly (within a mean deviation of 1 cm^{-1} only). The crystal field parameters in our theory are somewhat different from those of Gruber and Satten. Gruber and Satten evaluated them by fitting the predicted levels obtained by using IC wave functions of $NdCl_3$ instead of NES with the observed levels within a mean deviation of 4 cm^{-1}. However, with the correct IC wave functions of NES their parameters predict the crystal field levels which deviate considerably (about 12 cm^{-1} in some cases) from the observed spectra (see table III.1.5).

Having found the 'free-ion' and crystal field parameters which fit the predicted and observed spectra so nicely, it is expected that they should also faithfully reproduce the observed g-values and magnetic susceptibilities. On actual calculation with the crystal field parameters obtained by us and with the correct IC wave functions of NES without taking covalency effect into consideration (i.e. $k_{\parallel} = k_{\perp} = 1$) g-values come out to be $g_{\parallel} = 3.674$, $g_{\perp} = 2.052$ as against the recent values determined by Fisher et al.[97] $g_{\parallel} = 3.594$, $g_{\perp} = 2.039$. Moreover, both the principal susceptibilities $K_{\parallel}$ and $K_{\perp}$ are found to be larger than the experimental values.

However, if we introduce a very small covalency effect on the orbital angular momentum operator by using the covalency reduction factors $k_{\parallel} = 0.987$ and $k_{\perp} = 0.997$, we arrive at a good fitting of not only the g-values but also the principal magnetic susceptibilities, with the same set of parameters that explained the optical spectra with remarkable success. The predicted g-values are $g_{\parallel} = 3.596$, $g_{\perp} = 2.041$ in excellent agreement with the observed values. Also the theory is found to fit the magnetic data almost exactly (within 0.37%) at the lowest temperature of measurement (14K). At room temperature the theory is found to agree with the magnetic data within 1.4% and the maximum deviation that occurs at some intermediate temperature is found to be about 6% of the observed values.

The values of $k_{\parallel}$ and $k_{\perp}$ indicate that the covalency effect is very small as expected in the case of rare-earth ions. The covalency should also affect all parameters. In fact, Ellis and Newman[106] carried out an ab initio calculation for the theoretical estimates of the contribution from various factors including covalency to the CF parameters. However, in a theory using adjustable parameters to be evaluated from experiment, the values of the parameters deduced from experiment will automatically include the effect of covalency.

Some of the CF parameters given by Gruber and Satten have been slightly modified in the present investigation to

improve the fitting of the theory with the experiments on g-values and magnetic susceptibilities. In the present work B_4^o remains unchanged at the value given by Gruber and Satten, B_2^o changes from 58.4 to 56.8 cm^{-1}, B_6^o from -42.7 to -46.4 cm^{-1} and B_6^6 from 595 to 602.8 cm^{-1}. Since these changes are small, the present values of the parameters are expected not to disturb seriously the whole crystal field spectra. In fact, with the present CF parameters energy values of the CF components of the ground term have already been determined in the course of our calculation on the magnetic properties. They are shown in table III.1.7 alongwith the experimental results. The table III.1.5 shows that the small changes in the values of some of the CF parameters from those of Gruber and Satten in no way disturb the fitting of the CF spectra of the ground group of levels. We expect that excited CF levels will also not be seriously affected owing to the small changes that have been made in the values of the CF parameters given by Gruber and Satten.

In the present investigation we have considered that the crystal field parameters are independent of temperature as otherwise the solution of the parameters from the available experimental data will be nonunique. In the iron group the anisotropic component of the ligand field is found to vary with temperature in many cases[107-109]. Variation of the

crystal field parameters in our case, if any, must be small as found from the nature of agreement of the theory with the magnetic data and may account for the slight discrepancy that still persists at some temperature. There may also exist a very slight distortion from the C_{3h} symmetry to C_{3v} symmetry as was postulated by Elliott and Stevens[110] in the case of Ce-ethylsulphate. However, for further refinement of the theory a redetermination of the magnetic data with the presently available refined technique and purer samples is considered to be imperative. The magnetic measurements were done long ago and an accurate redetermination will ascertain whether the small discrepancy that still persists while interpreting the magnetic data with the present theory is really of any significance.

Numerical computation was done with the help of the computer (Burroughs 6700) at the Regional Computer Centre, Calcutta as far as practicable leaving hand calculation to the minimum.

Table III.1.1

IC wave functions and corresponding energies of Nd^{3+} for J = 9/2[a], [b]

Energy	14645.51	20877.77	47738.63	19375.66	32560.43	12475.50	0
Eigen Vectors							
^4F	0.8703	0.2766	0.0156	-0.1959	0.0037	-0.3570	0.0031
$^2G_{20}$	-0.1325	0.6020	0.6436	-0.3026	-0.0159	0.3372	-0.0170
$^2G_{21}$	0.0909	-0.4911	0.7598	0.2869	-0.1000	-0.2842	0.0151
^4G	-0.0339	0.5190	-0.0218	0.8394	0.0655	-0.1415	0.0076
$^2H_{11}$	-0.1570	0.0045	0.0814	-0.1296	0.9283	-0.2947	0.0577
$^2H_{21}$	0.4306	-0.2234	0.0341	0.2552	0.3517	0.7403	-0.1636
^4I	0.0746	-0.0244	0.0004	0.0345	0.0048	0.1527	0.9845

(a) $F_2 = 331.33\ cm^{-1}$, $F_4 = 47.956\ cm^{-1}$, $F_6 = 5.313\ cm^{-1}$, $\zeta = 880.11\ cm^{-1}$

(b) Energy of IC wave functions are given at the top of the columns. For the IC wave function of a particular energy the co-efficient of each constituent $^{2S+1}L_{Uv}$ state shown in the first column is given by the corresponding entry in the column where this energy occurs.

Table III.1.2

IC wave functions and the corresponding energies of Nd^{3+} for J = 11/2[a], [b]

Energy	21432.40	33902.63	15770.0	28459.26	1867.66
Eigen Vectors					
^4G	0.9642	0.1128	-0.2308	-0.0661	0.0071
$^2H_{11}$	-0.2109	0.8372	-0.3746	-0.2362	0.0367
$^2H_{21}$	0.1598	0.4005	0.8910	-0.1059	-0.0945
^2I	0.0101	0.3548	-0.0520	0.9333	-0.0151
^4I	0.0162	0.0117	0.0994	0.1700	0.9947

(a) Parameters same as Table III.1.1 .

(b) Explanation of the table same as Table III.1.1 .

Table III.1.3

IC wave functions and the corresponding energies of Nd^{3+} for $J = 13/2$[a], [b]

Energy	29770.80	3856.16	18040.81
Eigen Vectors			
^2I	0.9948	-0.0231	-0.0995
^4I	0.0166	0.9977	-0.0664
^2K	0.1008	0.0644	0.9928

(a) Parameters same as Table III.1.1 .

(b) Explanation of the table same as Table III.1.1 .

Table III.1.4

IC wave functions and the corresponding energies of Nd^{3+} for J = 15/2[a),(b)] .

Energy	5921.36	20777.68	29233.16
Eigen Vectors			
^4I	0.9930	-0.1166	-0.0161
^2K	0.1174	0.9705	0.2107
^2L	-0.0090	-0.2111	0.9774

(a) Parameters same as Table III.1.1

(b) Explanation of the table same as Table III.1.1 .

Table III.1.5

Comparison of the calculated crystal field energy levels with the experimentally observed levels[96].

Crystalline Stark Component	Experimental energy level	Predicted energy level considering second order correction with present set of parameters: $B_2^0 = 56.8\ cm^{-1}$, $B_4^0 = -68.2\ cm^{-1}$, $B_6^0 = -46.4\ cm^{-1}$, $B_6^6 = 602.8\ cm^{-1}$	Predicted energy level considering second order correction with the Gruber's set of parameters: $B_2^0=58.4\ cm^{-1}$, $B_4^0=-68.2\ cm^{-1}$ $B_6^0=-42.7\ cm^{-1}$, $B_6^6=595\ cm^{-1}$
$\pm 5/2$	0	0	0
$\pm 3/2$	149	149	142
$\pm 1/2$	154	155	154
$\pm 5/2$	279	279	268
$\pm 3/2$	311	310	299

Table III.1.6

Comparison between calculated and experimental g-values (Covalency reduction factors $k_{\parallel} = 0.989$, $k_{\perp} = 0.998$).

Calculated	Experimental
$g_{\parallel} = 3.608$	$g_{\parallel} = 3.594$[97], $g_{\parallel} = 3.61$[3]
$g_{\perp} = 2.044$	$g_{\perp} = 2.039$[97], $g_{\perp} = 2.05$[3]

Table III.1.7

Comparison of calculated values $K_{\parallel}$, $K_{\perp}$ with the experimentally observed values.

Temp. (T) °K	Predicted results		Experimental results[104]	
	$K_{\parallel} \times 10^6$, c.g.s. e.m.u.	$K_{\perp} \times 10^6$, c.g.s e.m.u	$K_{\parallel} \times 10^6$, c.g.s. e.m.u.	$K_{\perp} \times 10^6$, c.g.s. e.m.u
14.27	90525.34	34619.00	90257.08	34623.54
17.70	73949.83	29296.33	72873.73	29490.34
20.34	64998.27	26422.75	64625.1	26572.67
64.6	23113.42	13455.66	21616.72	12877.31
71.0	21225.60	12906.89	20246.49	12270.60
77.7	19553.10	12402.42	18644.50	11895.67
139.3	11264.58	9100.89	10682.24	8643.96
216.8	7261.65	6560.05	7103.31	6455.70
226.8	6938.90	6319.62	6905.62	6278.46
249.8	6293.15	5822.57	6292.09	5787.63
287.5	5456.17	5147.12	5474.05	5119.57
291.5	5380.00	5083.94	5378.61	4996.86

III.2. INTERPRETATION OF THE OPTICAL, MAGNETIC AND THERMAL BEHAVIOURS OF THULIUM ETHYL SULPHATE

III.2.1. INTRODUCTION

The present section aims at a consistent interpretation of the optical absorption spectra, magnetic heat capacity and magnetic susceptibility of Thulium ethyl sulphate (Tm.ES.) with a single set of parameters. From the results of optical absorption experiment on concentrated Tm.ES. Gruber and Conway[111-112] first determined a set of electrostatic (ES), spin-orbit (SO) and crystal field (CF) parameters that accounted for the observed levels which were limited in number. Wong and Richman[113] also did the spectroscopic investigation on the diluted crystals of Tm.ES. and gave a different set of crystal field parameters. Gerstein et al.[114] measured the magnetic susceptibility and magnetic heat capacity of concentrated Tm.ES. at different temperatures and tried to fit their experimental data theoretically with the parameters obtained from Wong and Richman[113] and Gruber and Conway[112]. Gerstein et al found that Wong's crystal field parameters which actually referred to the diluted crystals of Tm^{3+} in $La(C_2H_5SO_4)_3.9H_2O$ gave a better fitting of the magnetic susceptibility and magnetic heat capacity data than the parameters given by Gruber et al for undiluted crystals of Tm.ES.

In a later investigation more levels were observed by Krupke and Gruber[115] in optical absorption experiment on undiluted crystal of Tm.ES. But all the crystal field calculations on Tm.ES. primarily meant to fit the optical data were restricted to first order perturbation calculations (i.e., neglecting J-mixing among the states). But in the present work we have carried out the diagonalisation of the matrix of spin-orbit (SO), electrostatic (ES) and the crystal field (CF) interaction of Tm.ES. considered together, the matrix being constructed in a basis of all states of Tm^{3+} ion in the $4f^{12}$ configuration. Thus the full J-mixing was taken into account and which is the most realistic approach. Finally these results were used to obtain the magnetic susceptibility and magnetic heat capacity data. We find that the set of parameters given by Krupke and Gruber[115] when used in our full J-mixing calculation, can fit very well the magnetic susceptibility, optical levels and the magnetic heat capacity data, though slight discrepancies arise in some optical levels which will be discussed later.

III.2.2. SPECTRA OF Tm.ES.

The effective Hamiltonian of Tm^{3+} in Tm.ES. crystal having a D_{3h} symmetry is given by

$$\mathcal{H}_{eff} = \sum_{i<j} \frac{e^2}{r_{ij}} + \sum_i \zeta_i \cdot s_i + A_{20}U_o^{(2)} + A_{40}U_o^{(4)} + A_{60}U_o^{(6)} + A_{66}(U_6^{(6)} + U_{-6}^{(6)})$$

where $U_q^{(k)} = r^k y_k^q$ is an irreducible tensor operator. A_{kq}'s are the crystal field parameters which are related with Stevens form B_k^qs as shown in chapter II.

The matrix of the effective Hamiltonian $\mathcal{H}_{eff}$ is constructed in a basis of states represented by $|USLJM\rangle$. All states belonging to the different multiplet terms $^3PFH\,^1SDGI$ of Tm^{3+} have been taken into consideration for the representation of the above matrix and it turns out to be a 91x91 matrix. The matrix elements of ES interaction for $4f^2$ configuration expressed in terms of Slater-Condon parameters F_k's have been tabulated by Nielson and Koster[77] . We used those for our f^{12} system since it will be exactly same. The SO matrix elements can be easily calculated by using the formula given by Elliott et al.[89] The SO matrix elements for f^2 system have also been already calculated by Spedding[79] . We use these results of f^2 in our f^{12} system by reversing the sign of each matrix element of the spin-orbit interaction. The matrix element of $U_q^{(k)}$ was obtained by procedure described earlier (Chapter II), using tensor operator technique and thus the 91x91 full matrix is set up. But due to the crystal symmetry the whole matrix splits up into 2 matrices of dimension 16x16

(crystal quantum number $\bar{\mu} = \pm 2$), 3 matrices of dimension 14x14 (of which 2 matrices have $\bar{\mu} = \pm 1$ and another $\bar{\mu} = 3$) and one matrix of dimension 17x17 ($\bar{\mu} = 0$).

A complete computer program was then made in which the CF matrix elements were automatically generated and then added up to spin-orbit and electrostatic contribution and after that 6 matrices were diagonalized individually by the same program. The program then invokes a second portion of the program which automatically calculates the susceptibilities and the magnetic heat capacity at different temperatures.

III.2.3. CALCULATION OF SUSCEPTIBILITY

A significant contribution to the magnetic susceptibility of Tm^{3+} comes from only the lowest multiplet of $^3H_6$. It contains 13 crystal field states Φ_i's of which 4 are doublets and 5 are singlets. The general expression for calculating the ionic susceptibility is given in chapter II. The 13 CF states are given in Appendix III.2 at the end of this section.

III.2.4. CALCULATION OF MAGNETIC HEAT CAPACITY

The magnetic heat capacity of Tm.ES. is theoretically obtained from

$$C_m = \frac{R}{Z^2}\left[Z\sum_{m=1}^{n}\left(\frac{E_m^o}{kT}\right)^2 \exp\left(-\frac{E_m^o}{kT}\right) - \sum_{m=1}^{n}\frac{E_m^o}{kT}\exp\left(-\frac{E_m^o}{kT}\right)\right]$$

$E_m^o = W_m^o - W_1^o$ where W_1^o = Energy of lowest CF level. Here n = 13 since for Tm^{3+} ion $^3H_6$ is the ground term and it splits into 13 levels in a crystal field, where

k = Boltzman constant,

R = Nk ,

T = Temperature.

We then calculate the magnetic heat capacity of Tm.ES. at different temperatures using the energy values of the CF levels which give the best fit to the experimental crystal field energy levels and the magnetic susceptibility.

III.2.5. RESULTS AND DISCUSSION

In our present calculation we have done an exhaustive trial method to see which set of parameters can give an overall good fitting. We found that Krupke and Gruber's set of parameters gave an overall good agreement. The parameters taken are as follows :

$F_2 = 449.16\ cm^{-1}$, $F_4 = 64.57\ cm^{-1}$, $F_6 = 7.065\ cm^{-1}$, $\zeta = 2667.9\ cm^{-1}$, $B_2^o\langle r^2\rangle = 135.3\ cm^{-1}$, $B_4^o\langle r^4\rangle = -71.35\ cm^{-1}$, $B_6^o\langle r^6\rangle = -28.8\ cm^{-1}$, $B_6^6\langle r^6\rangle = 428.1\ cm^{-1}$. Table III.2.1 shows the experimental crystal field levels and the theoretical levels obtained from the above exact calculation by using Krupke and Gruber's set of parameters. Fig. III.2.1 shows

the theoretical points and the experimental curves of $K_{\parallel}$ and $K_{\perp}$ at different temperatures. Fig. III.2.2 shows the theoretical points and the experimental curve of C_m at different temperatures.

We find that Johnsen[116] and all the subsequent workers wrongly assigned the $^3F_4$ level. In a recent work on Tm^{3+} in $LaCl_3$ Gruber et al[10] obtained the $^3H_4$ multiplet at about 12624 cm^{-1} (mean value) from the ground level. But in his works on Tm.ES. which were done earlier it was wrongly interpreted that the $^3F_4$ manifold lies at about 12600 cm^{-1} from the ground term. It now appears from our theoretical calculation that it is the $^3H_4$ and not $^3F_4$ which lies at 12600 cm^{-1} and $^3F_4$ lies at 6000 cm^{-1} . The observed levels of Tm^{3+} in $LaCl_3$ also confirm this. We also find that Krupke and Gruber's set of parameters can fit almost all the experimental optical levels with the theoretical levels except the $^1I_6$ level. We also find that no new set of parameters can improve the $^1I_6$ level without affecting the other levels like $^1G_4$ and so on. This discrepancy in $^1I_6$ may be due to the configuration mixing. Fig. III.2.1 shows that above 24K a good fit is obtained between the theoretical points and the experimental curve for $K_{\parallel}$. Gerstein et al also could not fit this portion with Wong's parameters. They expressed doubt about the reliability of the absolute values of experimental data in this portion due to some experimental inaccuracies. The theoretical values

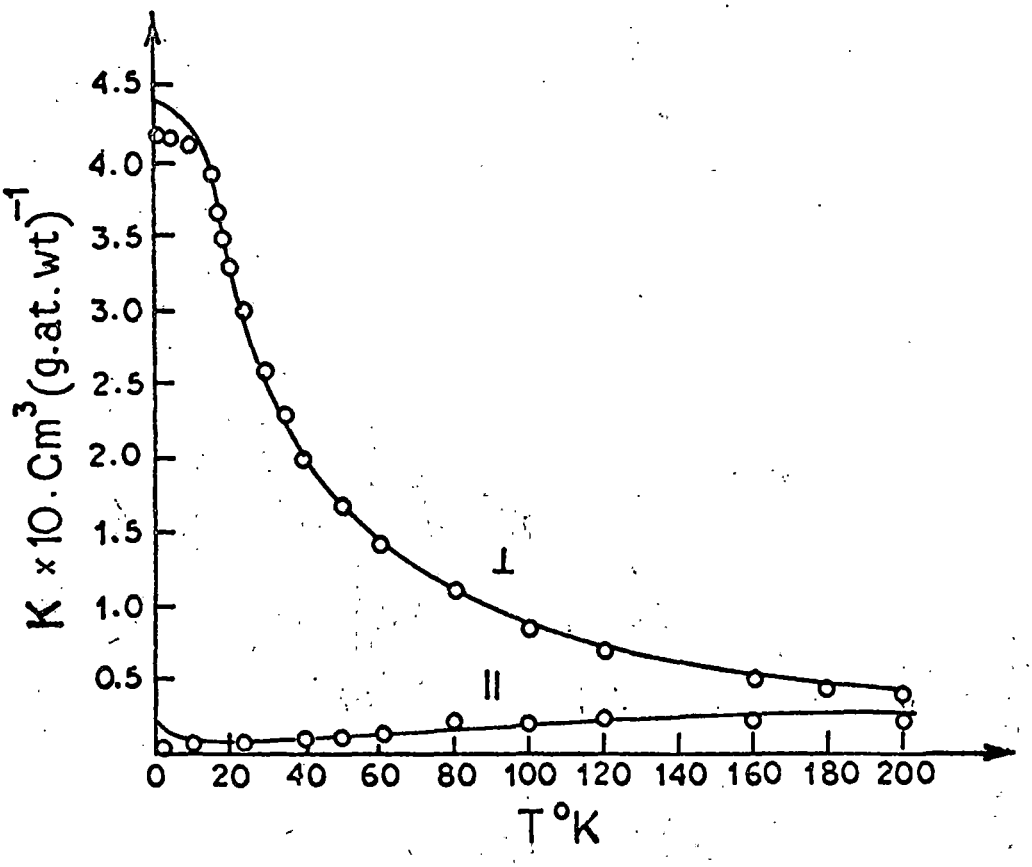

Fig. III.2.1. $K_{||}$ and $K_{\perp}$ of Tm.E.S., cm^3 (g.at. wt)$^{-1}$.

o Theoretical points.

— Experimental smoothed curve.

of $K_\perp$ are very close to the experimental curve. From Fig. III.2.2 we find that there is a sharp rise of experimental curve of C_m values upto 16K and then a gradual decrease in the value upto 40K then again a gradual rise in the value upto 80K after that again a rapid fall occurs. Fig. III.2.2 also shows that the theoretical values do not fit well at low temperatures but at higher temperatures they are almost on the experimental curve.

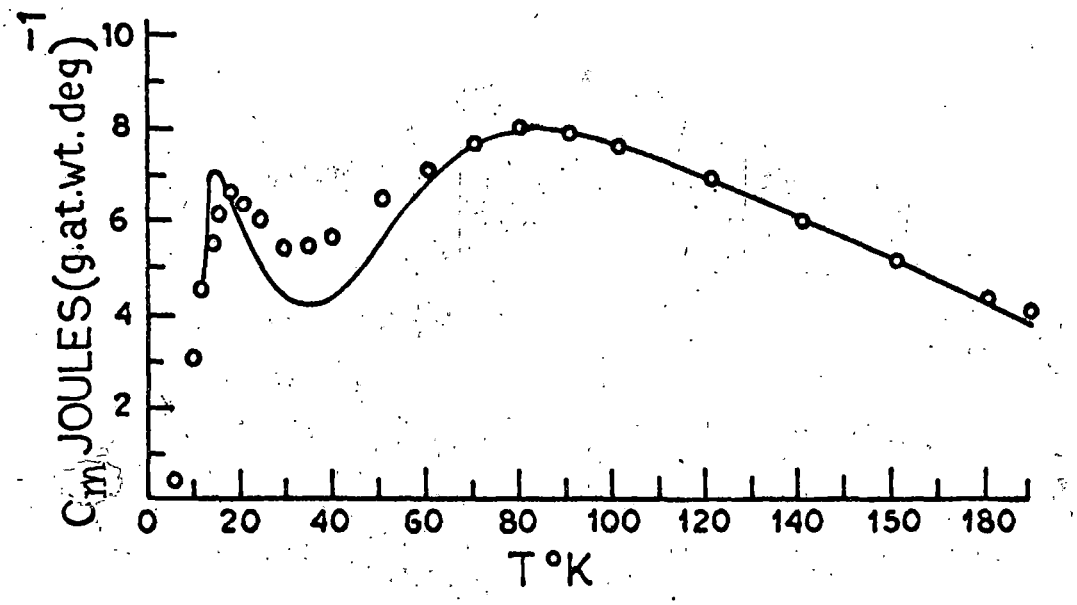

Fig. III.2.2. C_m of Tm.ES., J (g.at. wt.deg)$^{-1}$.

o Theoretical points.

— Experimental smoothed curve.

Table III.2.1

Comparison between experimental and theoretical values of crystal field splitting.

Terms	$\bar{\mu}$	Experimental levels	Theoretical levels
$^3H_6$	0	0	0
	±1	32	33
	±2	112	115
	3	176	165
	±1	201	207
	0	-	219
	0	-	224
	±2	277	278
	3	305	305
$^3H_4$	0	-	12592
	3	-	12637
	±1	-	12672
	±2	-	12692
	3	-	12785
	±2	-	12820
$^3F_3$	3	14407	14402
	±1	14466	14455
	±2	14486	14483
	3	14487	14493
$^3F_2$	±2	15079	14966
	±1	15106	14983
$^1G_4$	±2	21168	21120
	±1	21191	21138
	0	21255	20945
	±2	21279	21233
	3	21341	21276
	3	21379	21420
$^1D_2$	±2	27906	27885
	±1	27977	27951
$^1I_6$	±2	34844	33801
	3	34871	33825
	±2	34900	33854
$^3P_0$	0	35442	35456
$^3P_1$	0	36401	36304
	±1	36486	36385
$^3P_2$	±2	38147	38166
	±1	38188	38200
	0	38312	38350

APPENDIX III.2.

CF wave functions and the energy values of the ground term ($^3H_6$) of Thulium ethyl sulphate obtained from Krupke and Gruber's[115] set of parameters

$$\Phi_1 = 0.1154|^3H_6 6\rangle + 0.9820|^3H_6 0\rangle + 0.1154|^3H_6 -6\rangle - 0.0000|^3H_5 0\rangle - 0.0025|^3H_4 0\rangle - 0.0018|^3F_4 0\rangle - 0.0000|^3F_3 0\rangle + 0.0028|^3F_2 0\rangle - 0.0021|^3P_2 0\rangle - 0.0000|^3P_1 0\rangle - 0.0009|^3P_0 0\rangle + 0.0109|^1I_6 6\rangle + 0.0936|^1I_6 0\rangle + 0.0109|^1I_6 -6\rangle + 0.0009|^1G_4 0\rangle - 0.0017|^1D_2 0\rangle + 0.0002|^1S_0 0\rangle \quad W_1^{(0)} = 0$$

$$\Phi_2 = 0.2858|^3H_6 5\rangle + 0.9535|^3H_6 -1\rangle - 0.0021|^3H_5 5\rangle - 0.0065|^3H_5 -1\rangle - 0.0007|^3H_4 -1\rangle + 0.0002|^3F_4 -1\rangle + 0.0032|^3F_3 -1\rangle + 0.0007|^3F_2 -1\rangle - 0.0021|^3P_2 -1\rangle - 0.0009|^3P_1 -1\rangle + 0.0272|^1I_6 5\rangle + 0.0910|^1I_6 -1\rangle + 0.0005|^1G_4 -1\rangle - 0.0009|^1D_2 -1\rangle \quad W_2^{(0)} = 33 \text{ cm}^{-1}$$

$$\Phi_{2'} = 0.2858\,|^3H_6\,{-5}\rangle + 0.9535\,|^3H_6 1\rangle - 0.0021\,|^3H_5\,{-5}\rangle$$
$$-0.0065\,|^3H_5 1\rangle - 0.0007\,|^3H_4 1\rangle + 0.0002\,|^3F_4 1\rangle$$
$$+0.0032\,|^3F_3 1\rangle + 0.0007\,|^3F_2 1\rangle - 0.0021\,|^3P_2 1\rangle$$
$$-0.0009\,|^3P_1 1\rangle + 0.0272\,|^1I_6 5\rangle + 0.0910\,|^1I_6 1\rangle$$
$$+0.0005\,|^1G_4 1\rangle \quad -0.0009\,|^1D_2 1\rangle \qquad W_2^{(0)} = 33\ \text{cm}^{-1}$$

$$\Phi_3 = 0.8964\,|^3H_6 2\rangle + 0.4327\,|^3H_6\,{-4}\rangle + 0.0058\,|^3H_5 2\rangle$$
$$+0.0068\,|^3H_5\,{-4}\rangle + 0.0024\,|^3H_4 2\rangle + 0.0013\,|^3H_4\,{-4}\rangle$$
$$+0.0015\,|^3F_4 2\rangle - 0.0069\,|^3F_4\,{-4}\rangle - 0.0002\,|^3F_3 2\rangle$$
$$-0.0027\,|^3F_2 2\rangle - 0.0017\,|^3P_2 2\rangle + 0.0859\,|^1I_6 2\rangle$$
$$+0.0414\,|^1I_6\,{-4}\rangle - 0.0010\,|^1G_4 2\rangle - 0.0031\,|^1G_4\,{-4}\rangle$$
$$+0.0005\,|^1D_2 2\rangle \qquad W_3^{(0)} = 115\ \text{cm}^{-1}$$

$$\Phi_{3'} = 0.8964\,|^3H_6\,{-2}\rangle + 0.4327\,|^3H_6 4\rangle + 0.0058\,|^3H_5\,{-2}\rangle$$
$$+0.0068\,|^3H_5 4\rangle + 0.0024\,|^3H_4\,{-2}\rangle + 0.0013\,|^3H_4 4\rangle$$
$$+0.0015\,|^3F_4\,{-2}\rangle - 0.0069\,|^3F_4 4\rangle - 0.0002\,|^3F_3\,{-2}\rangle$$
$$-0.0027\,|^3F_2\,{-2}\rangle - 0.0017\,|^3P_2\,{-2}\rangle + 0.0859\,|^1I_6\,{-2}\rangle$$
$$+0.0414\,|^1I_6 4\rangle - 0.0010\,|^1G_4\,{-2}\rangle - 0.0031\,|^1G_4 4\rangle$$
$$+0.0005\,|^1D_2\,{-2}\rangle \qquad W_3^{(0)} = 115\ \text{cm}^{-1}$$

$$\Phi_4 = 0.7038\,|^3H_6 3\rangle + 0.7038\,|^3H_6\,{-3}\rangle - 0.0033\,|^3H_5 3\rangle$$
$$+0.0033\,|^3H_5\,{-3}\rangle + 0.0034\,|^3H_4 3\rangle + 0.0034\,|^3H_4\,{-3}\rangle$$
$$-0.0023\,|^3F_4 3\rangle - 0.0023\,|^3F_4\,{-3}\rangle + 0.0045\,|^3F_3 3\rangle$$
$$-0.0045\,|^3F_3\,{-3}\rangle + 0.0676\,|^1I_6 3\rangle + 0.0676\,|^1I_6\,{-3}\rangle$$
$$-0.0029\,|^1G_4 3\rangle - 0.0029\,|^1G_4\,{-3}\rangle \qquad W_4^{(0)} = 165\ \text{cm}^{-1}$$

$$\Phi_5 = 0.9535\,|^3H_6 5\rangle - 0.2857\,|^3H_6 -1\rangle + 0.0020\,|^3H_5 5\rangle$$
$$+0.0099\,|^3H_5 -1\rangle + 0.0024\,|^3H_4 -1\rangle + 0.0079\,|^3F_4 -1\rangle$$
$$+0.0049\,|^3F_3 -1\rangle + 0.0029\,|^3F_2 -1\rangle + 0.0011\,|^3P_2 -1\rangle$$
$$+0.0009\,|^3P_1 -1\rangle + 0.0913\,|^1I_6 5\rangle - 0.0275\,|^1I_6 -1\rangle$$
$$+0.0012\,|^1G_4 -1\rangle - 0.0008\,|^1D_2 -1\rangle \qquad W_5^{(0)} = 207 \text{ cm}^{-1}$$

$$\Phi_5' = 0.9535\,|^3H_6 -5\rangle - 0.2857\,|^3H_6 1\rangle + 0.0020\,|^3H_5 -5\rangle$$
$$+0.0099\,|^3H_5 1\rangle + 0.0024\,|^3H_4 1\rangle + 0.0079\,|^3F_4 1\rangle$$
$$+0.0049\,|^3F_3 1\rangle + 0.0029\,|^3F_2 1\rangle + 0.0011\,|^3P_2 1\rangle$$
$$+0.0009\,|^3P_1 1\rangle + 0.0913\,|^1I_6 -5\rangle - 0.0275\,|^1I_6 1\rangle$$
$$+0.0012\,|^1G_4 1\rangle - 0.0008\,|^1D_2 1\rangle \qquad W_5^{(0)} = 207 \text{ cm}^{-1}$$

$$\Phi_6 = -0.7039\,|^3H_6 6\rangle - 0.0000\,|^3H_6 0\rangle + 0.7039\,|^3H_6 -6\rangle$$
$$-0.0068\,|^3H_5 0\rangle + 0.0000\,|^3H_4 0\rangle + 0.0000\,|^3F_4 0\rangle$$
$$-0.0079\,|^3F_3 0\rangle + 0.0000\,|^3F_2 0\rangle + 0.0000\,|^3P_2 0\rangle$$
$$-0.0020\,|^3P_1 0\rangle + 0.0000\,|^3P_0 0\rangle - 0.0670\,|^1I_6 6\rangle$$
$$-0.0000\,|^1I_6 0\rangle + 0.0670\,|^1I_6 -6\rangle + 0.0000\,|^1G_4 0\rangle$$
$$-0.0000\,|^1D_2 0\rangle - 0.0000\,|^1S_0 0\rangle \qquad W_6^{(0)} = 219 \text{ cm}^{-1}$$

$$\Phi_7 = 0.6944|^3H_6 6\rangle - 0.1632|^3H_6 0\rangle + 0.6944|^3H_6 -6\rangle$$
$$+0.0000|^3H_5 0\rangle + 0.0028|^3H_4 0\rangle + 0.0000|^3F_4 0\rangle$$
$$-0.0079|^3F_3 0\rangle + 0.0000|^3F_2 0\rangle + 0.0000|^3P_2 0\rangle$$
$$-0.0020|^3P_1 0\rangle + 0.0000|^3P_0 0\rangle - 0.0670|^1I_6 6\rangle$$
$$-0.0000|^1I_6 0\rangle + 0.0670|^1I_6 -6\rangle + 0.0000|^1G_4 0\rangle$$
$$-0.0000|^1D_2 0\rangle - 0.0000|^1S_0 0\rangle \qquad W_7^{(0)} = 224 \text{ cm}^{-1}$$

$$\Phi_8 = -0.4327|^3H_6 2\rangle + 0.8961|^3H_6 -4\rangle - 0.0121|^3H_5 2\rangle$$
$$+0.0020|^3H_5 -4\rangle + 0.0007|^3H_4 2\rangle + 0.0013|^3H_4 -4\rangle$$
$$+0.0070|^3F_4 2\rangle - 0.0197|^3F_4 -4\rangle - 0.0040|^3F_3 2\rangle$$
$$+0.0026|^3F_2 2\rangle + 0.0011|^3P_2 2\rangle - 0.0417|^1I_6 2\rangle$$
$$+0.0864|^1I_6 -4\rangle + 0.0019|^1G_4 2\rangle - 0.0076|^1G_4 -4\rangle$$
$$-0.0007|^1D_2 2\rangle \qquad W_8^{(0)} = 278 \text{ cm}^{-1}$$

$$\Phi_{8'} = -0.4327|^3H_6 -2\rangle + 0.8961|^3H_6 4\rangle - 0.0121|^3H_5 -2\rangle$$
$$+0.0020|^3H_5 4\rangle + 0.0007|^3H_4 -2\rangle + 0.0013|^3H_4 4\rangle$$
$$+0.0070|^3F_4 -2\rangle - 0.0197|^3F_4 4\rangle - 0.0040|^3F_3 -2\rangle$$
$$+0.0026|^3F_2 -2\rangle + 0.0011|^3P_2 -2\rangle - 0.0417|^1I_6 -2\rangle$$
$$+0.0864|^1I_6 4\rangle + 0.0019|^1G_4 -2\rangle - 0.0076|^1G_4 4\rangle$$
$$-0.0007|^1D_2 -2\rangle \qquad W_8^{(0)} = 278 \text{ cm}^{-1}$$

$$\Phi_9 = -0.7037\,|^3H_6 3\rangle + 0.7037\,|^3H_6 -3\rangle - 0.0072\,|^3H_5 3\rangle$$
$$-0.0072\,|^3H_5 -3\rangle - 0.0015\,|^3H_4 3\rangle + 0.0015\,|^3H_4 -3\rangle$$
$$+0.0089\,|^3F_4 3\rangle - 0.0089\,|^3F_4 -3\rangle - 0.0068\,|^3F_3 3\rangle$$
$$-0.0068\,|^3F_3 -3\rangle - 0.0680\,|^1I_6 3\rangle + 0.0680\,|^1I_6 -3\rangle$$
$$+0.0040\,|^1G_4 3\rangle - 0.0040\,|^1G_4 -3\rangle$$

$$W_9^{(0)} = 305 \text{ cm}^{-1}$$

III.3. INTERPRETATION OF THE OPTICAL SPECTRA, MAGNETIC SUSCEPTIBILITY AND g-VALUE OF PRASEODYMIUM ETHYL SULPHATE

III.3.1. INTRODUCTION

In this section we aim at a consistent interpretation of the magnetic susceptibility, optical absorption spectra and e.p.r data of praseodymium ethyl sulphate (Pr.ES.) . Previous workers have reported different values of some parameters to interpret the different experimental results such as optical absorption[117,118], magnetic susceptibility and anisotropy. We shall investigate to what extent it is possible to interpret the available optical, magnetic susceptibility and e.p.r data simultaneously with a unique set of parameters. The diagonalisation of the complete Hamiltonian consisting of interelectronic repulsion (ES), spin-orbit interaction (SO) and the crystal field interaction (CF) considered together has been carried out. The full J-mixing is thus taken into account. The same type of treatment was done by Gruber to interpret the optical data of Pr.ES. and he deduced the ES parameters (F_2 , F_4 , F_6) SO coupling constant (ζ) and CF parameters by fitting a large number of optical levels to within 0.1% . But he did not test whether his parameters deduced from optical data were consistent with the magnetic

susceptibility and e.p.r data. It is to be noted that e.p.r , optical absorption and magnetic measurements were not performed with the identical samples of Pr.ES. The e.p.r experiment was performed at low temperature for Pr^{3+} in yttrium ethyl sulphate[119] . The optical absorption experiment for concentrated crystal of Pr.ES. was done by Hüfner[117] . For diluted crystal of Pr^{3+}, the same experiment was done by Hellwege et al[120] and by Gruber[118] . The magnetic susceptibility measurements of concentrated crystal of Pr.ES. were performed earlier by Van den Handel[121] and later by Hellwege et al[122] at different temperatures. But nobody made any attempt to fit theoretically the three experiments: optical absorption, magnetic susceptibility and e.p.r measurements of concentrated Pr.ES. with a single set of parameters. This invokes us to reinvestigate the problem systematically.

III.3.2. CRYSTAL FIELD ENERGY LEVELS

The Pr^{3+} ion in Pr.ES. crystal is considered to be in a D_{3h} symmetry. So the effective hamiltonian of Pr^{3+} ion in D_{3h} site symmetry and in absence of configuration interaction (C.I.) is given by

$$\mathcal{H}_{eff} = \sum_{i<j} \frac{e^2}{r_{ij}} + \zeta \sum_{i} \underset{\sim}{l}_i \cdot \underset{\sim}{s}_i + A_{20} U_o^{(2)} + A_{40} U_o^{(4)} + A_{60} U_o^{(6)} + A_{66} (U_6^{(6)} + U_{-6}^{(6)}) \qquad \text{(III.3.1)}$$

Gruber diagonalised the matrix of (III.3.1) in a basis of all the states belonging to $^3PFH^1SDGI$ terms of the Pr^{3+} ion. But he did not quote the various CF states in his paper which are required to calculate the magnetic susceptibilities and the g-values. So we repeat the diagonalisation of the complete energy matrix. Equation (III.3.1) does not include the term arising from C.I. which has been discussed earlier in chapter I and which was actually introduced by Rajnak and Wybourne[49] . In course of our investigation we find that unless these C.I. terms are included, a satisfactory agreement of the theory with the experiment is not possible. So by introducing the C.I. term the form of $\mathcal{H}_{eff}$ becomes

$$\mathcal{H}_{eff} = \sum_{i<j} \frac{e^2}{r_{ij}} + \zeta \sum_i \underset{\sim}{l}_i \cdot \underset{\sim}{s}_i + A_{20}U_o^{(2)} + A_{40}U_o^{(4)} + A_{60}U_o^{(6)}$$

$$+ A_{66}(U_6^{(6)} + U_{-6}^{(6)}) + \alpha L(L+1) + \beta G(G_2) + \gamma G(R_7) \qquad \text{(III.3.2)}$$

where $G(G_2)$ and $G(R_7)$ are the eigen values of Casimir's operators for the groups G_2 and R_7 used to classify the states of f^n configuration. These eigenvalues may be calculated in terms of the integers (u_1u_2) and $(w_1w_2w_3)$ used to label the irreducible representations of the groups G_2 and R_7 and are tabulated by Wybourne[102] . We use those values. α, β, γ are to be treated as adjustable parameters. In both the above equations A_{kq}'s are the crystal field parameters in tensor operator form and $U_q^{(k)}$ is the irreducible tensor operator.

The matrix elements of (III.3.1) or (III.3.2) were obtained by the same procedure as was mentioned in section III.2 .

III.3.3. COVALENCY REDUCTION OF ORBITAL ANGULAR MOMENTUM

We find that (as in the case of NES) it is impossible to achieve a good fit to the g-values and magnetic susceptibilities unless a reduction of the orbital angular momentum is used in the calculation of these quantities. So a small covalency reduction is introduced here to fit the experimental results. The details of the covalency reduction of the orbital angular momentum has been discussed earlier (chapter II).

III.3.4. CALCULATION OF THE PARAMAGNETIC SUSCEPTIBILITY

Significant contribution to the magnetic susceptibility of Pr^{3+} comes from only the lowest multiplet of $^3H_4$. $^3H_4$ contains 9 crystal field states of which 3 are doublets and 3 are singlets. The paramagnetic ionic susceptibility at different temperatures is obtained from Van Vleck's expression as given in chapter II. The 9CF states are given in Appendix III.3 at the end of this section.

III.3.5. CALCULATION OF g-VALUES

For the calculation of principal g-values one is interested only in the lowest doublet (Φ_1 , Φ_1') in the CF level

pattern. With the introduction of the covalency reduction factors ($k_{\parallel}$ and $k_{\perp}$) for the orbital angular momentum operator, the expressions for the g-values are

$$g_{\parallel} = g_Z = \left| \langle \Phi_1 | k_{\parallel} L_Z + 2S_Z | \Phi_1 \rangle - \langle \Phi_1' | k_{\parallel} L_Z + 2S_Z | \Phi_1' \rangle \right| ,$$

$$g_{\perp} = g_x = g_y = 2 \left| \langle \Phi_1 | k_{\perp} L_x + 2S_x | \Phi_1' \rangle \right| = 2 \left| \langle \Phi_1 | k_{\perp} L_y + 2S_y | \Phi_1' \rangle \right|$$

$$= 0$$

III.3.6. RESULTS AND DISCUSSION

Before we start interpreting the experimental data with the present theory it should be noted that the e.p.r, optical absorption and magnetic measurements were not performed with identical samples of Pr.ES. The e.p.r experiment was performed at low temperature for Pr^{3+} in Yttrium ethyl sulphate[119]. There are three sets of optical data that are available, one for the concentrated crystal of Pr.ES.[117] and two others for the diluted crystals of Pr^{3+} in lanthanum ethyl sulphate[118,120]. Magnetic measurements at different temperatures were however performed for the undiluted crystals of Pr.ES. The levels that could only be observed in the spectrum of concentrated crystals of Pr.ES. are $^3H_4$, $^3P_1$, $^1I_6$ and $^3P_2$. Our aim will be to have a good fit of these levels along with the magnetic susceptibility data, g-value and structural observation.

Earlier Gruber claimed to fit the whole spectrum having a large number of levels by exact diagonalisation of the energy

matrix. He quoted the values of three electrostatic parameters, one spin-orbit coupling parameter and four crystal field parameters. We repeated the calculation as we needed crystal field wave functions. After diagonalising the same matrix with Gruber's set of parameters, we were surprised to observe that not only the centre of gravity of all the levels were shifted but also $^3P_1$ multiplet goes above the $^1I_6$ multiplet contrary to Gruber's calculation and experimental findings. Also the position of ± 1 and 0 components of $^1I_6$ manifold are reversed. The separation between ± 2 and 3 components of $^3H_4$ manifold comes out to be 17.2 cm^{-1} against 12.2 cm^{-1} as quoted by Gruber . The separation between ± 2 and 3 components plays an important role in the calculation of the susceptibility. So at this stage we are unable to find any reason for having results different from those of Gruber even though calculation with identical set of parameters was done. When the results obtained from CF calculations by using Gruber's set of parameters are used further for g-value and magnetic susceptibility calculation, it is found that the g-value comes out to be large (2.26 compared to the experimental value 1.525), about 48% larger than the observed value. Experimental data shows that at lower temperature $K_{\parallel}$ is smaller than $K_{\perp}$ and around 137K the two curves cross over. But unfortunately we could not reproduce it with Gruber's set of parameters. No reversal of anisotropy ($K_{\perp} - K_{\parallel}$) occurs at any temperature in

the entire range from liquid helium upto room temperature, but $K_{||}$ is smaller than $K_{\perp}$ throughout the range. It is also noticed that for $K_{||}$ the calculated values are higher than the experimental one throughout the whole range of temperature. The difference between the observed and the calculated values varies from 102.8% to 5.9% . It is pronounced at low temperature region and it is largest (102.8%) at the lowest temperature of measurement (6.25K). On the other hand in the case of $K_{\perp}$ this difference between calculated and observed values is less pronounced (varying from 18.5% to 4.2%) and the calculated values are higher than observed values except at the temperatures 6.25K and 12.5K . Now from the large values of $g_{||}$ and also $K_{||}$ and $K_{\perp}$ one may suggest that a covalency reduction should be introduced in the orbital angular momentum. Next introducing covalency reduction for the orbital moment we made exhaustive trials and found that to have an appropriate reduction in $g_{||}$ value a covalency reduction factor as high as 0.8 should be introduced in the calculation of the $K_{||}$ and about 0.95 in the $K_{\perp}$. The $g_{||}$ value comes down to within 1% but the deviation of the susceptibility still remains as high as 41.7% and the reversal point does not occur. Thus we are unable to fit the susceptibility data even within 10% with Gruber's set.

While fitting the observed splitting between the crystal field levels of the concentrated crystals of Pr.ES. using

R-S coupling and without doing J-mixing, Hüfner quoted four crystal field parameters. Although such calculation cannot give electrostatic and SO parameter as it concerns with the splitting of individual free ion levels in a crystal field, it was found that fitting of the crystal field splittings was more or less satisfactory. But there were discrepancies in the assignment of the different crystal field components. The lowest crystal field component of ground term $^3H_4$ according to their calculation was the doublet ($\bar{\mu} = \pm 1$), whereas from the later experiment of Gruber it is the doublet ($\bar{\mu}=\pm 2$) which is lowest. Also in Hüfner's calculation the components 0 and ± 1 of $^1I_6$ multiplet and ± 2 and ± 1 components of $^3P_2$ multiplet interchanged their positions when compared with the observed spectra. We first used these CF parameters of Hüfner along with the spectrF_2, F_4, F_6 and ζ of Gruber to diagonalise exactly the full matrix and obtained the g-value and susceptibility. While carrying out the exact diagonalisation the fitting becomes worse, the optical absorption spectra cannot be explained, the lowest CF component of ground level comes out to be a singlet $\bar{\mu} = 3$ in complete disagreement with the observed spectra.

So it was clear that both Gruber's and Hüfner's parameters were not satisfactory for a consistent study of all the physical properties mentioned earlier. If the theory is made to agree with results of one type of experiment, it deviates

considerably from the other types of experiment. We made an extensive trial method and the following facts were revealed :

i) It is only possible to fit the theory with all the experimental data within some optimum limit with a single set of parameters but an exact agreement between the theory and all the experiments is too much to be expected.

ii) To change the centre of gravity of the multiplets, so that all of them come in right order, introduction of C.I. parameters α, β, γ in our calculation becomes imperative.

iii) The covalency reduction factors ($k_{\parallel}$ and $k_{\perp}$) for the orbital angular momentum are to be introduced for having a good fit to (a) the g-values, (b) to reproduce the reversal of the anisotropy ($K_{\perp} - K_{\parallel}$) at about 137K, and (c) the susceptibilities within 10% throughout the entire range of temperature.

We use the following set of parameters which gave a good fit to the optical, e.p.r and magnetic susceptibility data :

$F_2 = 307.5\ cm^{-1}$, $F_4 = 50\ cm^{-1}$, $F_6 = 5.0\ cm^{-1}$, $\zeta = 727.9\ cm^{-1}$, $\alpha = 11.0$, $\beta = -450.0$, $\gamma = 1000.0$, $B_2^0\langle r^2\rangle = 32.94\ cm^{-1}$, $B_4^0\langle r^4\rangle = -77.57\ cm^{-1}$, $B_6^0\langle r^6\rangle = -53.33\ cm^{-1}$, $B_6^6\langle r^6\rangle = 985.49\ cm^{-1}$, $k_{\parallel} = 0.99$, $k_{\perp} = 0.98$.

The set of parameters which were used by Gruber[118] are as follows :

$F_2 = 307.4\ cm^{-1}$, $F_4 = 49.44\ cm^{-1}$, $F_6 = 5.138\ cm^{-1}$, $\zeta = 727.9\ cm^{-1}$, $B_2^0\langle r^2\rangle = 15.31\ cm^{-1}$, $B_4^0\langle r^4\rangle = -88.32\ cm^{-1}$, $B_6^0\langle r^6\rangle = -48.76\ cm^{-1}$, $B_6^6\langle r^6\rangle = 548.48\ cm^{-1}$.

The set of parameters due to Hüfner[117] are as follows :

$B_2^o\langle r^2\rangle = 23\ cm^{-1}$, $B_4^o\langle r^4\rangle = -80\ cm^{-1}$, $B_6^o\langle r^6\rangle = -44\ cm^{-1}$, $B_6^6\langle r^6\rangle = 695\ cm^{-1}$.

In table III.3.1 we have presented the experimental optical levels and also the theoretical levels with different sets of parameters chosen. In the same table we have also placed the results obtained by Gruber from their own calculation. Fig. III.3.1 shows that the maximum deviation in $K_{\parallel}$ is about 10% and in $K_{\perp}$ is about 6% from the experimental curve. Our calculated $g_{\parallel}$ value deviates from the experimental value by 1.3% (the experimental $g_{\parallel} = 1.52$ and the theoretical $g_{\parallel}$ is 1.54). The slight discrepancy in $g_{\parallel}$ value is quite expected as the theoretical value is referred to the concentrated crystal of Pr.ES. but the experimental result obtained for the diluted crystal of Pr.ES. Table III.3.1 shows that there remains slight discrepancies in $^1I_6$ multiplets and $^3P_2$ multiplets when we use our own set of parameters. Two components ± 1 and 0 of $^1I_6$ manifold have interchanged their positions and two components ± 2 and ± 1 of $^3P_2$ have interchanged their normal positions. These discrepancies cannot be improved by any adjustment of the 13 parameters which we have mentioned earlier. The possible corrections which may improve the results are the following :

i) Small distortion in the crystals of Pr.ES. may exist even at room temperature. A small departure from reflection symmetry in X-Y plane will change the symmetry of the ion from pure C_{3h} and introduce terms $Y_4^{\pm 3}$ and $Y_6^{\pm 3}$ into the crystal potential, i.e. the new potential will be C_{3v} in which A_{43}, A_{63} parameters will have very low value. Noting that the new potential does not further lift the degeneracy found with pure C_{3h}, such distortion was suggested by Elliott and Stevens[110] for Ce-ethyl sulphate to interpret simultaneously the temperature variation of susceptibility and the observed g-values, the latter being much less than the values calculated on the assumption of a pure C_{3h} symmetry. The second one is that we have assumed in our calculation that all the CF parameters are temperature independent. There may be some temperature dependence of the CF parameters.

Finally we conclude that for future refinement of the theory in the light of the above discussion precise and more experimental data for the concentrated crystal, particularly the optical data of the ground manifold are necessary. This will help to calculate the magnetic susceptibilities and the g-values accurately.

All the calculations which have been presented here were done by computer B6700 using a complete program developed by us.

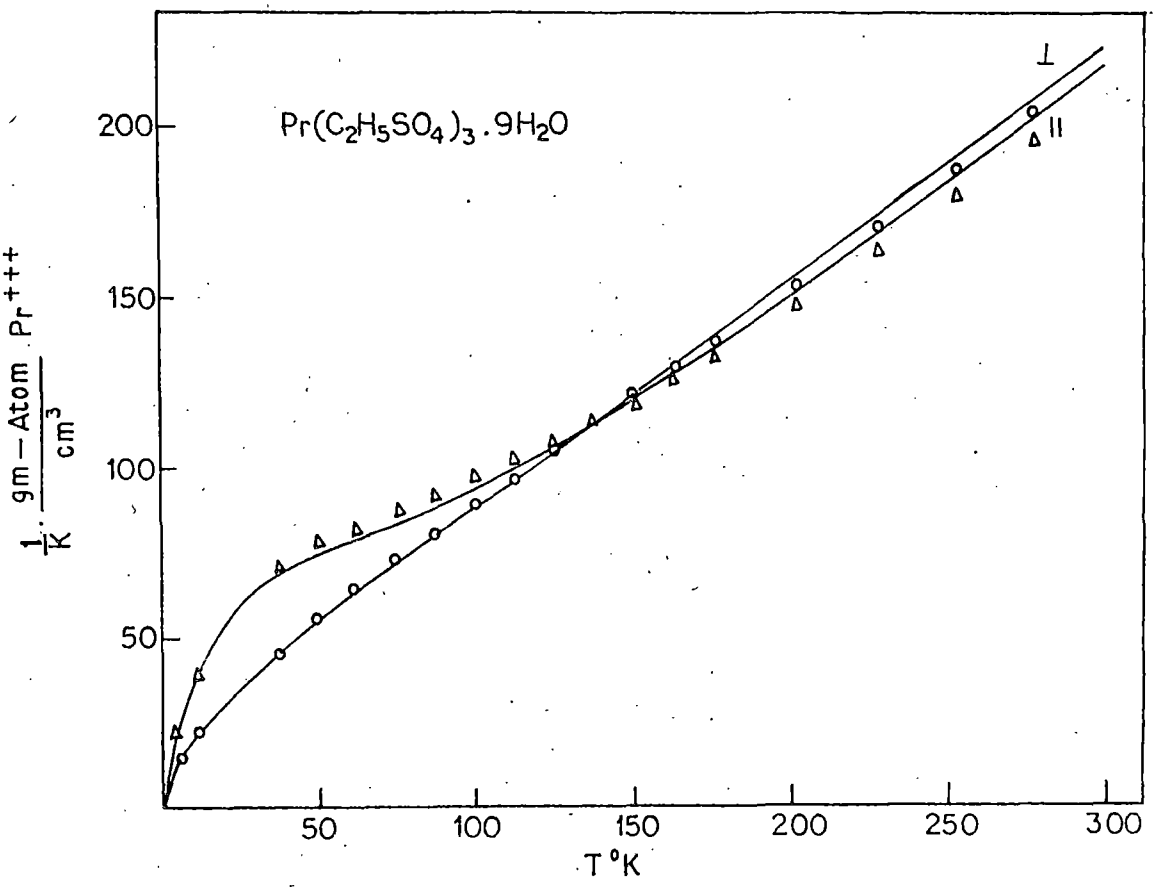

Fig. III.3.1. $\frac{1}{K_{\parallel}}$ and $\frac{1}{K_{\perp}}$ of Pr.ES. (gm - atom) cm^{-3} at different temperatures (T) in K.

Δ,o Theoretical points.

— Experimental smoothed curve.

Table III.3.1.

Comparison of the experimental and the theoretical crystal field levels

Terms	$\bar{\mu}$	Experimental levels	Theoretical levels obtained from the best fit parameters	Theoretical levels obtained by using Gruber's set of parameters in our calculations	Results obtained from Gruber's[118] original Table II
$^3H_4$	±2	0[a,b]	0	0	0
	3	11.9[a] 12.2[b]	12	17	15
	±1	(175±2)[b]	190	172	176
	±2	(188±28)[a]	303	192	192
	3	(181±2)[b]	241	180	181
	0	-	314	288	288
$^3F_3$	3	-	6345	6266	6330
	0	6310[b]	6344	6251	6309
	±2	6331[b]	6358	6264	6330
	±1	6383[b]	6417	6317	6383
	3	-	6458	6346	6413
$^3F_4$	3	-	6917	6763	6767
	3	-	6972	6810	6798
	±2	6831[b]	6990	6841	6825
	±1	6863[b]	7025	6882	6864
	0	6872[b]	7027	6886	6873
	±2	6896[b]	7060	6916	6895
$^1G_4$	3	-	9749	9566	9476
	3	-	10091	9804	9736
	0	9794[b]	10070	9858	9789
	±2	9811[b]	10071	9864	9806
	±1	9863[b]	10162	9930	9867
	±2	-	10399	10055	10000
$^1D_2$	0	16709[b]	16994	17051	16724
	±2	16858[b]	17144	17184	16857
	±1	16955[b]	17203	17267	16951
$^3P_0$	0	20687[b]	20651	20720	20687
$^3P_1$	±1	21276[a] 21281.1[b]	21234	21302	21281
	0	21290[a] 21290.6[b]	21254	21311	21290
$^1I_6$	0	21399[a]	21367	20867	21401
	0	21408[a]	21384	20880	21410
	±1	21447[a]	21426	20909	21443
	0	21456[a]	21417	20893	21447
	±2	-	21515	21009	21540
	±1	-	21527	21038	21570
	3	-	21570	21078	21610
	±2	-	21639	21138	21672
	3	-	21665	21146	21679
$^3P_2$	0	22425[a]	22447	22521	21422
	±2	22441[a]	22473	22524	22443
	±1	22448[a]	22466	22531	22450

[b]Results of diluted crystal of Pr.ES.[117], [a]Results of concentrated crystal of Pr.ES[118,120].

APPENDIX III.3.

CF wave functions and the energy values of the ground term ($^3H_4$) of Praseodymium ethyl sulphate obtained from our own set of fitted parameters

$$\Phi_1 = -0.0054\,|^3H_6 2\rangle - 0.0188\,|^3H_6 -4\rangle - 0.0229\,|^3H_5 2\rangle$$
$$+0.0587\,|^3H_5 -4\rangle + 0.9066\,|^3H_4 2\rangle - 0.3904\,|^3H_4 -4\rangle$$
$$-0.0099\,|^3F_4 2\rangle - 0.0057\,|^3F_4 -4\rangle - 0.0119\,|^3F_3 2\rangle$$
$$+0.0314\,|^3F_2 -2\rangle + 0.0037\,|^3P_2 2\rangle + 0.0008\,|^1I_6 2\rangle$$
$$+0.0017\,|^1I_6 -4\rangle + 0.1314\,|^1G_4 2\rangle - 0.0530\,|^1G_4 -4\rangle$$
$$+0.0027\,|^1D_2 2\rangle \qquad \Big\} \; W_1^{(0)} = 0$$

$$\Phi_1' = -0.0054\,|^3H_6 -2\rangle - 0.0188\,|^3H_6 4\rangle - 0.0229\,|^3H_5 -2\rangle$$
$$+0.0587\,|^3H_5 4\rangle + 0.9066\,|^3H_4 -2\rangle - 0.3904\,|^3H_4 4\rangle$$
$$-0.0099\,|^3F_4 -2\rangle - 0.0057\,|^3F_4 4\rangle - 0.0119\,|^3F_3 -2\rangle$$
$$+0.0314\,|^3F_2 -2\rangle + 0.0037\,|^3P_2 -2\rangle + 0.0008\,|^1I_6 -2\rangle$$
$$+0.0017\,|^1I_6 4\rangle + 0.1314\,|^1G_4 -2\rangle - 0.0530\,|^1G_4 4\rangle$$
$$+0.0027\,|^1D_2 -2\rangle \qquad \Big\} \; W_1^{(0)} = 0$$

$$\Phi_2 = -0.0061\,|^3H_6 3\rangle + 0.0061\,|^3H_6 -3\rangle + 0.0754\,|^3H_5 3\rangle$$
$$+0.0754\,|^3H_5 -3\rangle + 0.6942\,|^3H_4 3\rangle - 0.6942\,|^3H_4 -3\rangle$$
$$-0.0198\,|^3F_4 3\rangle + 0.0198\,|^3F_4 -3\rangle + 0.0308\,|^3F_3 3\rangle$$
$$+0.0308\,|^3F_3 -3\rangle + 0.0008\,|^1I_6 3\rangle - 0.0008\,|^1I_6 -3\rangle$$
$$+0.1050\,|^1G_4 3\rangle - 0.1050\,|^1G_4 -3\rangle \qquad W_2^{(0)} = 12 \text{ cm}^{-1}$$

$$\Phi_3 = -0.0156\,|^3H_6 5\rangle + 0.0079\,|^3H_6 -1\rangle - 0.0503\,|^3H_5 5\rangle$$
$$+0.0668\,|^3H_5 -1\rangle + 0.9844\,|^3H_4 -1\rangle - 0.0267\,|^3F_4 -1\rangle$$
$$-0.0122\,|^3F_3 -1\rangle - 0.0113\,|^3F_2 -1\rangle - 0.0032\,|^3P_2 -1\rangle$$
$$-0.0034\,|^3P_1 -1\rangle + 0.0019\,|^1I_6 5\rangle - 0.0012\,|^1I_6 -1\rangle$$
$$+0.1502\,|^1G_4 -1\rangle - 0.0003\,|^1D_2 -1\rangle \qquad W_3^{(0)} = 190 \text{ cm}^{-1}$$

$$\Phi_3' = -0.0156\,|^3H_6 -5\rangle + 0.0079\,|^3H_6 1\rangle - 0.0503\,|^3H_5 -5\rangle$$
$$+0.0668\,|^3H_5 1\rangle + 0.9844\,|^3H_4 1\rangle - 0.0267\,|^3F_4 1\rangle$$
$$-0.0122\,|^3F_3 1\rangle - 0.0113\,|^3F_2 1\rangle - 0.0032\,|^3P_2 1\rangle$$
$$-0.0034\,|^3P_1 1\rangle + 0.0019\,|^1I_6 -5\rangle - 0.0012\,|^1I_6 1\rangle$$
$$+0.1502\,|^1G_4 1\rangle - 0.0003\,|^1D_2 1\rangle \qquad W_3^{(0)} = 190 \text{ cm}^{-1}$$

$$\Phi_4 = -0.0071\,|^3H_6\,2\rangle - 0.0019\,|^3H_6\,-4\rangle - 0.0479\,|^3H_5\,2\rangle + 0.0351\,|^3H_5\,-4\rangle + 0.3854\,|^3H_4\,2\rangle + 0.9066\,|^3H_4\,-4\rangle - 0.1091\,|^3F_4\,2\rangle - 0.0272\,|^3F_4\,-4\rangle - 0.0370\,|^3F_3\,2\rangle - 0.0071\,|^3F_2\,2\rangle - 0.0043\,|^3P_2\,2\rangle + 0.0010\,|^1I_6\,2\rangle + 0.0008\,|^1I_6\,-4\rangle + 0.0626\,|^1G_4\,2\rangle + 0.1395\,|^1G_4\,-4\rangle + 0.0005\,|^1D_2\,2\rangle \qquad W_4^{(0)} = 203 \text{ cm}^{-1}$$

$$\Phi_4' = -0.0071\,|^3H_6\,-2\rangle - 0.0019\,|^3H_6\,4\rangle - 0.0479\,|^3H_5\,-2\rangle + 0.0351\,|^3H_5\,4\rangle + 0.3854\,|^3H_4\,-2\rangle + 0.9066\,|^3H_4\,4\rangle - 0.0191\,|^3F_4\,-2\rangle - 0.0272\,|^3F_4\,4\rangle - 0.0370\,|^3F_3\,-2\rangle + 0.0008\,|^1I_6\,4\rangle + 0.0626\,|^1G_4\,-2\rangle + 0.1395\,|^1G_4\,4\rangle + 0.0005\,|^1D_2\,-2\rangle \qquad W_4^{(0)} = 203 \text{ cm}^{-1}$$

$$\Phi_5 = -0.0150\,|^3H_6\,3\rangle - 0.0150\,|^3H_6\,-3\rangle - 0.0071\,|^3H_5\,3\rangle + 0.0071\,|^3H_5\,-3\rangle + 0.6957\,|^3H_4\,3\rangle - 0.6957\,|^3H_4\,-3\rangle - 0.0424\,|^3F_4\,3\rangle - 0.0424\,|^3F_4\,-3\rangle - 0.0051\,|^3F_3\,3\rangle + 0.0051\,|^3F_3\,-3\rangle + 0.0025\,|^1I_6\,3\rangle + 0.0025\,|^1I_6\,-3\rangle + 0.1178\,|^1G_4\,3\rangle + 0.1178\,|^1G_4\,-3\rangle \qquad W_5^{(0)} = 241 \text{ cm}^{-1}$$

$$\Phi_6 = -0.0121\,|^3H_6 6\rangle + 0.0146\,|^3H_6 0\rangle - 0.0121\,|^3H_6 -6\rangle$$
$$-0.0000\,|^3H_5 0\rangle + 0.9867\,|^3H_4 0\rangle - 0.0373\,|^3F_4 0\rangle$$
$$+0.0000\,|^3F_3 0\rangle + 0.0027\,|^3F_2 0\rangle + 0.0028\,|^3P_2 0\rangle$$
$$-0.0000\,|^3P_1 0\rangle + 0.0049\,|^3P_0 0\rangle + 0.0015\,|^1I_6 6\rangle$$
$$-0.0024\,|^1I_6 0\rangle + 0.0015\,|^1I_6 -6\rangle + 0.1566\,|^1G_4 0\rangle$$
$$-0.0006\,|^1D_2 0\rangle + 0.0008\,|^1S_0 0\rangle$$

$W_6^{(0)} = 314 \text{ cm}^{-1}$

III.4. STUDY OF THE CRYSTAL FIELD SPECTRA, MAGNETIC SUSCEPTIBILITIES AND THE g-VALUES OF $Pr_2Mg_3(NO_3)_{12}\cdot 24H_2O$

III.4.1. INTRODUCTION

The present section attempts a consistent interpretation of the results of the optical absorption experiment, the magnetic susceptibility measurement and the g-values of $Pr_2Mg_3(NO_3)_{12}\cdot 24H_2O$, (Pr.DN.) with the help of a single set of parameters. Here we have presented a rigorous theoretical approach to the problem. The optical absorption experiment of Pr.DN. was performed by Hellwege and Hellwege[123] . They performed their experiment at about 58K and observed certain crystal field levels. Later Judd[124] tried to explain theoretically the crystal field levels which were obtained by Hellwege and Hellwege[123] . Judd[124] supposed that the rare-earth ion in a double nitrate crystal has a C_{3v} point group symmetry. He did a first order perturbation calculation for crystal field splitting. Judd was the pioneer worker in the theoretical calculation of crystal field splitting of Pr.DN. He concluded that the Russell-Saunders coupling is totally inadequate to explain the various multiplets. However, he did not carry out the intermediate coupling calculation. The first

order perturbation calculation for the crystal field splitting does not necessarily take into account the J-mixing which has an important role in the crystal field splitting. It is therefore quite natural that such calculation will give only an approximate fit to the crystal field components of the various levels. The first order calculation of the crystal field levels by Judd gave the six crystal field parameters $A_2^o\langle r^2\rangle$, $A_4^o\langle r^4\rangle$, $A_6^o\langle r^6\rangle$, $A_6^6\langle r^6\rangle$, $A_4^3\langle r^4\rangle$, $A_6^3\langle r^6\rangle$. The values of the electrostatic parameters F_2 , F_4 , F_6 and spin-orbit coupling constant ζ cannot be obtained from the first-order calculation.

Cooke and Duffus[90] obtained the $g_{\parallel}$ value of Pr^{3+} diluted in $La_2Mg_3(NO_3)_{12}\cdot 24H_2O$. The parallel and perpendicular susceptibility measurements of Pr.DN. from 4.4K to 300K were done by Hellwege et al.[125] . But nobody made any attempt to fit the magnetic susceptibility results and the g-value as yet with the values of the parameters that fit the optical absorption results. It was already pointed out by Judd that the parameter deduced by him, using R.S. coupling will not faithfully reproduce the results of optical absorption measurement. Hence, one would therefore cannot expect that simultaneous fitting of the optical, e.p.r and magnetic susceptibility measurements can be made with this set of parameters.

We have presented a rigorous approach which takes into account not only the intermediate coupling but also all possible J-mixing under the crystal field. We have carried out diagonalisation of the matrix of spin-orbit (SO), electrostatic (ES) and crystal field (CF) interaction considered together, the matrix being constructed in a basis of all states of Pr^{3+} in $4f^2$ configuration. This takes into account the full J-mixing. When the parameters given by Judd were used in such calculation it is found that not only the optical levels deviate from the experimental results (see table III.4.1), but also the g-value and susceptibility results deviate considerably from the observed values, the g-value comes out to be $g_{\parallel} = 1.26$ against the experimental $g_{\parallel} = 1.55$ and maximum deviations of the parallel and perpendicular susceptibility from the experimental value come out to be about 17% and 51% respectively.

The aim of this chapter is to see whether it is possible to interpret the optical data, the magnetic susceptibility results and the g-value of Pr.DN. with a single set of parameters which gives a good fit to these experiments simultaneously.[126]

III.4.2. CRYSTALLOGRAPHIC BACKGROUND

The detailed X-ray crystallographic study of $Ce_2Mg_3(NO_3)_{12}\cdot 24H_2O$ has been carried out by Zalkin et al[127]. $Pr_2Mg_3(NO_3)_{12}\cdot$

$24H_2O$ is considered to be isomorphous to the cerium crystal. The crystals are rhombohedral, space group is $R\bar{3}$. The lanthanide ion is surrounded by twelve oxygen atoms at an average distance of 0.264 nm . These atoms belonging to six nitrate ions, are at the corners of a somewhat irregular icosahedron. The Mg atoms are of two kinds, each surrounded by six water molecules whose oxygen atoms lie at the corners of an octahedron with Mg-O distance of 0.207 nm (see Fig. III.4.1). The site symmetry at the lanthanide ion found by Zalkin et al[127] (Fig.III.4.2) is C_3 . But the spectroscopic and the resonance data have mostly been interpreted assuming the symmetry to be C_{3v} . Later Devine[128] suggested that T_h symmetry is a more realistic approximation to the nearest neighbours of the rare-earth ion than C_{3v} as there is a complete absence of mirror plane. But T_h site symmetry disregards the presence of A_2^o parameter in the crystal field which actually governs the splitting of $^3P_1$ level. On the other hand the IIa line in the transition $^3H_4 \rightarrow {}^3P_1$ of Pr.DN.is comparatively weak. This led Hellwege and Hellwege[125] to decide on C_{3v} rather than C_3 for the site symmetry, as an extra selection rule arises owing to the two types of A levels in the irreducible representations of C_{3v} . Devine also could not fit very well the spectroscopic results of Pr.DN. due to the absence of A_2^o term in T_h crystal field.

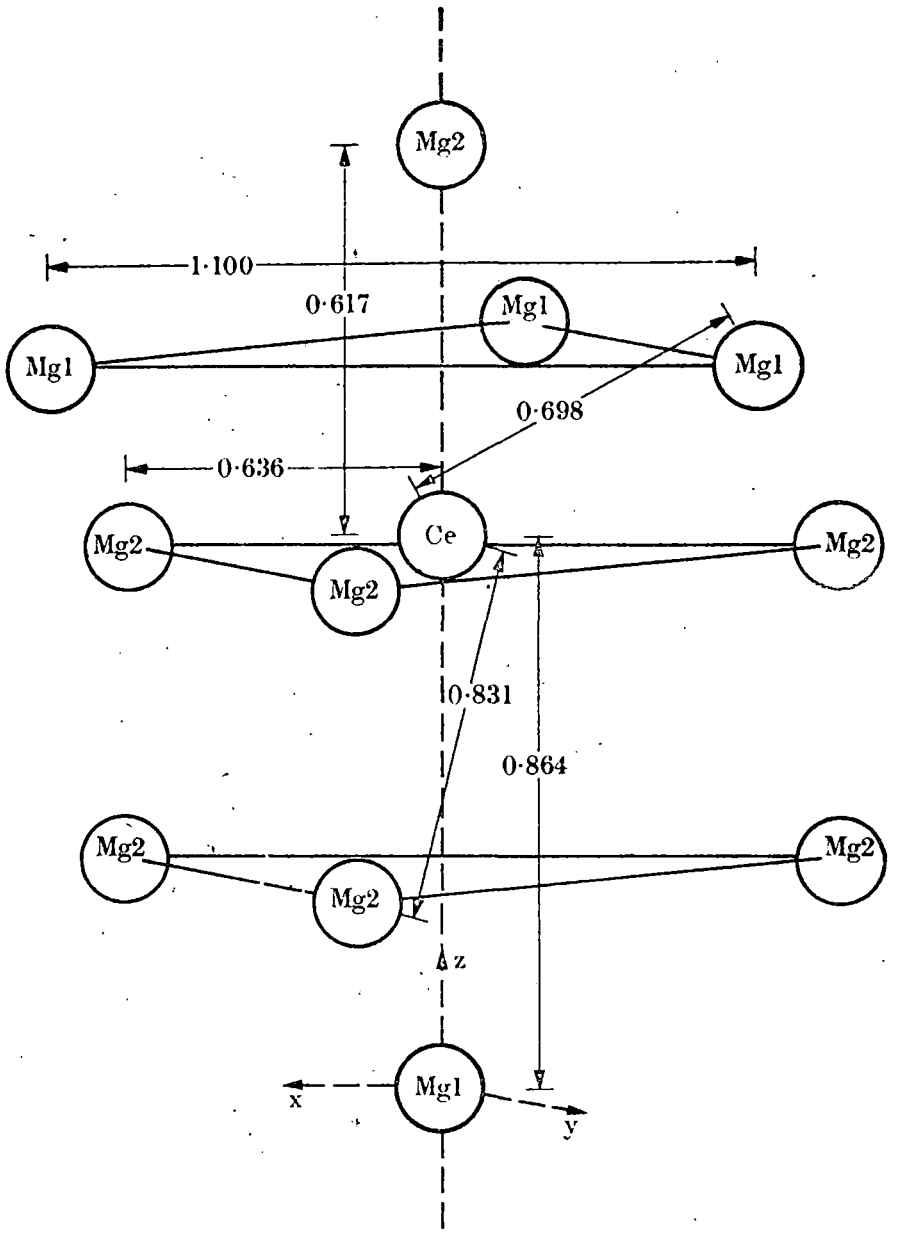

Fig. III.4.1. Positions of the magnesium ions (distances in nanometres) relative to a cerium ion in cerium magnesium nitrate (Zalkin, Forrester and Templeton 1963).

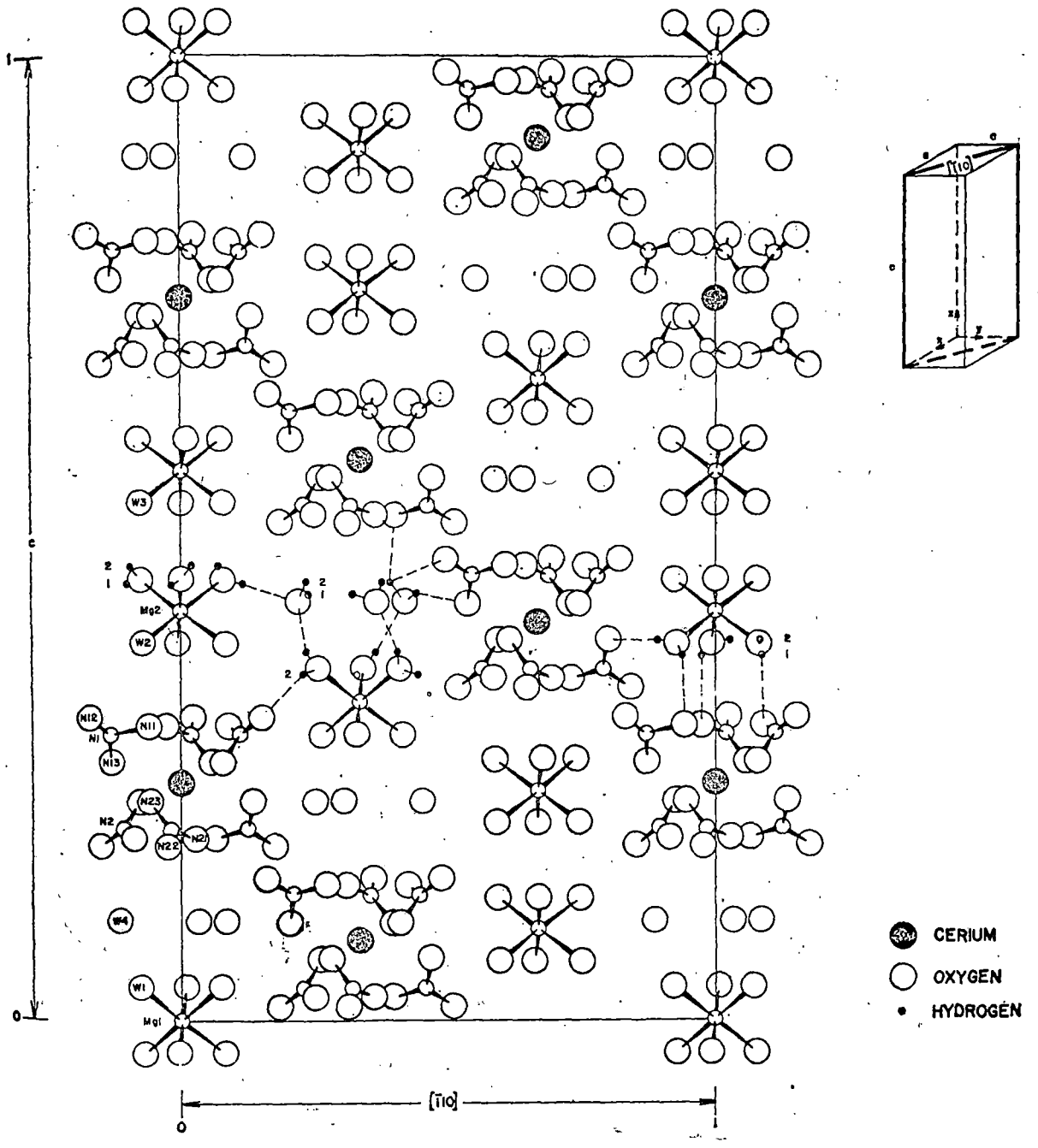

Fig. III.4.2. Crystal structure of $Ce_2Mg_3(NO_3)_{12}\cdot 24H_2O$. Atoms of Ce and Mg which lie in a section parallel with c and $\bar{1}10$ are shown together with nitrate ions and water molecule, near this section. Examples are shown of each kind of hydrogen atom and bond.

So this invokes us to take the site symmetry of Pr.DN. as C_{3v} where the six order parameters should be of high values in comparison to A_{20} , A_{40} , A_{43} parameters. This indicates that the actual symmetry is somewhat a distorted icosahedron having a 3-fold highest symmetry axis.

III.4.3. INTERPRETATION OF THE SPECTRA OF $Pr_2Mg_3(NO_3)_{12}\cdot 24H_2O$

The effective Hamiltonian of Pr^{3+} in a crystal is given by

$$\mathcal{H}_{eff} = \sum_{i<j} \frac{e^2}{r_{ij}} + \zeta \sum_i \underset{\sim}{l}_i \cdot \underset{\sim}{s}_i + H_c$$

H_c = crystal field interaction of the 4f electrons with the ligands.

Assuming a C_{3v} site symmetry H_c may be written as

$$H_c = A_{20}U_o^{(2)} + A_{40}U_o^{(4)} + A_{60}U_o^{(6)} + A_{66}(U_6^{(6)} + U_{-6}^{(6)})$$
$$+ A_{43}(U_3^{(4)} - U_{-3}^{(4)}) + A_{63}(U_3^{(6)} - U_{-3}^{(6)})$$

where $U_q^{(k)} = r^k Y_k^q$ is an irreducible tensor operator.

The crystal field parameter A_{kq}'s are related with the Stevens parameters B_k^q by a constant factor. The matrix elements of the effective Hamiltonian $\mathcal{H}_{eff}$ is constructed in a basis of states represented by $|UvSLJM\rangle$. All states belonging to the different multiplet terms $^3PFH\,^1SDGI$ have been taken into consideration for the representation of the above matrix

and it turns out to be 91 x 91 matrix. The matrix elements of electrostatic part for $4f^2$ configuration expressed in terms of Slater-Condon parameters F_k's have been tabulated by Nielson and Koster. We use those values. The matrix elements of spin-orbit interaction for $4f^2$ configuration have also been calculated by Spedding . We use those results of Spedding for $4f^2$ configuration. The matrix element of U^k_q was obtained by the same procedure as mentioned in chapter II. Thus the 91x91 matrix is set up. But due to the crystal symmetry the whole matrix splits up into 2 matrices of dimension 30x30 (crystal quantum number $\bar{\mu} = \pm 1$) and one matrix of dimension 31x31 ($\bar{\mu} = 0$).

A computer program was then developed in which the crystal field matrix elements were automatically generated and then added up to SO and ES contribution and after that the three matrices were diagonalised individually giving the crystal field states and corresponding energies. The program was then extended so that the crystal field results can invoke a second portion of the program which automatically calculates the parallel and perpendicular susceptibilities at different temperatures. It also calculates the g-values for the lowest doublet of the ground term $^3H_4$.

III.4.4. CALCULATION OF g-VALUES

For the calculation of the principal g-values one is interested only in the lowest doublet in the CF level pattern. The two components of the lowest doublet arises from the two 30x30 matrices mentioned above. The components of the lowest doublet are denoted by Φ_1 and $\Phi_{1'}$.

$$g_{\parallel} = g_Z = \left|\langle\Phi_1|L_Z + 2S_Z|\Phi_1\rangle - \langle\Phi_{1'}|L_Z + 2S_Z|\Phi_{1'}\rangle\right|$$

$$g_{\perp} = 2\left|\langle\Phi_1|L_x + 2S_x|\Phi_{1'}\rangle\right| = 2\left|\langle\Phi_1|L_y + 2S_y|\Phi_{1'}\rangle\right| = 0$$

III.4.5. CALCULATION OF PARAMAGNETIC SUSCEPTIBILITY

Significant contribution to the paramagnetic susceptibility of Pr^{3+} comes from only the lowest multiplet of $^3H_4$. $^3H_4$ contains 9 crystal field states Φ_i's of which 3 are doublets and 3 are singlets. The ionic susceptibility is calculated using the formula (II.11.4) discussed earlier. The 9 CF states are given in Appendix III.4 at the end of this section.

III.4.6. RESULTS AND DISCUSSION

We use the following set of parameters which give a good fit to the optical, e.p.r and paramagnetic susceptibility data

$F_2 = 303\ cm^{-1}$, $F_4 = 60.5\ cm^{-1}$, $F_6 = 5.65\ cm^{-1}$, $\zeta = 730\ cm^{-1}$,
$B_2^0\langle r^2\rangle = -75.02\ cm^{-1}$, $B_4^0\langle r^4\rangle = -19.39\ cm^{-1}$, $B_6^0\langle r^6\rangle = -49.91\ cm^{-1}$,
$B_6^6\langle r^6\rangle = 702.74\ cm^{-1}$, $B_6^3\langle r^6\rangle = \mp 2907.92\ cm^{-1}$, $B_4^3\langle r^4\rangle = \pm 393.3\ cm^{-1}$.

The crystal field parameters which were given by Judd as follows

$B_2^0\langle r^2\rangle = -70\ cm^{-1}$, $B_4^0\langle r^4\rangle = -20\ cm^{-1}$, $B_6^0\langle r^6\rangle = -50\ cm^{-1}$,

$B_6^6\langle r^6\rangle = 700\ cm^{-1}$, $B_6^3\langle r^6\rangle = \mp 2300\ cm^{-1}$, $B_4^3\langle r^4\rangle = \pm 420\ cm^{-1}$.

It is found that our values of the three CF parameters B_4^0 , B_6^0 and B_6^6 differ only very slightly from the corresponding values given by Judd, but the values of the B_2^0 and B_4^3 differ by about 7% from those of Judd and our value of B_6^3 differs very appreciably from that of Judd by about 26% .

Table III.4.1 shows the calculated and the observed crystal field levels of Pr.DN. The experimental levels which were observed are only $^3H_4$, $^1D_2$, ^3P_o, $^3P_1$ and $^3P_2$ multiplets. Regarding $^3P_2$ multiplets one should note that Hellwege and Hellwege[123] obtained the two multiplets $\bar{\mu} = \pm 1$ and $\bar{\mu} = 0$ within 3 cm^{-1}. But it is very much doubtful. Since at that time the optical instrument was not so much sophisticated that this amount of resolution may be reliably done. After an extensive trial with several sets of parameters we also found that it is actually impossible to fit these two levels of $^3P_2$ as were given by Hellwege and Hellwege. We also found that $^1D_2$ level could not be fitted very well by any adjustment of the parameters. The discrepancy probably be explained if we consider the effect of configuration interaction on the crystal field

splitting and also the actual site mymmetry of Pr^{3+} ion in the double nitrate. Other crystal field levels are in close agreement with the experimental levels. The calculated g-values $g_{\parallel} = 1.58$, $g_{\perp} = 0$ show excellent agreement with the experimental g-values. The calculated $g_{\parallel}$ value differs from the experimental value only by 0.03 . One should also note that the experimental g-value refers to diluted crystal while the theoretical value refers to the concentrated crystal. This may account for the slight discrepancy in the theoretical and experimental g-values. For Nd^{3+} in ethyl sulphate[55] crystal, such differences between the diluted and undiluted crystals are already known to exist. Fig. III.4.3 shows the experimental curves for $\frac{1}{K_{\parallel}}$ and $\frac{1}{K_{\perp}}$ plotted against temperature along with the theoretical values at intervals of 20K. It clearly shows an overall good agreement between the theoretical and experimental susceptibility values over a wide range of temperatures with a maximum deviations of about 10% for $K_{\perp}$ and 4% for $K_{\parallel}$.

So we find that C_{3v} symmetry can successfully explain g-values the optical and magnetic data of Pr.DN. On the other hand T_h site symmetry as assumed by Devine will not be able to account for the splitting of $^3P_1$. This splitting entirely depends on the parameter B_2^o which does not exist in the T_h symmetry. There may be a slight improvement in the crystal

field levels of Pr.DN. ' ' done by adopting a least square technique. But due to small number in crystal field levels we do not attempt any least square fitting. All calculations presented in this section were done by a complete program developed by us in B6700 computer.

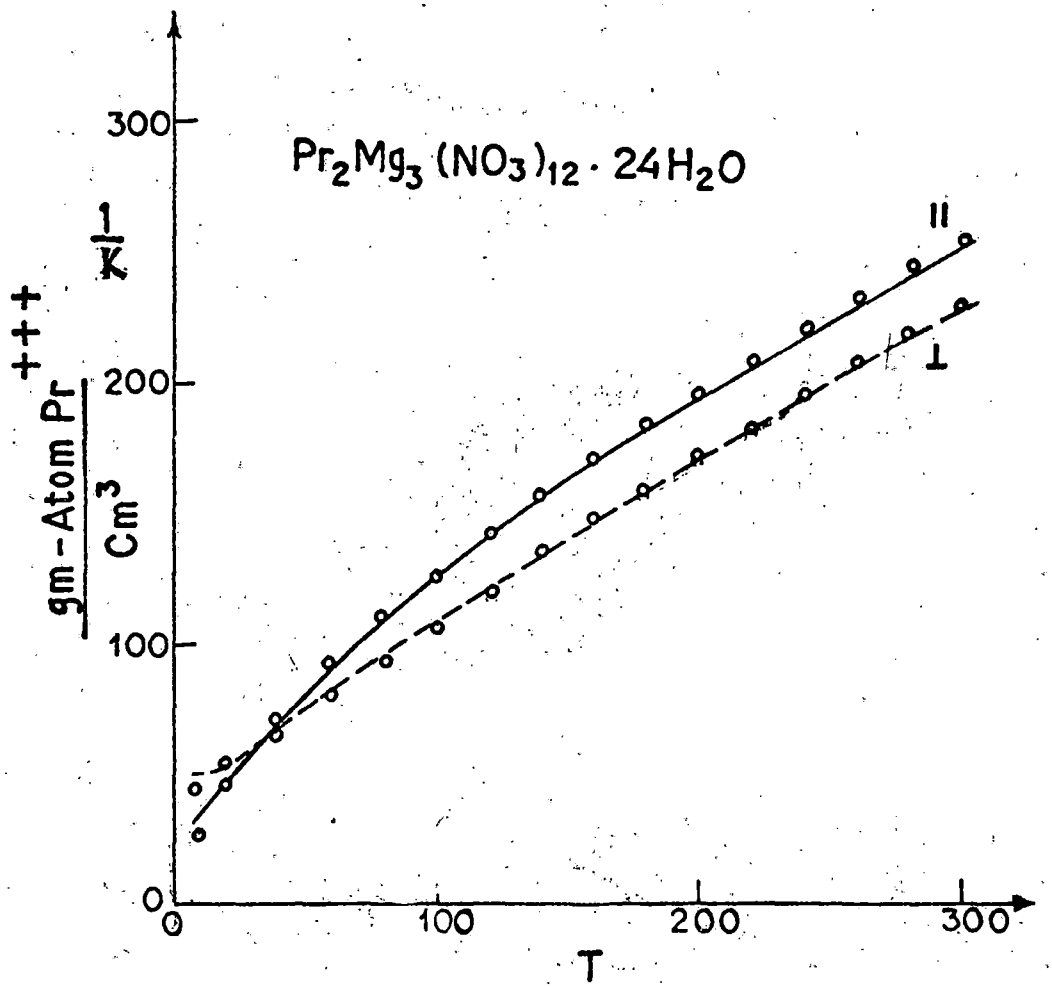

Fig. III.4.3. $\frac{1}{K_{\parallel}}$ and $\frac{1}{K_{\perp}}$ of Pr.DN. (gm - atom) cm^{-3} at different temperatures (T) in ^{o}K .

o Theoretical points.

— and -- Experimental curve.

Table III.4.1.

Comparison between the calculated and experimental values for the crystal field energy levels.

Terms	$\bar{\mu}$	Experimental energy levels in cm^{-1}	Predicted energy levels in cm^{-1} when our own set of parameters were used	Predicted energy levels when Judd's set of parameters were used
$^3H_4$	±1	0	0	0
	0	38	36.5	31.9
	±1	96	92.4	56.6
	0	-	419.9	362.4
	0	-	499.5	396.1
	±1	-	566.5	461.7
$^1D_2$	±1	16872	16888.8	16853.2
	±1	16920	16965.5	16931.5
	0	16934	17005.5	16930.4
$^3P_0$	0	20846	20875.0	20797.1
$^3P_1$	0	21422	21409.5	21333.3
	±1	21461	21453.5	21374.0
$^3P_2$	±1	22630	22650.0	22556.1
	0	22696	22681.9	22598.1
	±1	22693	22705.1	22605.7

APPENDIX III.4.

CF wave functions and the energy values of the ground term ($^3H_4$) of Praseodymium double nitrate (hydrated) obtained from our own set of fitted parameters

$$
\begin{aligned}
\Phi_1 = {} & 0.0034\,|^3H_6 6\rangle - 0.0365\,|^3H_6 3\rangle + 0.0326\,|^3H_6 0\rangle \\
& - 0.0165\,|^3H_6 -3\rangle - 0.0787\,|^3H_6 -6\rangle - 0.0576\,|^3H_5 3\rangle \\
& + 0.0516\,|^3H_5 0\rangle + 0.1013\,|^3H_5 -3\rangle + 0.4316\,|^3H_4 3\rangle \\
& + 0.7459\,|^3H_4 0\rangle + 0.4659\,|^3H_4 -3\rangle + 0.0058\,|^3F_4 3\rangle \\
& + 0.0042\,|^3F_4 0\rangle + 0.0076\,|^3F_4 -3\rangle + 0.0195\,|^3F_3 3\rangle \\
& + 0.0122\,|^3F_3 0\rangle - 0.0200\,|^3F_3 -3\rangle - 0.0242\,|^3F_2 0\rangle \\
& - 0.0084\,|^3P_2 0\rangle - 0.0070\,|^3P_1 0\rangle - 0.0003\,|^3P_0 0\rangle \\
& - 0.0003\,|^1I_6 6\rangle + 0.0032\,|^1I_6 3\rangle - 0.0030\,|^1I_6 0\rangle \\
& + 0.0017\,|^1I_6 -3\rangle + 0.0507\,|^1I_6 -6\rangle + 0.0889\,|^1G_4 3\rangle \\
& + 0.0541\,|^1G_4 0\rangle - 0.0005\,|^1G_4 -3\rangle - 0.0016\,|^1D_2 0\rangle
\end{aligned}
\Bigg\} \; W_1^{(0)} = 0
$$

$$\Phi_1' = 0.0034\,|^3H_6 6\rangle - 0.0365\,|^3H_6 3\rangle + 0.0326\,|^3H_6 0\rangle$$
$$-0.0165\,|^3H_6 -3\rangle - 0.0787\,|^3H_6 -6\rangle - 0.0576\,|^3H_5 3\rangle$$
$$+0.0516\,|^3H_5 0\rangle + 0.1013\,|^3H_5 -3\rangle + 0.4316\,|^3H_4 3\rangle$$
$$+0.7459\,|^3H_4 0\rangle + 0.4659\,|^3H_4 -3\rangle + 0.0058\,|^3F_4 3\rangle$$
$$+0.0042\,|^3F_4 0\rangle + 0.0076\,|^3F_4 -3\rangle + 0.0195\,|^3F_3 3\rangle$$
$$+0.0122\,|^3F_3 0\rangle - 0.0200\,|^3F_3 -3\rangle - 0.0242\,|^3F_2 0\rangle$$
$$-0.0084\,|^3P_2 0\rangle - 0.0070\,|^3P_1 0\rangle - 0.0003\,|^3P_0 0\rangle$$
$$-0.0003\,|^1I_6 3\rangle + 0.0032\,|^1I_6 0\rangle - 0.0030\,|^1I_6 -3\rangle$$
$$+0.0017\,|^1I_6 -6\rangle + 0.0507\,|^1G_4 3\rangle + 0.0889\,|^1G_4 0\rangle$$
$$+0.0541\,|^1G_4 0\rangle - 0.0005\,|^1G_4 -3\rangle - 0.0016\,|^1D_2 0\rangle$$

$$W_1^{(0)} = 0$$

$$\Phi_2 = -0.0278\,|^3H_6 6\rangle - 0.0126\,|^3H_6 3\rangle - 0.0289\,|^3H_6 0\rangle$$
$$+0.0126\,|^3H_6 -3\rangle - 0.0278\,|^3H_6 -6\rangle + 0.1070\,|^3H_5 3\rangle$$
$$-0.0000\,|^3H_5 0\rangle + 0.1070\,|^3H_5 -3\rangle + 0.5252\,|^3H_4 3\rangle$$
$$+0.6387\,|^3H_4 0\rangle - 0.5252\,|^3H_4 -3\rangle + 0.0067\,|^3F_4 3\rangle$$
$$+0.0026\,|^3F_4 0\rangle - 0.0067\,|^3F_4 -3\rangle - 0.0197\,|^3F_3 3\rangle$$
$$-0.0000\,|^3F_3 0\rangle - 0.0197\,|^3F_3 -3\rangle + 0.0155\,|^3F_2 0\rangle$$
$$+0.0114\,|^3P_2 0\rangle + 0.0000\,|^3P_1 0\rangle - 0.0005\,|^3P_0 0\rangle$$
$$+0.0026\,|^1I_6 6\rangle + 0.0012\,|^1I_6 3\rangle + 0.0024\,|^1I_6 0\rangle$$
$$-0.0012\,|^1I_6 -3\rangle + 0.0026\,|^1I_6 -6\rangle + 0.0620\,|^1G_4 3\rangle$$
$$+0.0762\,|^1G_4 0\rangle - 0.0620\,|^1G_4 -3\rangle - 0.0008\,|^1D_2 0\rangle$$
$$-0.0001\,|^1S_0 0\rangle$$

$$W_2^{(0)} = 36.5\ cm^{-1}$$

$$\Phi_3 = -0.0313\,|^3H_6 5\rangle + 0.0054\,|^3H_6 2\rangle + 0.0199\,|^3H_6 -1\rangle$$
$$+0.0254\,|^3H_6 -4\rangle + 0.0945\,|^3H_5 5\rangle - 0.0196\,|^3H_5 2\rangle$$
$$+0.1853\,|^3H_5 -1\rangle - 0.0213\,|^3H_5 -4\rangle - 0.7929\,|^3H_4 2\rangle$$
$$+0.1191\,|^3H_4 -1\rangle + 0.5429\,|^3H_4 -4\rangle + 0.0158\,|^3F_4 2\rangle$$
$$-0.0037\,|^3F_4 -1\rangle - 0.0064\,|^3F_4 -4\rangle + 0.0088\,|^3F_3 2\rangle$$
$$-0.0052\,|^3F_3 -1\rangle - 0.0037\,|^3F_2 2\rangle + 0.0291\,|^3F_2 -1\rangle$$
$$-0.0063\,|^3P_2 2\rangle + 0.0105\,|^3P_2 -1\rangle - 0.0005\,|^3P_1 -1\rangle$$
$$+0.0031\,|^1I_6 5\rangle - 0.0002\,|^1I_6 2\rangle - 0.0020\,|^1I_6 -1\rangle$$
$$-0.0019\,|^1I_6 -4\rangle - 0.1003\,|^1G_4 2\rangle + 0.0158\,|^1G_4 -1\rangle$$
$$+0.0668\,|^1G_4 -4\rangle + 0.0008\,|^1D_2 2\rangle + 0.0008\,|^1D_2 -1\rangle \qquad W_3^{(0)} = 92.4 \text{ cm}^{-1}$$

$$\Phi_3' = -0.0313\,|^3H_6 -5\rangle + 0.0054\,|^3H_6 -2\rangle + 0.0199\,|^3H_6 1\rangle$$
$$+0.0254\,|^3H_6 4\rangle + 0.0945\,|^3H_5 -5\rangle - 0.0196\,|^3H_5 -2\rangle$$
$$+0.1853\,|^3H_5 1\rangle - 0.0213\,|^3H_5 4\rangle - 0.7929\,|^3H_4 -2\rangle$$
$$+0.1191\,|^3H_4 1\rangle + 0.5429\,|^3H_4 4\rangle + 0.0158\,|^3F_4 2\rangle$$
$$-0.0037\,|^3F_4 1\rangle - 0.0064\,|^3F_4 4\rangle + 0.0088\,|^3F_3 -2\rangle$$
$$-0.0052\,|^3F_3 1\rangle - 0.0037\,|^3F_2 -2\rangle + 0.0291\,|^3F_2 1\rangle$$
$$-0.0063\,|^3P_2 -2\rangle + 0.0105\,|^3P_2 1\rangle - 0.0005\,|^3P_1 1\rangle$$
$$+0.0031\,|^1I_6 -5\rangle - 0.0002\,|^1I_6 -2\rangle - 0.0020\,|^1I_6 1\rangle$$
$$-0.0019\,|^1I_6 4\rangle - 0.1003\,|^1G_4 -2\rangle + 0.0158\,|^1G_4 1\rangle$$
$$+0.0668\,|^1G_4 4\rangle + 0.0008\,|^1D_2 -2\rangle + 0.0008\,|^1D_2 1\rangle \qquad W_3^{(0)} = 92.4 \text{ cm}^{-1}$$

$$\Phi_4 = -0.0155\,|^3H_6 6\rangle - 0.0016\,|^3H_6 3\rangle - 0.0000\,|^3H_6 0\rangle$$
$$-0.0016\,|^3H_6 -3\rangle + 0.0155\,|^3H_6 -6\rangle + 0.0078\,|^3H_5 3\rangle$$
$$+0.0113\,|^3H_5 0\rangle - 0.0078\,|^3H_5 -3\rangle + 0.6954\,|^3H_4 3\rangle$$
$$-0.0000\,|^3H_4 0\rangle + 0.6954\,|^3H_4 -3\rangle - 0.0374\,|^3F_4 3\rangle$$
$$+0.0000\,|^3F_4 0\rangle - 0.0374\,|^3F_4 -3\rangle - 0.0126\,|^3F_3 3\rangle$$
$$-0.0956\,|^3F_3 0\rangle + 0.0126\,|^3F_3 -3\rangle + 0.0000\,|^3F_2 0\rangle$$
$$+0.0000\,|^3P_2 0\rangle + 0.0014\,|^3P_1 0\rangle - 0.0000\,|^3P_0 0\rangle$$
$$+0.0023\,|^1I_6 6\rangle + 0.0011\,|^1I_6 3\rangle + 0.0000\,|^1I_6 0\rangle$$
$$+0.0011\,|^1I_6 -3\rangle - 0.0023\,|^1I_6 -6\rangle + 0.0993\,|^1G_4 3\rangle$$
$$+0.0000\,|^1G_4 0\rangle + 0.0993\,|^1G_4 -3\rangle - 0.0000\,|^1D_2 0\rangle$$
$$-0.0000\,|^1S_0 0\rangle$$

$\Big\}\ W_4^{(0)} = 419.9\ \text{cm}^{-1}$

$$\Phi_5 = -0.0059\,|^3H_6 6\rangle + 0.0083\,|^3H_6 3\rangle - 0.0171\,|^3H_6 0\rangle$$
$$-0.0083\,|^3H_6 -3\rangle - 0.0059\,|^3H_6 -6\rangle - 0.0258\,|^3H_5 3\rangle$$
$$-0.0000\,|^3H_5 0\rangle - 0.0258\,|^3H_5 -3\rangle + 0.4565\,|^3H_4 3\rangle$$
$$-0.7398\,|^3H_4 0\rangle - 0.4565\,|^3H_4 -3\rangle - 0.0296\,|^3F_4 3\rangle$$
$$+0.0571\,|^3F_4 0\rangle + 0.0297\,|^3F_4 -3\rangle + 0.0571\,|^3F_3 3\rangle$$
$$-0.0000\,|^3F_3 0\rangle + 0.0571\,|^3F_3 -3\rangle + 0.0272\,|^3F_2 0\rangle$$
$$+0.0034\,|^3P_2 0\rangle - 0.0000\,|^3P_1 0\rangle - 0.0018\,|^3P_0 0\rangle$$
$$+0.0007\,|^1I_6 6\rangle - 0.0013\,|^1I_6 3\rangle + 0.0037\,|^1I_6 0\rangle$$
$$+0.0013\,|^1I_6 -3\rangle + 0.0007\,|^1I_6 -6\rangle + 0.0681\,|^1G_4 3\rangle$$
$$-0.1119\,|^1G_4 0\rangle - 0.0681\,|^1G_4 -3\rangle + 0.0023\,|^1D_2 0\rangle$$
$$-0.0003\,|^1S_0 0\rangle$$

$\Big\}\ W_5^{(0)} = 499.5\ \text{cm}^{-1}$

$$\Phi_6 = -0.0109\,|^3H_6 5\rangle - 0.0049\,|^3H_6 2\rangle - 0.0139\,|^3H_6 -1\rangle$$
$$-0.0133\,|^3H_6 -4\rangle + 0.0297\,|^3H_5 5\rangle - 0.0277\,|^3H_5 2\rangle$$
$$-0.0544\,|^3H_5 -1\rangle + 0.0500\,|^3H_5 -4\rangle - 0.3673\,|^3H_4 2\rangle$$
$$+0.6220\,|^3H_4 -1\rangle - 0.6614\,|^3H_4 -4\rangle + 0.0262\,|^3F_4 2\rangle$$
$$-0.0501\,|^3F_4 -1\rangle + 0.0449\,|^3F_4 -4\rangle + 0.0635\,|^3F_3 2\rangle$$
$$-0.0435\,|^3F_3 -1\rangle - 0.0082\,|^3F_2 2\rangle + 0.0066\,|^3F_2 -1\rangle$$
$$-0.0016\,|^3P_2 2\rangle + 0.0009\,|^3P_2 -1\rangle + 0.0002\,|^3P_1 -1\rangle$$
$$+0.0022\,|^1I_6 5\rangle + 0.0012\,|^1I_6 2\rangle + 0.0025\,|^1I_6 -1\rangle$$
$$+0.0016\,|^1I_6 -4\rangle - 0.0560\,|^1G_4 2\rangle + 0.0952\,|^1G_4 -1\rangle$$
$$-0.0983\,|^1G_4 -4\rangle - 0.0003\,|^1D_2 2\rangle + 0.0002\,|^1D_2 -1\rangle \Big\} W_6^{(0)} = 566.5 \text{ cm}^{-1}$$

$$\Phi_6' = -0.0109\,|^3H_6 -5\rangle - 0.0049\,|^3H_6 -2\rangle - 0.0138\,|^3H_6 1\rangle$$
$$-0.0133\,|^3H_6 4\rangle + 0.0297\,|^3H_5 -5\rangle - 0.0277\,|^3H_5 -2\rangle$$
$$-0.0544\,|^3H_5 1\rangle + 0.0500\,|^3H_5 4\rangle - 0.3673\,|^3H_4 -2\rangle$$
$$+0.6220\,|^3H_4 1\rangle - 0.6614\,|^3H_4 4\rangle + 0.0262\,|^3F_4 -2\rangle$$
$$-0.0501\,|^3F_4 1\rangle + 0.0449\,|^3F_4 4\rangle + 0.0635\,|^3F_3 -2\rangle$$
$$-0.0435\,|^3F_3 1\rangle - 0.0082\,|^3F_2 -2\rangle + 0.0066\,|^3F_2 1\rangle$$
$$-0.0016\,|^3P_2 -2\rangle + 0.0009\,|^3P_2 1\rangle + 0.0002\,|^3P_1 1\rangle$$
$$+0.0022\,|^1I_6 -5\rangle + 0.0012\,|^1I_6 -2\rangle + 0.0025\,|^1I_6 1\rangle$$
$$+0.0016\,|^1I_6 4\rangle - 0.0561\,|^1G_4 -2\rangle + 0.0952\,|^1G_4 1\rangle - 0.0982\,|^1G_4 4\rangle$$
$$-0.0982\,|^1G_4 4\rangle - 0.0003\,|^1D_2 -2\rangle + 0.0002\,|^1D_2 1\rangle \Big\} W_6^{(0)} = 566.5 \text{ cm}^{-1}$$

CHAPTER IV

INTERPRETATION OF THE ABSORPTION AND CIRCULAR DICHROISM SPECTRA OF THE OPTICALLY ACTIVE $K_3Pr_2(NO_3)_9$ SINGLE CRYSTAL

IV.1. INTRODUCTION

In this chapter we present a model calculation on optical activity to correlate the rotational strengths for different CF transitions of anhydrous $K_3Pr_2(NO_3)_9$ single crystal, experimentally obtained by Chatterjee[12] . Sen et al[69,130] developed a theoretical model to calculate the rotational strength for optically active lanthanide crystals. They did extensive studies on lanthanide dyglycolate (Ln.DG.) crystals. They calculated the magnetic dipole transition moment and the electric dipole transition moment considering the component to component transition of the CF states. They used the Judd-Ofelt mechanism to calculate the lanthanide intensities. Later Richardson and Faulkner[68] developed an elaborate theoretical model which takes into account in addition to 'static' contribution the 'dynamic' ligand polarization contribution to the lanthanide electric dipole moment. The details of the static and Dynamic contribution to the electric dipole moment has been discussed in chapter II. In collaboration with Chatterjee and Chowdhury[131] we tried to fit the relative change in sign of the theoretical $\frac{R_K}{D_K}$ (D_K is the dipole strength which is the sum of the squares of the absolute values of all the dipole moments) with the experimental one. The values of $\frac{R_K}{D_K}$ for the K-th band were obtained from experiment by Chatterjee . Our attempt is to see how far our theoretical model can explain the experimental results i.e. the CF spectra and the CD spectra.

The purpose of the present chapter is to see: (1) how far the model is successful in predicting the relative sign and order of magnitude of rotational strengths of our anhydrous praseodymium double nitrate crystal; (2) a comparative study between the results obtained from the best fitted CF parameters (emperical) and that obtained from the theoretical parameters ($\equiv A_{kq}$(total), which is the sum of point charge and polarizability contributions); (3) whether we can evaluate a best set of parameters which can explain simultaneously the all observed CF levels and the relative change in sign of $\frac{R_K}{D_K}$ of the CD spectrum.

IV.2. A BRIEF ACCOUNT OF THE EXPERIMENT

The experimental data (i.e. both the optical absorption spectra and the CD spectra) were obtained by Chatterjee using Cary 17D and JASCO 500 at room temperature and upto $20^{\circ}K$. They are reproduced in table IV.3 .

IV.3. CRYSTAL STRUCTURE

The crystal is cubic with the space group $P4_32_12$. The four body diagonals are the four three-fold axes. Eight RE-ions, having identical environments occupy the eight corners of the cube. The site symmetry of a RE ion is a twelve

coordinated polyhedron; the twelve oxygens come from six nitrate groups. The actual symmetry is C_3 which makes each unit optically active[132] (see Fig. IV.1) .

IV.4. METHOD OF CALCULATION

We can divide our calculation into three parts: In the first part we tried to calculate the various theoretical CF levels and their corresponding wave functions with some set of CF parameters. During our CF calculations we have taken the full J-mixing into consideration. Then in the second part we have calculated the electric dipole transition moment and the magnetic dipole transition moment and in each case the component to component CF transition was taken into account. Finally in the last portion of our calculation we have calculated the rotational strength (R_K) for different transitions. Now we shall discuss the calculations in details.

IV.4(a) CRYSTAL FIELD CALCULATIONS

The effective Hamiltonian of Pr^{3+} in a crystal assuming a C_3 site symmetry is given by

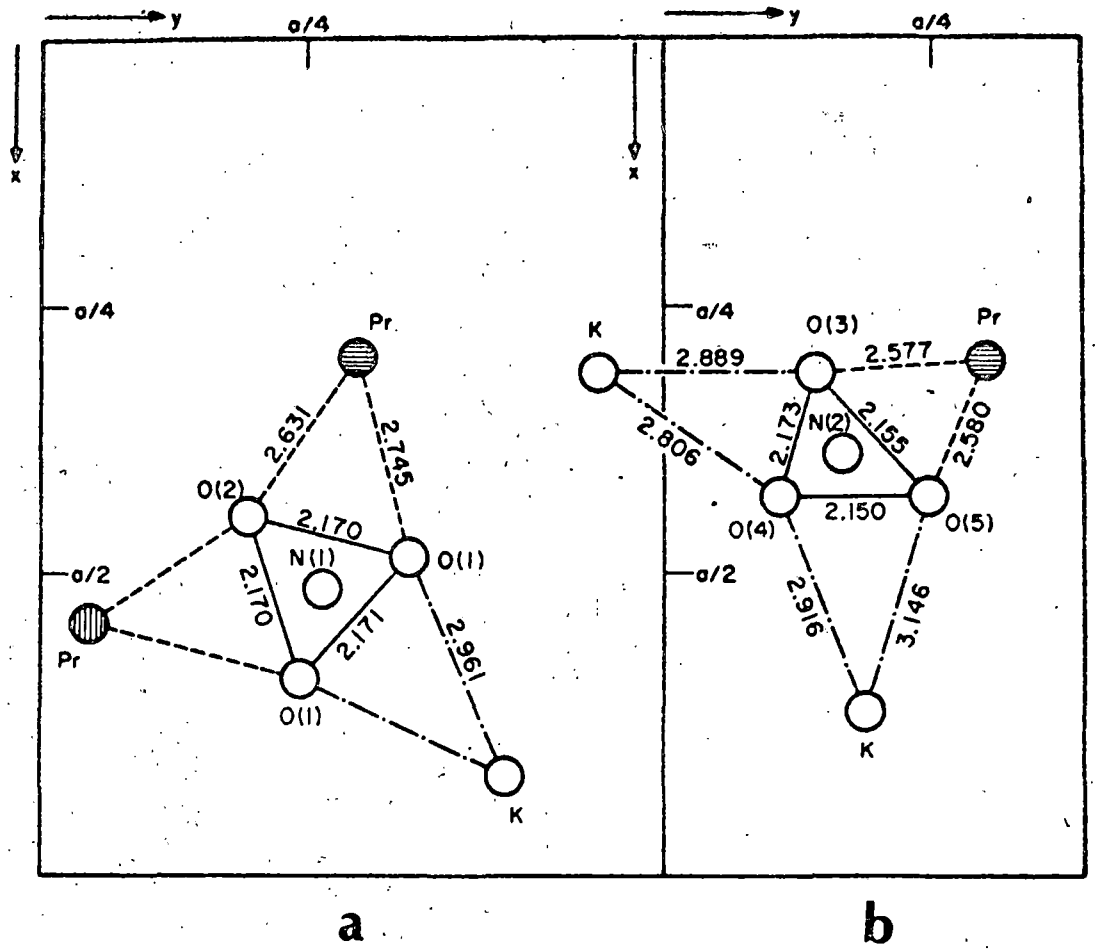

Fig. IV.1. Projection of "A" -type (a) and "B" -type (b) configurations, on the xy plane of $K_3Pr_2(NO_3)_9$.

$$\mathcal{H}_{eff} = \sum_{i<j} \frac{e^2}{r_{ij}} + \zeta \sum_i \underset{\sim}{l}_i \cdot \underset{\sim}{s}_i + A_{20}U_0^{(2)} + A_{40}U_0^{(4)} + A_{60}U_0^{(6)}$$

$$+ A_{66}(U_6^{(6)} + U_{-6}^{(6)}) + A_{43}(U_3^{(4)} - U_{-3}^{(4)}) + A_{63}(U_3^{(6)} - U_{-3}^{(6)})$$

$$+ iA'_{43}(U_3^{(4)} + U_{-3}^{(4)}) + iA'_{63}(U_3^{(6)} + U_{-3}^{(6)}) + iA'_{66}(U_6^{(6)} - U_{-6}^{(6)})$$

where A_{kq} and A'_{kq} are the real and imaginary part of the CF parameters in the tensor operator form. And $U_q^{(k)} = r^k Y_k^q$ is an irreducible tensor operator of rank k having q-th component.

The matrix elements of $\mathcal{H}_{eff}$ is constructed in a basis of states represented by $|UvSLJM\rangle$ (see chapter II). All states belonging to the different multiplet terms $^3P\,^3F\,^3H\,^1S\,^1D\,^1G\,^1I$ have been taken into consideration for the representation of the above matrix and it turns out to be a 91x91 matrix. The matrix element of the electrostatic part is obtained by a trial method by solving the Spedding's[79] matrix with a guess value of ζ so that it reproduces the free-ion energies given by Dieke[65]. The spin-orbit matrix elements for $4f^2$ configuration is given by Spedding[79]. We take those values. The value of ζ was determined by a trial procedure. The matrix element of $U_q^{(k)}$ is obtained by the tensor operator technique mentioned earlier in chapter II. Thus the 91x91 matrix is set up. But due to the crystal symmetry the whole matrix splits up into 2 matrices of dimension 30x30 (crystal quantum number $\bar{\mu} = \pm 1$) and one matrix of dimension 31x31 ($\bar{\mu} = 0$). Now one thing should be pointed here that the expansion of C_3 crystal field potential

contains both the 'C' term (real coefficient) and the 'S' term (imaginary coefficient) in the CF parameters.[133] The three CF parameters A'_{43} , A'_{63} and A'_{66} are coming from 'S' term. A'_{43} , A'_{63} and A'_{66} are individually real parameters. So iA'_{43}, iA'_{63} and iA'_{66} will be the crystal field parameters which are purely imaginary. Since the CF potential is always real so we take the combination of $U_3^{(4)}$ and $U_{-3}^{(4)}$; $U_3^{(6)}$ and $U_{-3}^{(6)}$ and $U_6^{(6)}$ and $U_{-6}^{(6)}$ in the last three combinations of CF interaction in such a way that the combination gives an imaginary i which on multiplication with iA'_{kq} parameters makes the CF interaction real. But according to the choice of our basis states the matrix element of the CF interaction part will be complex here. So this makes the three matrices complex. But still the whole matrix remains hermitian. One can solve the 3 above matrices by a direct complex matrix diagonalisation procedure. The same diagonalization can also be done by diagonalizing a real matrix in which the dimension of the whole matrix is made double of the original matrix. The detailed procedure has been described by Wilkinson[134] and we use the technique. So we have to diagonalize 2 matrices ($\bar{\mu} = \pm 1$) of dimension 60x60 and one matrix of dimension 62x62. During the diagonalisation of the matrix, the initial guess value of the different CF parameters were obtained as follows: A_{20} parameter was estimated from $^3P_1$ splittings, A_{40} and A_{43} parameters from $^1D_2$ splitting keeping A_{43}/A_{40} ratio as

obtained from point charge model. A_{60} , A_{63} and A_{66} parameters were guessed from the overall splittings of partially resolved $^3F_3$, $^3F_4$ and $^1G_4$ spectrum. The initial guess parameters A'_{43} , A'_{63} and A'_{66} were chosen directly from charge + polarizability contribution of the CF parameters (see chapter II). A complete computer program was then developed in which the CF matrix elements were automatically generated and then added up with SO and ES contribution and then the three matrices were diagonalized individually giving the different CF states and the corresponding energies. This takes into account the full J-mixing and also the intermediate coupling scheme which has already been discussed in chapter III. Starting with the guess value of the CF parameters we made an exhaustive trial method to see for which set of parameters the CF levels give the best fit with the experimental levels. The similar diagonalization was done with the parameters obtained from point charge + polarizability (theoretical) contribution. The two results were used to have a comparative study.

IV.4(b). CALCULATION OF THE MAGNETIC DIPOLE TRANSITION MOMENT AND THE ELECTRIC DIPOLE TRANSITION MOMENT

The contribution of the magnetic dipole transition moment between the different CF states was calculated using the computer diagonalised CF states and following the

appropriate selection rules for magnetic dipole transition (see chapter II). None of the transitions which we are considering, are directly magnetic dipole allowed but still the CF states contribute to the magnetic dipole intensity by mixing states of different J . The magnetic dipole moment calculation was done both for our fitted (emperical) CF parameters and also with the theoretical parameters independently. The details of the calculation of the magnetic dipole moment is given in chapter II.

The electric dipole transition moment arises in the $f^N \rightarrow f^N$ transitions by mixing with the odd parity states through the odd CF parameters, where

$$V = \sum_{t} A_{tp} D_p^{(t)}, \text{ with t odd .}$$

In the C_3 potential the allowed terms are $A_{3\pm3}$, $A_{5\pm3}$ and $A_{7\pm3}$. Foulkner and Richardson[68] gave a nice looking expression for the calculation of electric dipole transition moment both for static and the dynamic parts (see chapter II). The expression does not need the explicit values of odd CF parameters. We use their expressions for calculating the static and the dynamic contributions of the electric dipole moment and finally they were added up. While calculating the electric dipole moment we always consider the CF component to component transition. The electric dipole transition moment was calculated again with two sets of CF states (one is obtained from the emperical CF parameters and the other is obtained from the theoretical CF parameters).

The process for computing the magnetic dipole moment and the electric dipole moment was made in two separate computer programs.

IV.4(c). CALCULATION OF THE ROTATIONAL STRENGTH

The rotational strength (R_K) for a transition a → b is given by[67] the dot product

R_K = Imaginary part $\langle a|p|b\rangle . \langle b|m|a\rangle$

p and m are the electric and the magnetic dipole moment operators. We have already discussed how to obtain the contribution of the electric dipole moment and the magnetic dipole moment. As the CF states are complex for our system so the contribution of both the electric dipole moment and the magnetic dipole moments have real and the imaginary parts simultaneously. While calculating the rotational strength we need only the imaginary part of the product of electric dipole moment and the magnetic dipole moment. So in our case we can write the rotational strength as follows :

R_K = (Imaginary part of $\langle a|p|b\rangle$).(real part of $\langle a|m|b\rangle$) + (Real part of $\langle a|p|b\rangle$)x(Imaginary part of $\langle a|m|b\rangle$). The product of the total electric dipole moment and the magnetic dipole moment which has been calculated for the local axis system of each unit, was then re-expressed in terms of cubic

axis system and summed over the eight RE ions of the unit cell. It may be pointed out that the two ions located on opposite sides of any body diagonal of the cube are rotationally related (space group $P4_32$) and their contributions are added instead of cancelling. These are then compared with the experimental rotational strengths.

IV.5. RESULTS AND DISCUSSIONS

In the table IV.1 we have presented the values of ζ, $\langle r^2 \rangle$, $\langle r^4 \rangle$, $\langle r^6 \rangle$, $\overline{\alpha_L}$, q_L and C.I. parameters $\Xi_t(t,\lambda)$ which we have used in our calculations. The different set of CF parameters are presented in table IV.2 . Table IV.3 contains the different stark splitting and different $\frac{R_K}{D_K}$ obtained from experiment and from two sets of CF parameters. Where D_K is the dipole strength of the K-th band and it can be obtained theoretically by summing over the squares of all the dipole moments (i.e. both the electric and the magnetic dipole moments). The contribution of magnetic dipole moment is very small and hence the squares of this is again very small so we can neglect this safely from D_K . Since due to complex wave functions we have both the real part and the imaginary part of the electric dipole moment and the magnetic dipole moment, we can write

D_K = (Real part of the electric dipole moment)^2
+ (Imaginary part of the electric dipole moment)^2 .

We first tried to fit the experimental CF levels by adjusting the CF parameters. This was done by a trial procedure. The same CF level calculations were done by theoretical parameters alsp. In table IV.3 we have given the different stark splitting obtained for $^1D_2$, $^3P_0$, $^3P_1$ and $^3P_2$ manifold both from experiment and from our calculations. We find that overall stark splitting of the CF levels obtained from emperical parameters are in good agreement with the experimental findings. On the other hand the same thing obtained from theoretical parameters are significantly off from the experimental findings. So one may expect that the emperical CF parameters will give a better fitting with the experimental $\frac{R_K}{D_K}$ than that obtained from theoretical parameters. For a comparative study we have placed the experimental $\frac{R_K}{D_K}$ together with the theoretical $\frac{R_K}{D_K}$ (obtained both from emperical CF parameters and theoretical parameters) in table IV.3 . The results show that the theoretical values of $\frac{R_K}{D_K}$ are always higher in magnitude than the experimental ones. Specially some $\frac{R_K}{D_K}$ due to emperical set of CF parameters give very large values. Now, regarding the signs of $\frac{R_K}{D_K}$ we observe the following things :

In case of $^3H_4 \longrightarrow {}^1D_2$ transition the $\frac{R_K}{D_K}$ values for the theoretical parameters are as follows, out of four resolved

transitions all the four have the positive signs but in the experimental $\frac{R_K}{D_K}$ we have two are positive and two are negative. On the other hand $\frac{R_K}{D_K}$ obtained from emperical CF parameters gave a slight improvement in relative sign with the experimental findings. For the transition $^3H_4 \rightarrow {}^3P_0$ both the absolute and relative sign of $\frac{R_K}{D_K}$ obtained from theoretical CF parameters exactly match with the experiment. On the other hand only the relative sign of $\frac{R_K}{D_K}$ obtained from fitted set match with the experiment. For the fully resolved $^3H_4 \rightarrow {}^3P_1$ transitions we find that the signs of three experimental $\frac{R_K}{D_K}$ are positive and one is negative. The same results due to theoretical parameters show that the sign of three $\frac{R_K}{D_K}$ are positive and one is negative. We also find that the absolute sign of $\frac{R_K}{D_K}$ for two component to component transitions in both the above two-cases exactly match but the rest two transitions do not match exactly. For theoretical parameters we find that the relative sign of $\frac{R_K}{D_K}$ for last three consicutive transitions match with the experiment, but one component to component transition does not match at all.

In case of $^3H_4 \rightarrow {}^3P_2$ transition, the absolute and relative sign of $\frac{R_K}{D_K}$ with theoretical parameters exactly matches with the experiment, whereas in case of emperical parameters we succeed only in two.

So comparing the results obtained from theoretical parameters and the emperical parameters we conclude that optical activity calculation with the theoretical CF parameters is a better proposition for intensity matching than that with emperical CF parameters.

Table IV.1.

Values for Praseodymium ion Parameters

ζ_{so}/cm^{-1}	730
$\bar{\alpha}_L/A^3$	0.45
q_L/e.s.u.	-4.8×10^{-10}
$\langle r^2 \rangle/m^2$	3.04×10^{-21}
$\langle r^4 \rangle/m^4$	2.21×10^{-41}
$\langle r^6 \rangle/m^6$	3.45×10^{-61}
$H(1,2)/m^2J^{-1}$ *	-1.78×10^{-3}
$H(3,2)/m^4J^{-1}$	1.54×10^{-23}
$H(3,4)/m^4J^{-1}$	1.75×10^{-23}
$H(5,4)m^6J^{-1}$	-1.27×10^{-43}
$H(5,6)/m^6J^{-1}$	-5.45×10^{-43}
$H(7,6)/m^8J^{-1}$	4.54×10^{-63}

* $H(t,\lambda)$ —— : are the configuration interaction parameters.

Table IV.2

Values of Crystal field parameters (even ranked) for anhydrous and hydrated double nitrate single crystal.

A_{kq}	Values from Point charge + Polarizability model in cm^{-1}	Emperical parameters for $K_3Pr_2(NO_3)_9$ in cm^{-1}	Emperical parameters[124] for $Pr_2Zn_3(NO_3)_{12}\cdot 24H_2O$ in cm^{-1}
A_{20}	+72.3	+150	+191
A_{40}	-141.3	-107	-181
A_{60}	+96.7	+1296	+1022
A_{43}	+368.7	+202	±160
A_{63}	+241.7	+810	±2294
A_{66}	-191.0	+1755	-941
A'_{43}	+139.7	+89	-
A'_{63}	-85.0	+615	-
A'_{66}	+23.3	+203	-

Table IV.3.

Comparison of experimental, emperical and calculated $\frac{R_K}{D_K}$'s of $K_3Pr_2(NO_3)_9$

Transitions	Experimental results		Results with emperical CF parameters			Results with Theoretical (Point charge+Polarizability) CF parameters		
	Stark splitting in cm^{-1}	$\frac{R_K}{D_K} \times 10^4$	Stark splitting in cm^{-1}	Assignment of transition	$\frac{R_K}{D_K} \times 10^4$	Stark splitting in cm^{-1}	Assignment of transition	$\frac{R_K}{D_K} \times 10^4$
	0	+12.1	0	A→A	-20456.0	0	A→1E	+2.8
	61	-13.5	15	A→1E	+21.25	4	E→1E	+100.52
$^3H_4 \rightarrow {}^1D_2$	109	+6.12	61	E→A	+11.5	45	A→A	+190.6
			76	E→1E	+1205.10	50	E→A	+51.94
	152	-10.22	128	A→2E	-76.2	114	A→2E	+107.13
			189	E→2E	+452.60	118	E→2E	+201.5
$^3H_4 \rightarrow {}^3P_0$	0	+1.65	0	A→A	-3016.5	0	A→A	+21.08
	59	-0.93	60	E→A	+33.5	4	E→A	-137.0
$^3H_4 \rightarrow {}^3P_1$	0	+4.46	0	A→A	+45.9	0	A→A	+567.15
	32	+0.57	32	A→E	-164.6	5	E→A	+68.67
	59	-0.84	61	E→A	+68.07	16	A→E	+14.67
	96	+1.18	92	E→E	-1718.35	21	E→E	-193.6
$^3H_4 \rightarrow {}^3P_2$	0	+3.1	0	A→1E	-7.0	0	A→1E	+2.94
	53	-2.17	39	A→2E	-1.6	5	E→1E	-174.06
			61	E→1E	-10204.54	22	A→A	-16.86
			80	A→A	-2146.8	24	A→2E	-20.97
	106	-2.28	100	E→2E	-8125.66	27	E→A	+5.93
			141	E→A	+345.4	29	E→2E	-106.19

REFERENCES

[1] J.H. Van Vleck, Electric and magnetic susceptibilities, Oxford University Press (1932).

[2] H. Bethe, Ann. der. Phys. 3, 133 (1929).

[3] R.J. Elliott and K.W.H. Stevens, Proc. Roy. Soc. A 219, 387 (1953).

[4] E.Y. Wong and I. Richman, J. Chem. Phys. 34, 1182 (1962).

[5] W.T. Carnall, P.R. Fields and K. Rajnak, J. Chem. Phys. 49, 4424 (1968).

[6] H.M. Crosswhite and Hanah Crosswhite, F.W. Kaseta and R. Sarup, J. Chem. Phys. 64, 1981 (1976).

[7] W.T. Carnall, Hanah Crosswhite, H.M. Crosswhite and J.G. Conway, J. Chem. Phys. 64, 3582 (1976).

[8] H.M. Crosswhite, Hanah Crosswhite, N. Edelstein and K. Rajnak, J. Chem. Phys. 67, 3002 (1977).

[9] C.A. Morrison, R.P. Leavitt and D.E. Wortman, J. Chem. Phys. 73, 2580 (1980).

[10] J.B. Gruber, R.P. Leavitt and C.A. Morrison, J. Chem. Phys. 74, 2705 (1981).

[11] W.T. Carnall, H. Crosswhite and H.M. Crosswhite, Energy level structure and transition probabilities in the spectra of trivalent lanthanide in LaF_3, Argone National Laboratory Report (1977).

[12] T. Hayhurst, G. Shalimoff, N. Edelstein, L. A. Boatner and N. M. Abraham, J. Chem. Phys. 74, 5449 (1981).

[13] J. P. Morley, T. R. Faulkner, F. S. Richardson and R. W. Schwartz, J. Chem. Phys. 75, 539 (1981).

[14] Joma Hölsä and Pierre Porcher, J. Chem. Phys. 75, 2108 (1981).

[15] O. L. Malta, Chem. Phys. Lett. 87, 27 (1982).

[16] B. R. Judd, Proc. Roy. Soc. A241, 122 (1957).

[17] A. A. S. da gama, Gilbarto F. deså, P. Porcher and P. Caro, J. Phys. Chem. Solids. 42, 701 (1981).

[18] A. A. S. da Gama, Gilbarto F. de sá, P. Porcher and P. Caro, J. Chem. Phys. 75, 2583 (1981).

[19] B. R. Judd, J. Luminescence 18/19, 604 (1979).

[20] R. J. Elliott, Rev. Mod. Phys. 25, 167 (1953).

[21] R. A. Satten, J. Chem. Phys. 21, 637 (1953).

[22] B. R. Judd, Proc. Roy. Soc. A241, 122 (1957).

[23] B. R. Judd, Proc. Roy. Soc. A 241, 414 (1957).

[24] E. H. Erath, J. Chem. Phys. 34, 1985 (1961).

[25] E. Y. Wong, J. Chem. Phys. 34, 1989 (1961).

[26] J. D. Axe, and G. H. Dieke, J. Chem. Phys. 37, 2364 (1962).

[27] B. G. Wybourne, J. Chem. Phys. 36, 2295 (1962).

[28] D. K. Ray, Proc. Phys. Soc. 82, 47 (1963).

[29] B. M. Tinsley, J. Chem. Phys. 39, 3505 (1963).

[30] J. B. Gruber, W. F. Krupke and J. M. Poindexter, J. Chem. Phys. 41, 3363 (1964).

[31] J.A.Koningstein, Phys. Rev. 136, A717 (1964).

[32] J.A.Koningstein and J.E.Gensic, Phys. Rev. 136, A711 (1964a).

[33] J.A.Koningstein and J.E.Gensic, Phys. Rev. 136, A726 (1964b).

[34] H.M.Crosswhite, G.H.Dieke and W.J.Carter, J. Chem. Phys. 43, 2047 (1965).

[35] D.J.Newman, Adv. Phys. 20, 197 (1971).

[36] G.F.Herrmann, J.J.Pearson, K.A.Wickersheim and R.A.Buchanan, J. Appl. Phys. 37, 1312 (1966).

[37] T.Mookherji and A.Mookherji, Indian J. Pure and Appl. Phys. 4, 43 (1966).

[38] C.H.Brecher, H.Samelson, A.Lempicki, R.Riley and T.Peters, Phys. Rev. 155, 178 (1967).

[39] B.R.Judd, Proc. Roy. Soc. A 232, 458 (1955).

[40] R.S.Mulliken, J. Chem. Phys. 3, 375 (1935).

[41] K.W.H.Stevens, Proc. Roy. Soc. A 219, 542 (1953).

[42] J.Owen, Proc. Roy. Soc. A 227, 183 (1955).

[43] J.Owen, Farad. Soc. Discussion, No.19, 127, (1955).

[44] B.Bleaney, K.D.Bowers and M.H.L.Pryce, Proc. Roy. Soc. A 228, 166 (1955).

[45] A.Bose, A.S.Chakravarty and R.Chatterjee, Proc. Roy. Soc. A 255, 145 (1960).

[46] C.K.Jørgensen, Modern aspects of ligand field theory, Amsterdam, North-Holland Publishing Co (1971).

[47] A. Bose and R. Rai, Indian J. Phys. 39, 176 (1965).

[48] A. Bose, L. C. Jackson and R. Rai, Indian J. Phys. 39, 7 (1964).

[49] K. Rajnak and B. G. Wybourne, Phys. Rev. 132, No. 1, 280 (1963).

[50] B. R. Judd, Phys. Rev. 141, 4 (1966).

[51] B. R. Judd, H. M. Crosswhite and Hanah Crosswhite, Phys. Rev. 169, 130 (1968).

[52] B. R. Judd, Phys. Rev. 127, No. 3, 750 (1962).

[53] G. S. Ofelt, J. Chem. Phys. 37, 511 (1962).

[54] E. U. Condon and G. H. Shortley, Theory of Atomic Spectra, Cambridge (1953).

[55] A. Nath and U. S. Ghosh, Phys. Stat. Sol. (b) 112, 187 (1982).

[56] H. B. Jonassen and Arnold Weissberger, Techniques of Inorganic Chemistry, Vol. IV, page 249-368, Interscience Publishers (John Wiley and Sons), London (1965).

[57] C. W. Deutsche, D. A. Lightner, Robert W. Woody and Albert Moscowitz, Ann. Rev. Phys. Chem. 20, 407 (1969).

[58] S. F. Mason, Quart. Rev., The Chemical Society, 17, 20 (1963).

[59] A. D. Liehr, Optical activity in Inorganic and Organic Compounds - Transition metal chemistry, 2, 165 (1966).

[60] C. Djerassi, Optical rotatory dispersion (Application to Organic Chemistry), Mc Graw-Hill, New York, (1960).

[61] P. Pino, F. Ciardelli and M. Zandomeneghi, Ann. Rev. Phys. Chem. 21, 561 (1970).

[62] A. K. Mukherjee and M. Chowdhury, Phys. Rev. B 16, 3070 (1977).

[63] R.D.Peacock, Chem. Phys. Letts. 35, 420 (1975).

[64] E.V.Sayre, K.M.Sancier and S.Freed, J. Chem. Phys. 23, 2060 (1955).

[65] G.H.Dieke, Spectra and energy levels of rare-earth ions in crystals, Interscience publications (1968) and references therein.

[66] R.D.Peacock, J. Mol. Structure, 46, 203 (1978).

[67] H.Eyring, J.Walter and G.E.Kimball, Quantum Chemistry (Section 17C, p. 342), John Wiley and Sons, Inc. (1944).

[68] F.S.Richardson and T.R.Faulkner, J. Chem. Phys. 76, 1595, (1982).

[69] A.C.Sen and M.Chowdhury, Chem. Phys. Letts. 79, 165 (1981).

[70] A.C.Sen, Ph.D. thesis, Calcutta University, India (1980).

[71] A.Nath, C.Basu and U.S.Ghosh, Indian J. Phys. 55A, 227 (1981).

[72] J.C.Slater, The Quantum Theory of Atomic Structure, Vol. I and II, Mc Graw-Hill Book Company, New York (1960).

[73] G.Racah, Phys. Rev. 63, 367 (1943).

[74] P.E.Wigner, Group Theory (English Transl.) Academic Press, New York (1959).

[75] G.Racah, Phys. Rev. 62, 438 (1942).

[76] C.Basu, Ph.D. Thesis, Calcutta University, India (1976).

[77] C.W.Nielson and G.F.Koster, Spectroscopic coefficients for the p^n, d^n and f^n configurations, M.I.T. press, Cambridge, (1963).

[78] G.Racah, Phys. Rev. 76, 1352 (1949).

[79] F.H.Spedding, Phys. Rev. 58, 255 (1940).

[80] B.R.Judd and R.Loudon, Proc. Roy. Soc. A 251, 127 (1959).

[81] B.R.Judd, Operator techniques in atomic spectroscopy, Mc Graw-Hill Book Company, New York (1963).

[82] M.Mizushima, Quantum Mechanics of Atomic Spectra and Atomic Structure, W.A.Benzamin, New York (1970).

[83] K.W.H.Stevens, Proc. Phys. Soc. LXV, 209 (1952).

[84] Thomas R.Faulkner and F.S.Richardson, Mol. Phys. 39, 75 (1980).

[85] S.F.Mason (ed.), Optical activity and chiral discrimination, p.161-187, D.Reidel Publishing Company, England (1978).

[86] J.D.Saxe, T.R.Faulkner and F.S.Richardson, J. Chem. Phys. 76, 1607 (1982).

[87] W.F.Krupke, Phys. Rev. 145, No.1, 325 (1966).

[88] S.F.Mason, R.D.Peacock, B.Stewart, Mol. Phys. 30, 1829 (1975).

[89] J.P.Elliott, B.R.Judd and W.A.Runciman, Proc. Roy. Soc. A 240, 509 (1957).

[90] A.H.Cooke and H.J.Duffus, Proc. Roy. Soc. A 229, 407 (1955).

[91] B.Bleaney, H.E.D.Scovil and R.S.Trenam, Proc. Roy. Soc. A 223, 15 (1954).

[92] D.Neogy and A.Mookherji, J. Phys. Japan 20, 1332 (1965).

[93] A.Mookherji and S.P.Chachra, J. Phys. Chem. Solids 30, 2399 (1969).

[94] D.Neogy and A.Mookherji, Physica 31, 1325 (1965).

[95] A.Mahalanabis and S.P.Chachra, Indian J. Pure. and Appl. Phys. 6, 55 (1968).

[96] J.B.Gruber and R.A.Satten, J. Chem. Phys. 39, 1455 (1963).

[97] R.A.Fisher, G.E.Brodale, E.W.Hornung and W.F.Giauque, J. Chem. Phys. 68, 169 (1978).

[98] B.G.Wybourne, J. Chem. Phys. 34, 279 (1961).

[99] J.A.A.Ketelaar, Physica,'s Grav. 4, 619 (1937).

[100] D.R.Fitzwater and R.E.Rundle, Z. Kristrallogr. Kristallgeom, 112, 362 (1959).

[101] E.Y.Wong, J. Chem. Phys. 35, 544 (1961).

[102] B.G.Wybourne, Spectroscopic properties of rare-earths, John Wiley and Sons, Inc., New York, (1965).

[103] A.Abragam and B.Bleaney, Electronic paramagnetic resonance of transition ions, Clarendon Press, Oxford, (1970).

[104] J.V.D.Handel and J.C.Hupse, Physica 9, 225 (1942).

[105] E.Y.Wong, J. Chem. Phys. 35, 544 (1961).

[106] M.M.Ellis and D.J.Newman, J. Chem. Phys. 47, 1986 (1967).

[107] A.Bose, A.S.Chakravarty and R.Chatterjee, Proc. Roy. Soc. A 261, 43 (1961).

[108] A.Bose, R.Chatterjee and R.Rai, Proc. Phys. Soc. 83, 959 (1964).

[109] A.Bose, A.S.Chakravarty and R.Chatterjee, Proc. Roy. Soc. A 261, 207 (1961).

[110] R.J.Elliott and K.W.H.Stevens, Proc. Roy. Soc. A 64, 932 (1951).

[110a] A.Nath, Indian J. Phys. (in press).

[111] J.B.Gruber and J.G.Conway, J. Chem. Phys. 32, 1178 (1960).

112 J.B.Gruber and J.G.Conway 32, 1531 (1960).

113 E.Y.Wong and I.Richman, J. Chem. Phys. 34, 1182 (1961).

114 B.C.Gerstein, L.D.Jennings and F.H.Spedding, J. Chem. Phys. 37, 1496 (1962).

115 W.F.Krupke and J.B.Gruber, Phys. Rev. A 139, 2008 (1965).

116 U.Johnsen, Z. Physik 152, 454 (1958).

117 S.Hüfner, Z. Physik 169, 417 (1962).

118 J.B.Gruber, J. Chem. Phys. 38, 946 (1963).

119 J.M.Baker and B.Bleaney, Proc. Phys. Soc. A 68, 936 (1955).

120 K.H.Hellwege, G.Hess and H.G.Kahle, Z. Physik 159, 333 (1960).

121 J.V.D.Handel, J. Physica's Grav, 8, 513 (1941).

122 K.H.Hellwege, W.Schembs and B.Schneider, Z. Physik 167, 477 (1962).

123 A.M.Hellwege and K.H.Hellwege, Z. Physik 135, 92 (1953).

124 B.R.Judd, Proc. Roy. Soc. A 232, 458 (1955).

125 K.H.Hellwege, S.H.Kwan, W.Rummel, W.Schembs and B.Schneider, Z. Physik 167, 487 (1962).

126 A.Nath, J. Phys. Soc. Japan, 52, No.9 (1983) (in press).

127 A.Zalkin, J.D.Forrester and D.H.Templeton, J. Chem. Phys. 39, 2881 (1963).

128 S.D.Devine, J. Chem. Phys. 47, 1844 (1967).

129 P.K.Chatterjee, Ph.D. thesis, Calcutta University, India (submitted).

130 A.C.Sen, M.Chowdhury and R.W.Schwartz, J. Chem. Soc. Farad. Tr. II 77, 1293 (1981).

131 P.K. Chatterjee, A. Nath, A.C. Sen and M. Chowdhury, J. Chem. Soc. Farad. Tr. II. (in press).

132 W.T. Carnall, S. Siegel, J.R. Ferraro, B. Tani and E. Giebert, Inorg. Chem. 12, 560 (1973).

133 J.L. Prather, Atomic Energy levels in Crystals, NBS Monograph 19, U.S. Government Printing Office, Washington D.C. (1961).

134 J.H. Wilkinson, The Algebraic eigen value problem, p. 342-343, Clarendon press, Oxford (1965).